Université du Québec
à Rimouski

Conception, modélisation et simulation d'un bateau de pêche électrique à émission zéro

Mémoire présenté

dans le cadre du programme de maîtrise en ingénierie

en vue de l'obtention du grade de maître en sciences appliquées (M. Sc. A.)

PAR

© IMAN FOROUGHI

Avril 2023

Composition du jury :

Mazen Ghandour, président du jury, UQAR

Adrian Ilinca, directeur de recherche, UQAR

Mohamad Issa, codirecteur de recherche, Institut Maritime du Québec

Patrick Rizk, UQAR

Dépôt initial le 20 Décembre 2022 Dépôt final le 18 avril 2023

ACKNOWLEDGMENTS

I would like to express my gratitude to **Dr. Adrian Ilinca** for his support in accomplishing research in electrical engineering. Without his direction, supervision, patience, insightful comments, immense knowledge, and encouragement, I would not have finished this thesis. It is my pleasure to pursue a Master of Engineering degree at **UQAR** University.

I would also like to thank my co-director, Professor **Mohamad Issa,** from the Institut Maritime du Québec in Rimouski, for the interesting discussions we had and for his wise advice.

I would like to thank my family for their continuous assistance, patience, and encouragement throughout the coursework and research work.

Finally, I would like to dedicate this thesis to my parents, Yaghoub Foroughi and Farangis Azizi.

RÉSUMÉ

Dans cette thèse, on s'efforce de concevoir un système de propulsion entièrement électrique pour un bateau de pêche qui fonctionne en eau douce (comme une rivière) et qui n'a pas besoin d'utiliser de carburant. Le bateau étudié est un catamaran et mesure 23 pieds de long par 8 pieds de large. Une vitesse de 8 nœuds est considérée pour le bateau lorsqu'il se déplace vers le lieu de pêche et également entre les rivières, et la durée de l'activité quotidienne du bateau est de 8 heures. La consommation d'énergie pour chaque voyage est de 17.3 kWh.

Le modèle présenté est tout à fait général, mais les résultats peuvent être utilisés pour n'importe quel bateau dont la taille se situe dans la fourchette du modèle étudié. Un panneau solaire photovoltaïque, un moteur à courant continu, des batteries lithium-ion, un équipement de protection, un contrôleur MPPT et un contrôleur d'accélérateur sont tous proposés comme éléments du système d'alimentation. Les systèmes de batteries peuvent fournir de l'électricité jusqu'à 20 kWh. L'énergie électrique produite par le panneau solaire est stockée dans une banque de batteries pour être utilisée par l'équipement électrique à l'intérieur du bateau.

Un modèle 3D d'un toit rigide en aluminium est conçu pour monter les panneaux solaires sur le toit du bateau. Le toit rigide (créé avec Solidworks) a été examiné dans différentes conditions, notamment en ce qui concerne le vent et le poids, à l'aide d'Ansys Workbench. Tous les tests ont révélé un énorme facteur de sécurité. Les bons calculs sont effectués pour déterminer où placer les objets lourds tels que les batteries, les moteurs et les panneaux solaires et s'assurer que le bateau reste stable. Ensuite, un modèle 3D d'un bateau équipé du toit rigide conçu et d'autres équipements est présenté.

Le système de bateau alimenté par batterie proposé a été simulé par SIMULINK, puis la conception a été évaluée. Lorsque les pêcheurs appuient sur l'accélérateur du bateau

électrique développé, le système de propulsion électrique conçu peut immédiatement produire un couple adéquat, alors que les bateaux similaires équipés de moteurs à combustion mettent souvent plus de temps à atteindre cette puissance. La tension de charge continue est maintenue quel que soit le changement de la valeur de l'irradiation. Chaque fois que le pourcentage de charge de la batterie est inférieur à 55 %, les panneaux sont connectés à la batterie par l'intermédiaire du circuit de commutation et la batterie est ainsi chargée. Les résultats de la conception proposée montrent qu'elle maintient la vitesse et la stabilité par rapport à d'autres conceptions issues de recherches antérieures qui posaient des problèmes de continuité et de stabilité de l'alimentation en raison des variations des conditions météorologiques, telles que l'irradiation solaire. Les résultats montrent qu'un moteur à carburant traditionnel peut être remplacé par un moteur électrique sans perte de puissance et avec seulement de légers changements dans le poids du système de propulsion.

Mots clés : Bateau zéro émission, banc de batteries, propulsion électrique, module PV, énergie renouvelable, énergie solaire.

ABSTRACT

In this thesis, an effort is made to design an all-electric propulsion system for a fishing boat that works in freshwater (like a river) and does not have to use fuel. The boat under study is a catamaran and measures 23 feet long by 8 feet wide. A speed of 8 kn is considered for the boat when moving to the fishing place and also between rivers, and the duration of the boat operations is 8 hours. Energy consumption for each trip is 17.3 kWh.

The model shown is completely general, but the results can be used for any boat whose size is within the range of the model studied. A solar PV panel, a DC motor, lithium-ion batteries, protection equipment, an MPPT controller, and a throttle controller are all suggested as parts of the power system. The battery systems can sustain energy up to 20 kWh. The resulting electrical power from the solar panel is stored in a battery bank for use by electrical equipment inside the boat.

A 3D model of an aluminium hardtop is designed to mount the solar panels on the boat's roof. The designed hardtop (created with Solidworks) has been examined under different conditions, including wind and weight, using Ansys Workbench. In all tests, a huge safety factor was reported. The right calculations are done to figure out where to put heavy objects like batteries, motors, and solar panels and make sure the boat stays stable. Next, a 3D model of the boat equipped with the designed hardtop and other equipment is presented.

The proposed battery-powered boat system has been simulated by SIMULINK, and the design is then evaluated. When fishermen push the throttle on the developed electric boat, the designed electric propulsion system can immediately produce proper torque, while similar boats with combustion engines often take longer to reach this horsepower. The continuous charging voltage is maintained regardless of the change in the value of the irradiance.

Whenever the battery charge percentage reaches less than 55%, the panels are connected to the battery through the switching circuit, and the battery is consequently charged. The results of the proposed design show that it maintains speed and stability compared to other ones from previous research that had issues with power continuity and stability due to variations in weather conditions, such as solar irradiation. The results show that a traditional fuel engine can be replaced with an electric motor without losing power and with only slight changes in the weight of the propulsion system.

Keywords: Battery bank, Electric propulsion, PV module, Renewable energy, Solar energy, Zero emission boat.

TABLE OF CONTENTS

LIST OF TABLES

LIST OF FIGURES

LIST OF ABBREVIATION

IMO	International maritime organization
SPB	Solar powered boat
DC	Direct current
AC	Alternating current
PV	Photovoltaic
HP	Horsepower
V	Voltage
I	Current
MPPT	Maximum power point tracking
BB	Battery bank
SOC	State of charge
AGM	Absorbent glass mat
DOD	Depth of discharge
CC	Constant current
CV	Constant voltage
RPM	Revolutions per minute
DG	Diesel generator

MATLAB	Matrix laboratory
P&O	Perturbation and observation
D	Duty cycle
IGBT	Insulated-gate bipolar transistor
AWG	American wire gauge
COM	Common
CB	Circuit breaker
GND	Ground
LIBs	Lithium ion battery based
UUVs	Unmanned underwater vehicles
CIGS	Copper indium gallium diselenide
CdTe	Cadmium telluride
IC	Incremental conductance
BC	Before christ
CO2	Carbon dioxide
GPS	Global Positioning System
S/N	Serial number
QTY	Quantity
PbA	Lead acid
PbO2	Lead dioxide

PbSO4	Lead sulfate
KOH	Potassium hydroxide
Ni-Cd	Nickel-cadmium
Ni–MH	Nickel metal hydride
EV	Electric vehicle
R&D	Research and development
N	Newton
PWM	Pulse width Modulation
C	Collector
E	Emitter
A-Si	Amorphous silicon
LC	Inductor capacitor
ANSYS	Analysis of Systems

LIST OF SYMBOLS

A	Area	[m^2]
I	Electric current	[A]
V	Voltage	[V]
T	Motor torque	[N·m]
Kn	Speed	[knot]
P	Electric power	[Watt]
E	Electric energy	[kWh]
h	Hour	[h]
sec	**S**econd	[s]
Hz	Frequency	[hertz]
M	Mass	[kg]
R	Electrical resistance	[Ω]
F	Force	[N]
ω	Angular Rotational Speed	[rad/s]
Ah	Ampere-hour	[A.h]
G	Gravitational constant	[m/s^2]
L	Length	[m]

σ	Stress	[pa]
gal	Volume	[L]
mph	Speed	[m/s]
hp	Power	[watts]
m	Dimension	[meter]
min	Time	[minute]
n	Speed	[rpm]

GENERAL INTRODUCTION

1. INTRODUCTION

Greenhouse gases such as CO_2, water vapour, and methane are one of the current problems of human society. This affects not only human life but also the quality of life for many creatures. In the last few decades, the growth of large industries has led to more of these gases being released into the air. For example, the boating industry alone is responsible for the emission of about 3–5% of greenhouse gases [1, 2].

The most important sources of greenhouse gas emissions in the boating industry are combustion and diesel engines [2]. Consequently, the International Maritime Organization (IMO), responsible for a safe and pollution-free marine industry, monitors the emission of greenhouse gases by diesel engines used in the boating industry. In some cases, it has established regulations to control it [3]. Greenhouse gases emitted by diesel engines can travel up to 400 km and impact a large portion of the environment [4].

Most countries with a lot of inland waterways use boats for both cargo and passenger transportation. Most of the currently used boats run on diesel fuel [5]. The replacement of diesel engines with electric engines that work with batteries will make the transportation industry more environmentally friendly [6]. The fact that fossil fuels are running out and will most likely become more expensive justifies the switch from diesel to electric engines [7, 8]. In the past few years, it has become very important to replace engines that run on fossil fuels with engines that can get all or part of their power from renewable energy sources [9].

Millions of years are required for fossil fuels to form, which is why they are classified as non-renewable resources. Replacing these fuels can also slow down their depletion process and change the needs of the industry. Using renewable energy for propelling a boat is a new development in the boating industry [10].

One of the most significant renewable energy sources is solar energy, which is widely available around the world. One of the replacement propulsion solutions for boats is photovoltaic (PV) technology with energy storage.

Using solar boats in the boating industry lowers greenhouse gas emissions and reduces global warming. Such a change positively affects the survival of many creatures on this planet [11]. Also, electric boats do not need any fuel or oil, so apart from preventing air pollution, they do not cause oil pollution and do not endanger the lives of aquatic creatures [12].

All-electric boats also do not require ignition, their start-up time is much faster, and they have much less noise pollution than their diesel counterparts [13]. Electric engines have a much simpler operation; therefore, their maintenance and repair costs are much lower [13]. Repairs of these engines are possible with more straightforward tools. Also, carrying significant fuel for the boats can be dangerous and cause a fire, but using electric motors eliminates this risk [4, 14].

Several studies have been conducted on solar boats, but most of them have focused on hybrid designs. However, limited studies have been conducted on battery-powered boats that use only batteries and solar power. To maintain reliable propulsion during daily boat operations, more study is required for a battery-powered boat in terms of the appropriate selection of electrical components and the connection between them. In this study, the 3D design of the boat and its hardtop is also taken into account to analyze the boat's safety under various weather conditions. The developed model is evaluated for use in medium-sized catamaran fishing boats under different boat operating scenarios in terms of its reliability and autonomy.

2. PROJECT OBJECTIVES AND SCOPE

The main objective of this thesis is to make boats less harmful to the environment by stopping them from releasing greenhouse gases, stopping diesel engine oil leaks, and getting rid of noise pollution.

This study analyses how to design a boat whose propulsion can run on batteries and solar panels. All the parts of this model and their connections are examined. Most medium-sized fishing boats have hard tops, making it possible to put solar panels on them as the boat's roof. Designing the hardtop is also one of the goals of this thesis.

This thesis is based on the design of an electric catamaran boat. However, efforts have been made to use the results on boats of different sizes with as few changes as possible. The objectives of this thesis include the following:

- Fully electrifying the boat propulsion system;
- Sizing and choosing the necessary components for the propulsion of an electric boat, including solar panels, batteries, electric motors, and controllers;
- Appropriate connections and wiring for the boat's motor system;
- Choosing the most effective solar panels and batteries for the best performance;
- Analyzing and designing hardtop and boat in considerable detail, along with 3D modeling;
- Studying solar panel positioning;
- System modeling and simulation to analyze the propulsion system's reliability; and
- Identifying the remaining challenges for further improvements.

3. MODEL SELECTION

We decided to use the catamaran hull form as it provides greater space on top of the deck to put the solar array [15]. The boat design says that the roof of the superstructure is 7.01 m long and 2.43 m wide, giving a total of 17.03 m^2 to mount the solar array. Table 1 summarizes the features of the designed fishing boat.

Table 1. General specifications of the studied boat.

Parameters	Specifications
Boat × beam	23 × 8 (feet)
Passenger carrying capacity	4 to 6 people
Boat speed	8 kn
Boat operating duration/day	8 hours
The required energy to drive boat	17.3 kWh
Hull form	Catamaran

4. METHODOLOGY

This project presents an approach to the design of a zero-emission medium-sized catamaran boat based on modeling on Simulink software.

The proposed approach is based on a methodology structured into five steps: (i) optimal selection of power system components; (ii) designing electric connections between components; (iii) 3D modeling of the boat and its components; (IV) validation of the boat's hardtop using ANSYS software; (V) simulation of the developed boat in different situations using Simulink.

5. WORK PLAN

- **General introduction**

- **Chapter** 1

This chapter includes an overview of boat history, a review of boat and marine motor types, industrial motivations for research, and the global electric boat market.

- **Chapter 2**

The first part of the second chapter presents the size of the main components of an electric boat based on mathematical relationships, along with a comparison with similar

models of diesel boats. The daily load of the boat has been calculated, according to which the right size for the battery and solar panel has been chosen. The batteries, solar panels, and motor were evaluated in four different conditions: anchored, in port, sailing, and off position, and a proposed connection diagram was also made after appropriate cabling and safety equipment.

- **Chapter 3**

The third phase presents a 3D schematic of the boat and its equipment using SolidWorks. The space on the boat is calculated based on its size. A hard top is designed to hold the solar panels, and methods for connecting them are suggested. The designed hard top has been validated with the help of Ansys Workbench in different weather conditions by calculating the safety factor. A conceptual method is developed for how to position solar panels at different times of the year. At the end of the chapter, mathematical relationships were used to figure out how to place heavy objects on the deck to keep the boat stable.

- **Chapter 4**

This chapter focuses on the simulation of different boat scenarios using Simulink, then the simulation results are analyzed.

- **Chapter 5**

This chapter discusses the analysis of the results, recommendations, and future perspectives. Possible solutions are also presented for generalizing the research results to large-scale boats.

CHAPTER 1
AN OVERVIEW OF BOAT DEVELOPMENT

1.1 INTRODUCTION

Many industries across the globe are incorporating green technology into their operations due to the rise in pollution levels and increased awareness regarding climate change. Maritime transport is one of the main sectors in this field, which has seen significant progress. Switching from boats with fuel-powered engines to electric engines is one of the most significant actions in this industry. An electric boat uses batteries instead of fuel to propel the boat during marine operations [16].

The electric boat market is segmented according to system operation, range, ship type, power, application, type, boat size, battery type, boat length, run time, passenger capacity, and end use. Based on boat size, the electric boat market has been segmented into three categories: small, medium, and large. Considering the battery type, the electric boat market has been segmented into lead-acid, lithium-ion, and nickel-based batteries. Based on the run time, the electric boat market has been segmented into three categories: less than 7 hours, 7 to 12 hours, and more than 12 hours [17].

In the forecast period of 2021 to 2028, the electric boat market is expected to reach USD 230,180.50 million, growing at a rate of 11.20% [17, 18].

1.2 LITERATURE REVIEW

1.2.1 Introduction

Many studies have investigated how renewable energy can be used in transportation, especially in the boating industry.

Solar boats have become increasingly popular in recent years [19]. There are two methods for the development of an inventive solar-powered boat. The first is a hybrid PV-diesel system for large boats, and the second is an entirely PV-based system for small boats. The findings of studies show that both design methods can reduce fuel consumption and gas emissions [20].

1.2.2 Literature study

Simonetti et al. [21] sought to introduce an optimistic control strategy for an indirect vector-controlled induction motor driving a solar-powered boat that has been the subject of nearly 20 years of intensive research. The method revolves around the concept that the boat will follow an optimistic control strategy. This paper demonstrated the accuracy of the method by coupling a trial drive load and performing experiments within the laboratory to determine its accuracy. On the other hand, the results of field tests regarding the performance of solar power and induction motors were insufficient to support the conclusions of the paper. The authors proposed a fuzzy logic controller technique to control the speed and torque of solar-powered boats whose motors were controlled indirectly by vectors in the article. A fuzzy logic-based indirect vector controller was proposed by researchers to improve the efficiency of the system and consequently of the PV boat. There is, however, insufficient information in these studies on how solar power is used, the performance of induction motors, and their environmental effects.

A study by Spagnolo et al. [14] proposed a solar-electric tourist boat that could run pollution-free and had a low operating cost by utilizing advanced management technology to

accept and discharge energy at various times. The proposal included the installation of solar PV arrays, batteries (45 Ah), a catamaran boat, an MPPT controller, a boost converter (DC-DC), an inverter (DC/AC), a charge-discharge controller, and a power management controller. This paper described the design of solar boats to combine an innovative mechanism with an engineering method to create an intelligent design, a safe and trustworthy safety procedure, and a reliable policy.

Through their work, Postiglione et al. [22] introduced a zero-emission electric boat driven by a permanent magnet synchronous motor that was supposed to be used for public transportation and water sports competitions. They introduced two PMSM motors, both of which were rated at 12 kW and included a converter to provide stable DC-bus voltages. Having been designed as a wave-penetrating catamaran, the boat could be charged either at the harbor or using solar panels as part of the charging process. This paper concentrated on boat speed, battery power delivery duration, and motor control procedures, but it did not discuss charge control or motor control procedures.

In their paper, Mahmud et al. [23] examined the development of a small solar boat design that reduced the need for fossil fuels and resulted in minimal environmental pollution. The authors emphasized one limitation of the boats, which was their applicability for a certain distance and weight. The study proposed a solar-powered electric boat for a particular load and distance, but there was no comprehensive design technique available. The lightweight composite material was initially considered when designing the boat. In addition to calculating the boat's dimensions and hydrodynamics, they also calculated its propulsion system, solar panel capacity, and battery bank. However, the control system did not seem to be able to keep the boat moving at the same speed as the number of passengers increased.

In another study, N. A. S. Salleh et al. [24] demonstrated that solar PV and wind energy could be used to charge electric vessels connected to the grid in Kuala Terengganu. Various configurations of wind turbines, solar panels, converters, batteries, and grid power were used in the HOMER software for simulations. According to the findings, the most cost-effective and high-performance configuration was a hybrid grid-PV installation. However, there was

no information available for a solar tracking system capable of giving maximum output power from the system.

Chakraborty et al. [25] introduced a new MPPT-based solar power system that fishing trawlers could use to reduce their fuel consumption. However, there were no data concerning the cost, payback period, or applicability to fishing trawlers.

In Chittagong, Bangladesh, it was examined whether solar power could be utilized to make electricity in a fishing vessel's open area. As part of this survey, 200 fishing trawlers were examined to determine the amount of free roof space, the angle of the solar panels to receive the maximum amount of solar radiation throughout the year, and the amount of power generated by the solar panels. Yet, this paper did not address lifecycle cost analysis or MPPT implementation.

According to Kabir et al. [26], Bangladesh developed a conventional ferry boat into a solar-powered ferry boat capable of transporting 1200 kg of cargo. The boat was constructed out of local wood. The solar panels, motors, and battery storage system were designed, but no detailed information was provided on the total control system, nor was the water drag force used to run the boat discussed. The authors provided a detailed design methodology for solar-powered boats. The boat was converted into a solar-powered boat 6.5 m long with a beam of 2 m and a load capacity of 1200 kg.

In their study, Leung et al. [27] designed a solar-powered boat with zero greenhouse gases. Through modifications to the efficiency of the solar system, they could reduce CO_2 emissions significantly, resulting in an overall reduction in costs and greenhouse gas emissions for the project. The authors also mentioned that the main challenge in improving PV efficiency was to increase the battery capacity and discussed the drawbacks of diesel marine engines as well.

Obaid et al. [28] made an electric boat that used the MPPT system for a hybrid power system with solar and diesel power systems that utilized a three-phase asynchronous power source. They chose the MPPT system, which could maximize the output of the solar array,

to make the electric boat as efficient as possible. Using a neural network, the researchers could also predict how much solar irradiance the electric boat would need to run. This enabled them to plan hybrid power operations to protect the boat during times when there was not enough solar irradiance. They proposed an electric hybrid boat using three renewable energy sources, including a wind turbine that drove an induction generator, a solar PV panel with MPPT, and a polymer electrolyte membrane fuel cell.

As proved by Chao et al. [29], a standalone distributed photovoltaic system was capable of propelling vessels. Several technologies, such as MPPT, power optimization, motor controllers, solar power controllers, battery management systems (BMS), and UART interfaces for onboard control, were used to put the system together. The system was tested at the Love River in Kaohsiung City, Taiwan, where a PV boat was converted into a solar-powered boat and tested. Furthermore, a new solar-powered boat design was introduced using MPPT technology, a power optimizer, and a PV power controller with patented distribution PV power systems.

Ghenai et al. [30] designed a hybrid electric power system to meet the needs of Dubai passengers, combining PV, diesel, and fuel cells. HOMER software was used to configure and simulate a hybrid electric power system for Dubai passenger needs. They demonstrated that the proposed hybrid power system was the most environmentally friendly hybrid power system available, but they did not elaborate on how it would be repaid.

Sharma and Syal [20] examined two ways to make new and different solar boats. The first was a hybrid PV-diesel system for large watercraft, and the other was purely PV-based for small boats. All PV boats are simpler than their hybrid counterparts. Solar boats are one of the promising applications of solar energy. Solar or all-electric boats offer the opportunity to reduce greenhouse gas emissions and switch to renewable and sustainable energy. This article presented the research work done regarding the design for installing solar panels on the boat.

Padwad and Naidu's [31] paper reviews how the technology of FPV (floating photovoltaics) has been used in various projects across the globe. Pontoons or floats are used to keep all the grid-connected systems buoyant, along with solar panels. Various projects around the world have used floating photovoltaics to solve the energy crisis, which is why this paper discusses the technology of floating photovoltaics (FPV). As a grid-connected system, the buoyant pontoons or floats used to connect a grid with the grid are buoyant, on which solar panels are placed to provide electricity to all the systems.

This innovative concept of transparent solar cells using thin-film technology, in a similar concept to the floating solar system, can be applied to the Namami Gange project in India to create green energy power by generating electricity in small villages and towns.

Research conducted by Shahira et al. [16] demonstrated the electrical design of an electric boat powered by solar energy for recreational purposes in Malaysia. As the price of fossil fuels has increased in Malaysia, as have river pollution cases, this research sought to implement electric boats powered by solar energy to help reduce oil spills and pollution. A key challenge for this project was to design a zero-emission recreational boat powered by a photovoltaic panel integrated into the battery. Through their analysis, the researchers could identify the sizes and numbers of the parts required to build the solar boat. These parts included batteries, MPPT charge controllers, and BLDC motors.

This research has selected a catamaran boat, designed according to the shape and dimensions of the hull and the installation location of the solar panels on the roof, while also considering the stability of the boat when choosing the number of solar panels and batteries. In addition to the charge controller, other components, such as solar panels, a battery bank, an inverter, and a DC motor, are also considered. The model is assessed and validated using Simulink assessments.

1.3 INDUSTRIAL MOTIVATION

An all-electric and hybrid boat makes less noise, generates less pollution, and also uses less fossil fuel. Therefore, many companies that make electric motors, batteries, and solar panels have turned their attention to this area [32].

As the maritime logistics industry grows, companies are trying to cut costs by reducing the amount of fuel they use. Because of the interest of large corporations, the market value of electric boats in 2021 was approximately $5 billion and is predicted to reach $16.6 billion by 2031 [33].

In addition, the marine tourism industry has grown significantly in recent years [34]. As a result, recreational and fishing boats of various sizes need a reliable system to travel long distances and reduce costs.

Among the existing electric boats, those with power ranges from 75 kW to 745 kW account for the majority of the market. Also, boats with powers below 75 kW will witness the most significant growth in the coming years [17]. Figure 1 shows the size of the market for electric boats in Europe from 2016 to 2027. As is apparent from the graph, the market size of these boats is growing with a high slope, highlighting the increase and growth of the existing company in this field [35].

The number and market size of companies manufacturing electric boat parts or motors for electric boats have recently increased. These companies are ElectroVoya, General Dynamics, ePropulsion, and Elco. One of the motivations for this research is the increasing growth of the electric boat industry as a potential resource to address the challenges of this field.

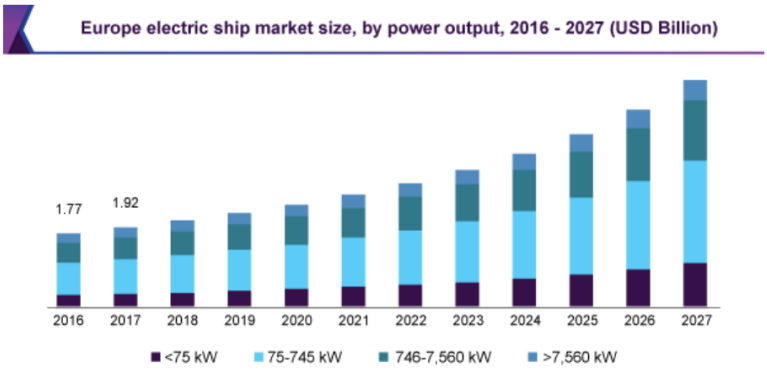

Figure 1. The market size of electric boats in Europe [35].

1.4 BOAT EVALUATION AND STATE OF THE ART

1.4.1 Boat history

The first boats were built around 4000 BC. However, the development and evolution of boats lasted until around the 19th century. Ancient Egyptian papyrus was typically designed for sailing in the Mediterranean's shallow waters, and their design, sail, and oars were used for movement. Figure 2 shows a view of these boats.

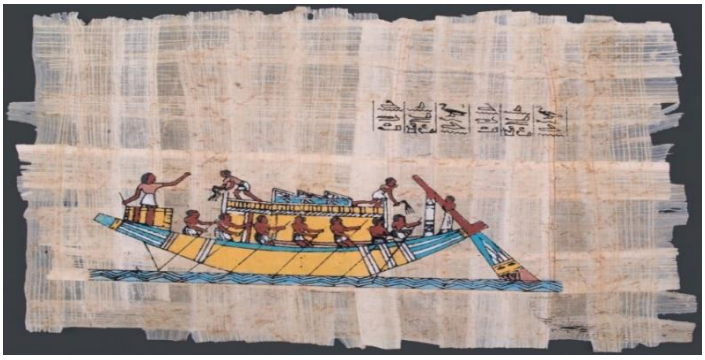

Figure 2. Ancient Egyptian papyrus [36].

The first sea voyages mentioned in the sources were two years long and made by the king of Egypt around 600 BC, when the capabilities of Egyptian boats increased. There were also ancient commercial ships and warships. Warships sought to carry more soldiers at high

speed, for which long and narrow boats were used. On the other hand, the primary purpose of commercial boats was to carry as many products as possible; therefore, the floor space of the boats increased in the design of these boats. Figure 3 shows an example of galley warships [37].

Figure 3. Galley warship [37].

Over time, as sailing boats became famous for traveling longer distances at sea, more complex sail structures were developed, enabling the boats to sail into the wind instead of just being driven by the wind direction. Figure 4 shows an example of these vessels [38]. The structural improvement of these ships continued until around 1500 AD. These ships have square sails.

Figure 4. Square sails [38].

In the 1840s, with the appearance of the first steam-powered ships, the last glorious years of wind-powered ships passed, causing almost all sail-powered ships to disappear. Figure 5 shows a view of boats based on steam engines [39].

Figure 5. Steam ship [39].

1.4.2 Recreational fishing boats

Today, there are various types of fishing boats in a variety of sizes available on the market, which provide different features for a wide range of tastes. In the following, we will introduce some of these boats.

1.4.2.1 Skiff

These boats are made in various models and sizes. Their bodies are usually made of wood, fiberglass, or a combination of the two, and they are mainly known for their shape. Usually, the miniature models do not have a hard top, while a small hard top can be seen in the larger models.

An outboard engine provides the propulsion for these boats. The 162 JLS model has a body length of about 16 feet, can carry about 21 gal of fuel, and has a maximum power of approximately 90 hp. Bigger boats of this model are also available; for example, the body length of the 26 ULTRA ELITE model is about 26 feet. Figure 6 shows 26 Ultra Elite models [40].

Figure 6. Skiff 26 ultra elite model [40].

1.4.2.2 Deck boat

As the name suggests, these boats have a lot of deck space, are usually made of fiberglass, and have a V-shaped hull. The size of these boats varies from 15 to 25 feet and is appropriate for sea sailing. Figure 7 shows a view of these boats. These boats can also reach speeds between 60 and 70 mph, and outboard engines are usually used in their design [41].

Figure 7. Deck boat [41].

1.4.2.3 Bass boat

These boats are suitable for fishing in lakes and rivers, but some models are also designed for open-water fishing. The length of these boats varies from 16 to 26 feet, and the propulsion power of the boat can be provided by an outboard motor and a trolling motor. Figure 8 shows a view of these boats. A model of this boat that works with 150 hp can move at 50 mph [42].

Figure 8. Bass boat [42].

1.4.2.4 Bay boat

These boats, powered by outboard engines, are highly efficient for sailing in bays. The boats range in size from 16 to 28 feet, and the material of the body is aluminum and sometimes fiberglass. These boats handle high speeds well. Figure 9 shows a view of these boats [42].

Figure 9. Bay boat [42].

1.4.2.5 Catamaran

Catamarans are famous for their multihulls, which are similar to each other. Compared to their single-hull counterparts, these boats usually have smaller hulls. Moreover, for long distances, for example, a monohull boat needs to be nearly 30 feet long for a specific volume

of cargo, while a catamaran needs an approximately 40 feet long for a higher speed and the same volume. One or two outboard motors are used, depending on the size of the catamarans. Figure 10 shows a view of these boats [43].

Figure 10. Catamaran boat [43].

1.4.2.6 Convertible

Convertible boats are usually large and suitable for saltwater. The size of these boats varies from 28 to 30 feet, and their hulls can be made of fiberglass, wood, or steel. These boats can use inboard or outboard engines and reach a speed of 30 mph in the ocean. Figure 11 shows a view of these boats [44].

Figure 11. Convertible boat [44].

1.5 EXISTING BOAT ENGINES

1.5.1 Outboard engines

These engines, typically installed in the rear part of the boat, are usually used to power small boats. The height of these motors can be adjusted, and the engine can adjust the boat's direction in addition to providing thrust. These engines can be easily disassembled for engine repairs, which is one of their advantages. The changes in the height of these engines can help them sail in shallow waters near the coast, which can avoid potential damage by raising the engine [45, 46]. Figure 12 shows the different parts of the outboard engine.

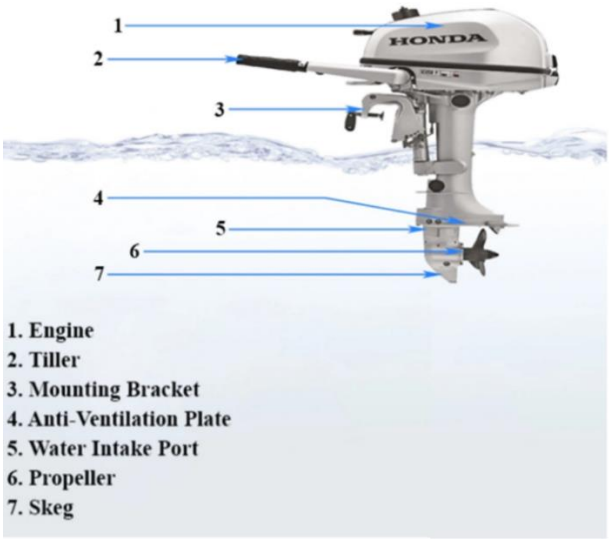

Figure 12. Different parts of the outboard motor [47].

Outboard engines have many advantages. For example, they are easier to put together and take apart compared to inboard engines, and their application and repair are also more straightforward. These engines are also more suitable for shallow waters and have less risk of damage due to the height adjustment feature. Also, these engines can give the boats more speed in shallow waters. In salt water, the engine can be removed from the water, as a result of which the engine life increases, which is not possible with the inboard engines.

Some of the most famous brands of outboard engines are:

- Evinrude Outboards
- Mercury outboard motors
- Minn Kota outboards
- Motorguide outboard motors
- Seven marine outboards
- Torqeedo outboard motors
- Yamaha outboards motors

1.5.2 Inboard engines

Unlike outboard engines, inboard engines are placed inside the boat's hull and are designed in various sizes and capacities depending on the size of the boat. These engines pump lake or bay water into themselves for the cooling process. Figure 13 shows a view of these engines.

Figure 13. Inboard engine [48].

These engines have a relatively more complicated structure compared to outboard ones. The two main parts of these engines are the power head, which is very similar to car engines, and the shaft, which is connected to the blades to provide the thrust of the boat. As shown in Figure 14, there are two main models of engines. In the direct-drive model, the engine is placed in the middle part of the boat and is connected to the thrust generator with a shaft. In V-type models, the motor is placed in the end part and makes a V-shape with the shaft.

In general, inboard engines have a longer lifespan than outboard engines; their repairs are more specialized, and their troubleshooting is more complicated. These engines are also much more efficient in terms of fuel consumption. The engine weight makes the boat more stable and consequently slows it down. These engines enable the boat to carry heavier loads. Important brands of these engines include Nanni, Volvo, and Yanmar.

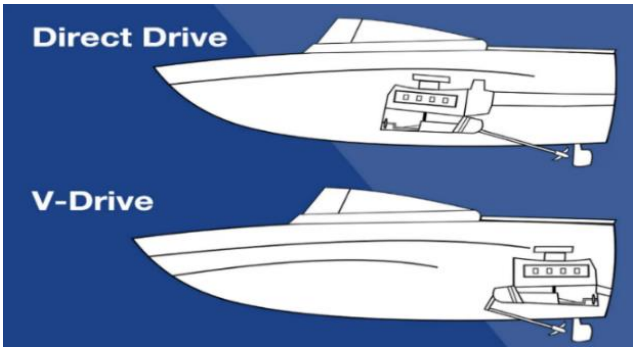

Figure 14. Direct and V-drive inboard engines [49].

1.5.3 Pod motors

In these engines, the engine and accelerator parts are located at the back of the boat and include two main parts. The upper unit and the lower unit control the rotation and orientation of the boat. For example, rotation in the horizontal direction guides the boat back and forth, while circulation in the vertical direction guides the boat on its sides. Figure 15 shows an example of these engines and their placement in the rear part of the boat. Table 2 provides an overview of the advantages and disadvantages of various types of boat engines [50, 51].

Figure 15. Pod motors [52].

Table 2. Advantages and disadvantages of different boat engines [50, 51].

Motor types	Advantages	Disadvantages
Inboard motors	• Excellent fuel efficiency • Quiet operation • Increased longevity – usually beyond 6.000 hours • Superior torque and power	• Less interior space • Higher upfront cost • More expensive maintenance • Significantly more complex repairs
Outboard motors	• Full portability • Far easier maintenance • Simple winterizing procedure and space-saving storage • Significantly lower price • Extra interior space • Higher top speed	• Insufficient torque to drive heavier boats
Electric pod motors	• Quiet, clean, and very efficient • Much better handling, maneuverability, and more thrust in the lower speed range • Cheaper maintenance • Safer than combustion engines • Environmentally friendly • Lower installation cost	• High technical skill required for installation • Drives location outside the boat under the hull

We will introduce the leading brands of electric motors in the market, including inboard, outboard, and pod motors.

Torqeedo: This brand is one of the leading manufacturers of electric motors and lithium batteries and manufactures engines for both inboard and outboard applications. For example, the inboard Deep Blue engine of this brand can produce up to 2500 rpm [53].

Minn Kota: The brand is also a manufacturer of lithium batteries and outboard motors. An example is the E-Drive Electric Outboard model, which works with 48 V and can provide up to 20 hp [54].

Ray: This brand is the premier manufacturer of outboard electric motors for boats and also makes all kinds of electric motors for salty and coastal water. Figure 16 shows the logo and brand names of these companies [55]**.**

Figure 16. Logos of electric motor brands [55].

1.6 EXISTING ELECTRIC BOATS AND ELECTRIC PROPULSION SYSTEMS (WITH SOLAR PANELS)

Today, there are many models of all-electric boats on the market with solar panels, some of which are introduced in this section:

1.6.1 Alfastreet 28 cabin

Different models of this boat are available with outboard engines. However, the interesting point is the existence of electric versions of these boats. The boats are about 28 feet in size and are designed to move at 5 to 6 kn with zero emissions. However, they can move up to the maximum speed of 7 kn. Two 25 kW batteries power this boat, and it is equipped with two 10 kW engines. Figure 17 shows a view of this boat [56].

Figure 17. Alfastreet 28 boat [56].

1.6.2 DutchCraft DC25

This electric boat has electric motors with 89, 112, and 134 kW. The boat is nearly 23 feet long and can travel at a maximum speed of approximately 23 kn in about 75 min. The engine is a 135 kW outboard type. Figure 18 shows a view of this boat [57].

Figure 18. DutchCraft DC25 [57].

1.6.3 SILENT 60

With its 60 feet length, this boat can generate 16 kW of electricity from the sun. This boat is suitable for long distances. It emits zero greenhouse gases and is quiet compared to its diesel counterparts. It can move at a speed of 6 to 8 kn with its 140 kWh batteries. Figure 19 shows a view of this boat [58].

Figure 19. Silent 60 [58].

1.6.4 Aquawatt 550 solar

This boat is 16 feet long and can move at a speed of 6 kn with its 1600 W motors. The boat's body is fiberglass, and the expected amount of greenhouse gases is zero. The average weight is 500 kg, the batteries are of the 24 V type, and the boat can carry four people. Figure 20 shows a view of this boat [59].

Figure 20. Aquawatt 550 solar [59].

CHAPTER 2
DESIGN OF THE ELECTRIC FISHING BOAT

2.1 INTRODUCTION

Global warming and climate change are undoubtedly among the most pressing concerns the world is facing today [60]. Using solar energy is one of the best ways to fight global warming because it does not lead to pollution or greenhouse gas production. Electric propulsion has become increasingly popular for driving boats in recent years [11]. As a result, solar-powered electric boats will be part of clean transportation in the future. The components of an electric boat are a PV array, a DC-DC converter, an MPPT, electric propulsion, and a battery management system. These boats are usually seen in two types, including PV-Diesel Hybrid and Stand-Alone PV systems in the marine transportation industries.

The PV-diesel hybrid system is made up of several parts, such as a PV module, DC-DC converter, MPPT, battery, controllers for charging and discharging, diesel generator, and inverter. In this type of boat, an onboard generator is required to keep charge in the batteries, both for the motor propulsion and those for the appliances. This arrangement makes it easier for the boat to stay at anchor for a long time without needing electricity from shore power or having to sail just to charge the batteries.

Another kind of solar-powered boat only relies on the power of solar PV output panels to supply load demands. This type of structure works best for small ships like cruise ships and fishing boats, only requiring power to run its electric motor to move and turn on some lights [61].

Figure 21 and 22 show the electrical schematics of hybrid and fully electric boats, respectively. A comprehensive analysis of the solar PV boat components and their function will be presented in the next section.

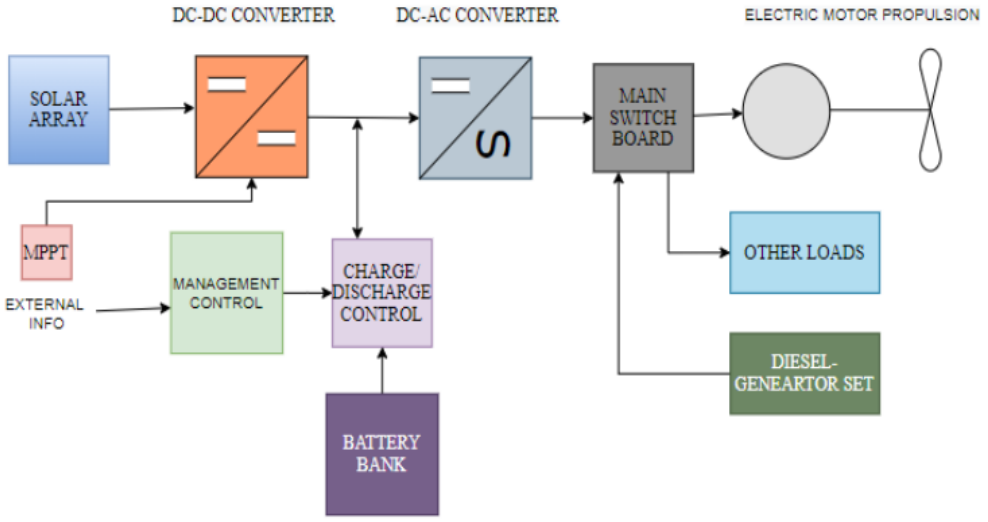

Figure 21. PV-Diesel Hybrid System Topology [20].

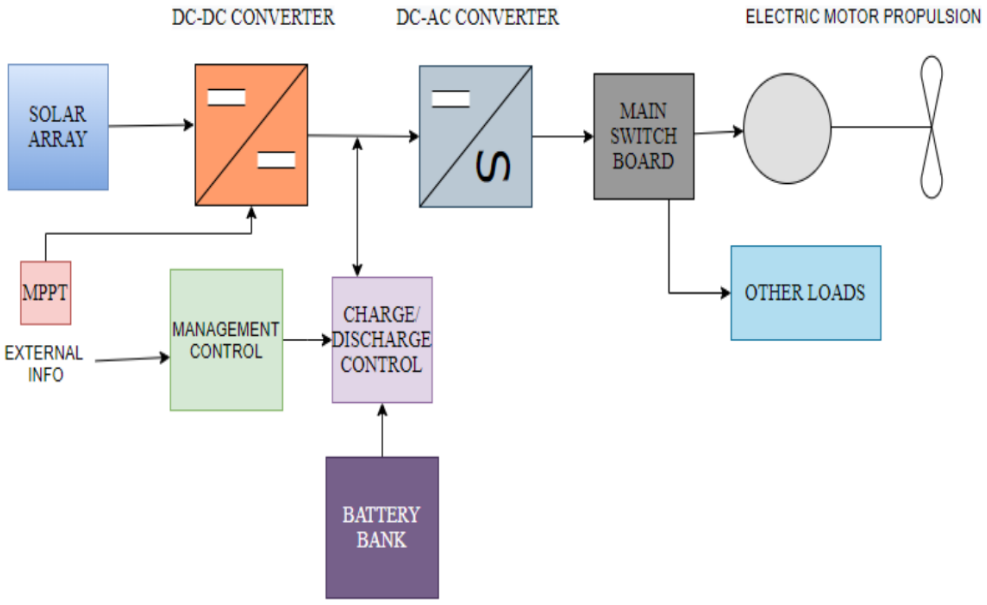

Figure 22. Boat topology with all-electric propulsion [20].

2.2 BASIC ELEMENTS OF A BOAT'S PROPULSION SYSTEM

2.2.1 Motor

2.2.1.1 Motor sizing analysis

A motor with the desired power rating is required to propel a boat. There are several different motors on the market, including DC shunt, brushless DC, and induction motors. Induction motors have limited applications since they require a driver to adjust speed and an inverter (DC to AC) and have also high maintenance costs [62]. Although a DC shunt motor might do the task, there is a chance that it will behave poorly in the field as a result of repeated use. The electric outboard motor is well known for use on a fishing boat [63]. An outboard electric motor from Turqeedo Company has been selected in this thesis to supply the propulsion system. Christoph Ballin and Friedrich Böbel established Torqeedo in Starnberg in 2005 [64]. Torqeedo makes marine electric motors and batteries and exports them worldwide. Torqeedo motors are commonly called torque motors due to their high torque.

Every Torqeedo motor model is synchronous and has a constant speed-to-supply voltage-frequency ratio. Synchronous motors often have torque control, constantly drawing the current required to produce the expected torque at the chosen speed. Hence, they are the preferred choice for use in fields with incredibly demanding torque requirements [65]. If the motor requires more power to keep the propeller spinning, it automatically draws more current. This motor uses a "frequency converter," an electric switching device, to provide the necessary alternating field. No brush loss is created, and the motors are maintenance-free. Additionally, permanent magnets produce the magnetic field. Only recently have significant developments in the manufacture of electronic power components and circuit design made it possible to build these high-performance motors at a low cost [66].

There are four different electric outboard versions of Torqeedo available, including ultralight (1 hp and 3 hp), travel (2 hp and 3 hp), cruise (6 hp and 25 hp), and deep blue (40 hp and 80 hp).

It is necessary to look at a similar boat that weight and measures identically to the boat studied to find out the size of the electric motor that will propel the boat. This boat should run on fuel, so we can analyze fuel motors with different powers and compare them to the electric boat under study to find the correct electric motor size.

The developed electric boat system needs a motor with the same characteristics as fuel-powered boats. Thus, we take advantage of the data of Quicksilver ACTIV boats, which only work with the fuel engine brand Mercury Marine. Two boats, ACTIV 505 and ACTIV 555, with fuel engines from Mercury 40 four-stroke, Mercury 40 Orion, and Mercury 50 four-stroke, have been analyzed. The maximum power allowed for the ACTIV 505 boat is 100 hp, while the ACTIV 555 boat has 115 hp. Table 3 shows the maximum speed for two boats, Activ 505 and Activ 555, with different fuel engines.

Table 3. Speed test results [67].

BOAT	ENGINE	HP (kW)	CRUISE SPEED (kn)	MAXIMUM SPEED (kn)
ACTIV 505	Mercury 40 Four Stroke	40 (29.83)	15.9	23.1
	Mercury 40 Orion	40 (29.83)	16.5	22.9
	Mercury 50 Four Stroke	50 (37.285)	17.9	25.8
ACTIV 555	Mercury 40 Orion	40 (37.285)	13.1	19.6
	Mercury 50 Four Stroke	50 (37.285)	15.1	23.7

According to the speed characteristics of the studied boat, the maximum speed for this thesis is 8 kn; a comparison of this speed with the data in the table above for similar boats shows that the Deep Blue model engines are not a good choice for this project. Therefore, it

is essential to choose a motor with power below 40.0 hp, necessitating the search between Cruise engines. Table 4 indicates the specifications of Turqeedo's cruise motors. The letters T and R on the table stand for the tiller throttle and remote throttle, respectively.

Table 4. Summary of Cruise motor specifications [68].

TECHNICAL DATA	**CRUISE 3.0 T/R**	**CRUISE 6.0 T/R**	**CRUISE 10.0 T**	**CRUISE 12.0 T/R**
Input power in W	3.000	6.000	10.000	12.000
Propulsive Power in W	1.530	3.504	5.600	6.720
Comparable petrol outboard (shaft power)	6 HP	9.9 HP	20 HP	25 HP
Comparable petrol outboard (thrust)	8 HP	15 HP	25 HP	25 HP
Maximum overall efficiency in %	51	58	56	56
Static thrust in lbs*	142	230	Up to 405	405
Nominal voltage in V	24	48	48	48
Total weight in kg	T:19.7 (S)/20.2 (L) R:18.9 (S)/19.4 (L)	T:21.3 (S)/21.8 (L) R:20.6 (S)/21.0 (L)	T:60.3 (S)/61.8 (L) /63.0 (XL) R:59.8 (S)/61.3 (L) /62.5 (XL)	59.8 (S)/61.3 (L) /62.5 (XL)
Shaft length in cm	62.5 (S)/75.5 (L)	62.5 (S)/75.5 (L)	38.5 (S)/51.2(L) /63.9 (XL)	38.5 (S)/51.2 (L) /63.9 (XL)

The motor's consumption and speed are examined to discover which of the three types of electric cruise motors (10.0 hp, 20.0 hp, and 25.0 hp) is best for the system's development. All cruising motors are electric outboards with a built-in GPS and an internal computer that shows speed, input power, the status of the battery, and the power left.

Cruises 3.0 and 6.0 are suitable for boats up to 3000 and 6000 kg, respectively, and cruises 10.0 and 12.0 are for boats up to 10000 kg. Furthermore, according to the product data table, the speed of each cruise engine (6.0, 10.0, and 12.0) in full-throttle mode will be

14.0 km/h, 26.5 km/h, and 28.3 km/h, respectively. Therefore, according to the speed range considered in this thesis, the cruise 10.0 and 12.0 motors are good choices. The latter is preferred because it includes a remote and tiller throttle, while the former has only introduced a tiller throttle recently. Table 5 displays the motor parameters for the Cruise 12.0 model.

Table 5. Electrical and mechanical data for Cruise 12.0 [69].

Model	**Cruise 12.0 R**
Continuous input power	12 kW continuous power 6 kW when using 1x power 48-5000
Rated Voltage	48 V
Nominal Shaft Power	10.2 kW
Weight (motor with propeller and cable set up to battery)	67.0 kg (RS),69.0 kg (RL), 70 kg (RXL)
Shaft length	38.5 kg (RS), 51.2 cm (RL), 63.9 cm (RXL)
Propeller rotational speed at max. Rotational speed	1400 rpm

Letters S, L, and XL refer to the length of the motor shaft and represent the words "short," "long," and "extra long." Also, Table 6 shows the engine's running time at different speeds (assuming the use of two Power 48-5000 batteries from the Torqeedo Company). Again, these values depend on the type of boat, load, propeller, and conditions.

Table 6. Motor speed, range, and performance for Cruise 12.0 [70].

Cruise 12.0 R With 2x Power 48-5000 (Battery)	
Speed in km/h	**Running time in hh:mm**
27.0 km/h	00:30
12.0 km/h	03:00
7.5 km/h	09:00

2.2.1.2 Overview of components

The motor body is made of high-grade, seawater-proof aluminum for long service life. It also has full protection against galvanic corrosion, accomplished by carefully combining and isolating materials with various electrochemical properties. Figure 23 shows other parts related to the cruise 12.0 motor body.

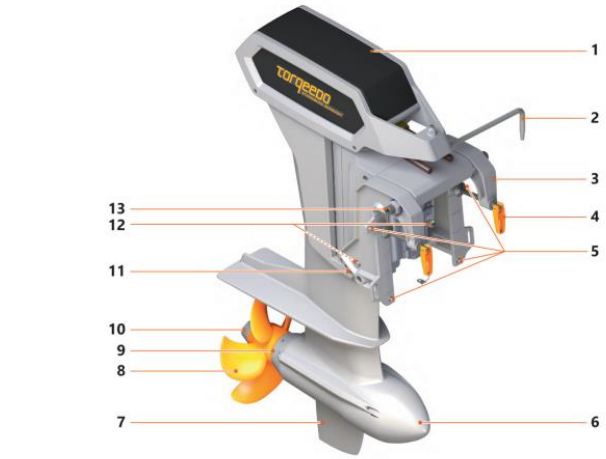

1	GPS receiver in the motor head	**8**	Propeller
2	Jointed rod	**9**	Half ring anodes
3	Transom bracket	**10**	Shaft galvanic anode
4	Transom clamp bolt	**11**	Trim rod (for fixing the indexing position of the motor)
5	Drill hole Ø 12 mm	**12**	Ring anodes on transom bracket
6	Pylon	**13**	Steering tube
7	Fin		

Figure 23. The outer mechanical part of Cruise 12.0 [69].

2.2.1.3 Motor electricity autonomous speed

The propulsion power needed for a boat to move across water increases based on the speed's cube. Accordingly, eight times as much power is required to double the speed [71, 72]. This assumption has been used to determine instantaneous power at various speeds, as indicated in Table 7. Torqeedo's range information allows for the computation of the maximum instantaneous power (27.0 kn). According to Torqeedo, a pair of batteries with a

maximum capacity of 10 kWh can operate at full speed for up to an hour. The second and third rows of the table have been computed using this information as a starting point and the explained assumption.

Table 7. Speed vs. Power points.

	BOAT SPEED (knots)	**INSTANTANEOUS POWER (kw)**
1	13.5	12.3
2	6.75	1.53
3	3.37	0.19
4	0	0

Figure 24 can be obtained by plotting these points. The graphic's Y and X axes represent instantaneous power and speed, respectively. The points' Equation and regression line have been also obtained. An analysis of the resulting Equation leads to the two viscous friction coefficients ($0.005 \cdot speed^3$) and dry friction (0.0012 speed). Other coefficients are not significant. Equation 1 can be used to determine the autonomous speed of the studied boat .

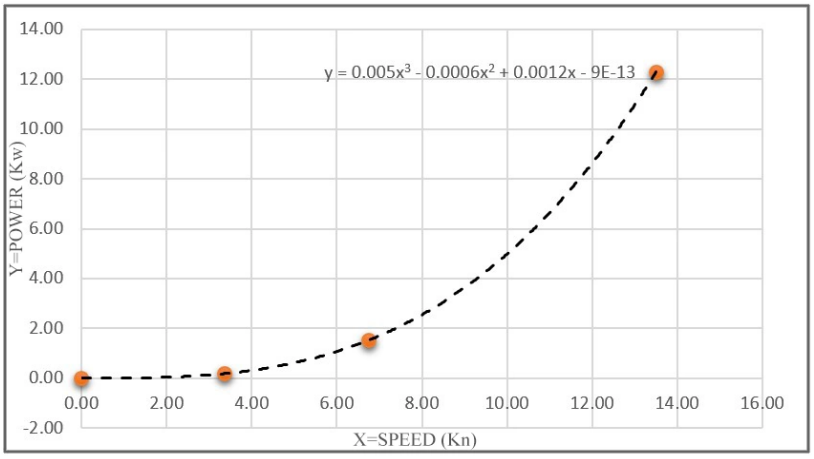

Figure 24. Speed (kn) vs Power (kw).

$$Power(kw) = 0.005(speed)^3 - 0.0006(speed)^2 + 0.0012(speed) - 9\times 10^{-13} \quad \textit{(Eq. 1)}$$

Taking into account the solar panels used (see Section 2.4.2), the solar modules can provide up to 990 W of power (110 W each). The efficiency of these solar panels will not be 100%. The calculation has been performed with the highest efficiency (100%) and a more reasonable efficiency (80%). The weather in the area where the boat is sailing affects its efficiency. Considering a solar panel efficiency of 100%, the maximum autonomous speed is 5.8 knots (Equation 2). Instead, assuming an efficiency of 80% for the solar panels, the actual autonomous speed (Equation 3) is 5.3 knots.

$$\text{Power} = 0.005(\text{speed})^3 - 0.0006(\text{speed})^2 + 0.0012(\text{speed}) - 9\times 10^{-13}$$

$$= (\quad). 1 = 0.990\ (\text{kw}) \rightarrow \text{speed} = 5.803\ \text{kn} \qquad \textit{(Eq. 2)}$$

$$\text{Power} = 0.005(\text{speed})^3 - 0.0006(\text{speed})^2 + 0.0012(\text{speed}) - 9\times 10^{-13}$$

$$= (\quad). 0.8 = 0.792\ (\text{kw}) \rightarrow \text{speed} = 5.385\ \text{kn} \qquad \textit{(Eq. 3)}$$

2.2.1.4 Motor electricity consumption

Considering the conditions for the boat studied in this thesis, the boat moves at 8 knots for one hour every day. In addition, the boat will spend about 6 to 7 hours with the engine off or at the minimum speed at the fishing location during each voyage. The maker's website provides performance data for the Cruise 12.0 R engine, as shown in Table 8, for various engine speeds, ranges, and powers. These data were obtained for a very light boat sailing in fresh water with a wind velocity of 8.5 km/h and two batteries with a total capacity of 10.0 kWh.

Table 8. Data for different powers from the Cruise 12.0 motor [73].

Input Power (W)	Speed (km/h)	Range (km)
500	5.0	100.0
1000	5.9	59.0
2000	8.0	40.0
3000	9.1	30.0
4000	9.8	23.3
5000	10.0	20.0
6000	10.6	17.7
7000	12.7	18.1
8000	16.2	20.3
8700	20.0	23.3
9400	23.0	24.5
10700	26.0	24.3
12300	28.3	23.0

Based on this information and Equation 1, the boat's motor is estimated to use an average of 7.5 kW of power per day at a speed of 8 kn, requiring between 500 W and 1 kW at the slowest speed. Finally, for 8 hours of daily boat activity in each daily voyage, the power consumption of the engine will equal 14.5 kW to provide top speed and fishing speed for the boat. The time duration for a boat sailing on fresh water is about 8 hours. Table 9 shows details of propulsion component calculations at top speed and fishing speed.

Table 9. Load profile.

S/N	COMPONENTS	QTY	POWER (WATT)	Hours of use per day	Energy per day (Wh)
1	Motor (up) Motor (down)	1	7.5×10^3 7×10^3	8	14.5×10^3
2	Lighting	5	20	4	400
3	Water Pump	1	350	1	350
4	Bilge Pump	2	30	1	60
5	Navigation Panel	2	8	8	128
6	Control Panel	1	5	8	40
7	Refrigrator	2	60	8	960

Table 10 indicates the estimated loads for all appliances on board.

Table 10. The power needed for a daily voyage.

Condition	Total Consumed Power
Maximum Speed (1 hour)	7.5 kW
Fishing (6-7 hours)	7.0 kW
Electrical/ Mechanical appliances	2.0 kW
Total	16.5 kW

The power needed to safely move the boat increases by adding 5% more P. Therefore, the daily energy requirement is 17.325 kWh. As a result, the load profile for the boat is 17325 Wh per day, which will be used to calculate the PV and battery power systems.

2.2.1.5 Throttle controller

The throttle controller contributes primarily to controlling the propeller's rotational speed and direction. Depending on the position of the lever, the throttle adjusts the power of the electric motor to increase the speed, keep the speed constant, or decrease it. The engine manufacturer advises using the throttle controller in Figure 25.

This throttle provides complete control for the selected cruise motor and has a colorful, clear, and bright screen. With the touch of a button, the system's necessary data will be shown, including built-in Bluetooth for simple mobile phone connectivity. This throttle display system represents a lot of information, such as speed, energy use, battery capacity, charging rate, and time left to charge.

Figure 25. Torqeedo throttle controller [74].

There are several advantages to using this throttle, including:

- Appropriate for an outboard motor with an input power of 12.0 kW or 25.0 HP.
- Effective efficiency in terms of runtime and range when using a Power 48-5000 battery.
- Compatible with different 48- V batteries.
- Marine weatherproof aluminium with the best lifetime, even in the most challenging environments.

2.3 BATTERIES

A battery uses an electrochemical oxidation-reduction (redox) reaction to convert the chemical energy in active materials directly into electric energy. In this reaction, electrons are transferred from one substance to another through an electrical circuit. Although the term battery is often used, a cell is an electrochemical entity utilized to generate or store electrical energy [75, 76].

Two of the essential components of the design are solar panels and batteries. Since solar power cannot support the load at night or in cloudy or wet conditions, the batteries must be able to run continuously for several hours. Since challenges may occur if electric propulsion stops operating mid-trip due to solar PVs not receiving enough sunlight to provide electricity, the battery serves as the main power source for this project. The boat's load supply

will be maintained throughout the voyage with the aid of the battery. There are typically two types of batteries based on whether they can be charged or not [77].

A type of battery that gives a small current for a long cycle is needed to store solar energy. Batteries that work in boats are classified based on their lead-acid, nickel-cadmium, and lithium-ion chemical compositions. In terms of battery capacity, power, and rate of discharge, lithium-ion batteries are the most preferred batteries nowadays [78, 79].

2.3.1 Battery types

2.3.1.1 Lead acid batteries

French physicist Gaston Planté invented the lead-acid (Pb-A) battery in 1859 [80]. In general, these batteries have a low DOD, a shorter lifecycle, and lower costs than other kinds of batteries. In a typical Pb-A battery cell, the anode and cathode are made of Pb and PbO_2, respectively. Sulfuric acid is used as the electrolyte [81]. During complete reversible charge/discharge reactions, lead and lead peroxide are converted into lead sulphate ($PbSO_4$). The oxygen created on the positive plates of lead-acid batteries is taken in by the negative plates located on the other side of the battery. In response, the negative plates generate water, facilitating the dissipation of heat generated by the electrolytes' chemical reaction. The user does not need to add water to these batteries, making them maintenance-free [82].

Lead-acid batteries lose useful capacity at high discharge rates, which is a major drawback. If a battery is completely drained in an hour, for instance, only roughly 50%–70% of its rated capacity will be used. There are other disadvantages, such as lower energy density and the usage of lead, a dangerous substance regulated or banned in some areas. The benefits include low initial investment, ease of use, and simple charging technology [83, 84].

Three primary lead-acid batteries are flooded, absorbed glass mat batteries (AGM), and gel batteries. Both AGM and GEL batteries belong to the class of valve-regulated lead-acid (VRLA) batteries. AGM batteries utilize a unique glass mat comprised of thin glass fibers. This absorbs the electrolytes between the battery plates. Gel batteries, on the other hand, use

a unique sort of silica gel that absorbs electrolytes. The material's thick consistency allows electrons to flow easily from the plates. Gel batteries often lose power more quickly than AGM batteries, particularly at lower temperatures, which is attributed to the battery's gelled thixotropic nature. AGM batteries work in bad weather, which makes them good for vehicles like snowmobiles that need a lot of power in the winter. When it comes to Depth of Discharge (DoD), Gel batteries use acid more effectively than AGM batteries [85].

Acid protects the plates of Gel batteries, making them more suitable for deep-discharge applications. However, Gel batteries must be recharged properly to avoid early failure. In terms of durability, lifespan, and charging, AGM batteries outsell gel types. They are also less costly and more useful in a wide range of climates [86]. In comparison to AGM batteries, gel batteries have a lower leakage percentage because of their gelled composition.

2.3.1.2 Nickel-cadmium batteries (Ni-Cd)

Waldemar Jungner, a Swedish engineer, patented the nickel-cadmium battery system in 1899 [87]. Metallic cadmium and nickel hydroxide are employed as an anode and cathode, respectively, in an aqueous alkali solution such as potassium hydroxide (KOH) as an electrolyte. A three-layer porous polymeric separator, typically composed of nylon, polypropylene, and nylon layers, separates the anode and cathode [88]. The most important advantage of the nickel–cadmium batteries is the delivery of nominal capacity even at high discharge rates. Although these batteries have a higher price than lead-acid batteries, they show a higher depth of discharge. For years, NiCd was the preferred battery for two-way radios, emergency medical equipment, and professional video cameras [89].

2.3.1.3 Lithium-ion batteries

Lithium batteries are the latest in marine battery technology. In portable electronics and medical equipment, lithium-ion batteries provide excellent results [90]. Since they are much lighter than other options, hold a charge better, and can handle more charge/discharge cycles than traditional marine batteries. The portable electronic sectors are the primary

consumers of Li-ion batteries at the moment, where their excellent properties, such as low maintenance, excellent cyclability, high voltage, low self-discharge, and very high specific energy, have led to the displacement of nickel-based battery systems (Ni-Cd and NiMH), which previously dominated the battery market. In addition, Li-ion batteries are increasingly used in several fields, including military, aerospace, and electric and hybrid vehicles (EVs and HEVs) [91]. Figure 26 shows the discharge process of a lithium battery.

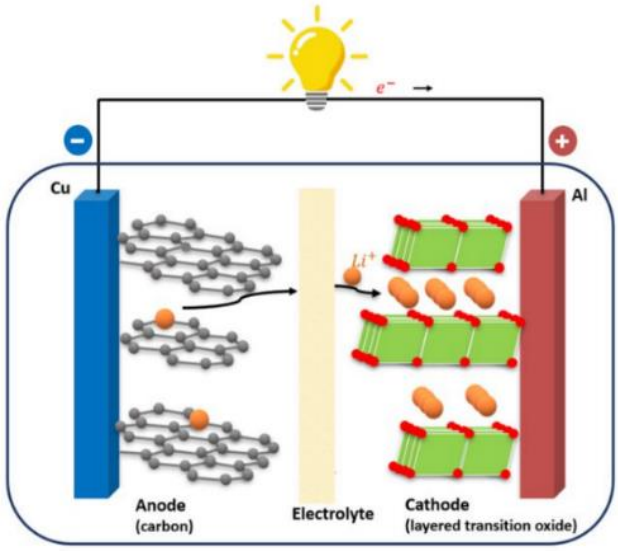

Figure 26. Schematic illustration of a lithium-ion battery under discharge [92].

A lithium-ion cell's positive and negative electrodes are often made of metal oxide and carbon, respectively. Of all metals, lithium is the lightest, offering the most specific energy per weight and showing the most significant electrochemical potential. However, this battery technology does have certain limitations. Lithium-ion batteries have an approximate lifetime of 3000 cycles at 80% depth of discharge. The temperature impacts life cycles, and heavy discharges would significantly reduce them. In addition, lithium-ion batteries need complex management systems and protection circuits to make sure they work safely [93].

2.3.2 Batteries brief review

Table 11 provides a summary of the advantages and disadvantages of rechargeable batteries.

Table 11. Advantages and disadvantages of different rechargable battery systems [92, 94].

Battery Type	Advantages	Disadvantages
Lead-acid	i) Mature technology ii) World-wide production iii) Low material cost iv) No memory effect v) Low self-discharge rate vi) Relatively low capital cost	i) Short life cycle ii) Modest energy/power density iii) Long charging time iv) Safety issues (gas discharge) v) Temperature-sensitive output vi) Poor reliability
Lithium-ion (Li-ion)	i) Long life cycle ii) High round trip efficiency iii) Global R&D efforts iv) Relatively fast charging v) Highly reliable vi) Low discharge rates vii) Excellent energy/power density	i) High capital cost ii) Safety issues (thermal runaway) iii) Toxic materials iv) Poor recovery/recycling v) Advanced battery management systems required
Nickel metal hydride (NiMH)	i) Modest initial cost ii) Acceptable energy/power density iii) Modest round-trip efficiency iv) Highly reliable v) Excellent safety record vi) Relatively fast charging vii) Eco-friendly materials viii) Low operational maintenance	i) Higher self-discharge rate ii) Memory effect iii) Relatively short life cycle iv) Poor recovery/recycling
Nickel-cadmium (Ni-Cd)	i) Comparatively low capital cost ii) Highly reliable iii) Mature technology iv) Superb safety record v) Wide operating temperatures vi) Relatively fast recharge vii) Excellent life cycle viii) Low operational maintenance	i) Modest energy/power density ii) Memory effect iii) Relatively poor round trip efficiency iv)Reliance on hazardous cadmium

2.3.3 Battery technology in marine applications

The batteries used on ships must be able to handle the harsh environment and work well in an emergency. A regular flooded lead-acid battery cannot stand up to the constant pounding and shaking of the waves. In this case, the sulfuric acid electrolyte in a flooded battery could completely evaporate, disrupting the function of the battery. High vibration and overturning can potentially loosen the battery cap, leading to venting holes that allow gases to escape [95].

Lead-acid batteries have been the standard way for marine vehicles to store energy for more than a century. They can power the main engine or contribute as a backup source. Yet, there is still a need for more powerful batteries since, for instance, submarines need to travel farther and quicker, which is impossible with the available batteries. A new generation of lithium-ion battery-based energy storage technology is necessary (LIBs). Lithium-ion batteries could change the way boats and ships work by becoming the main power source for torpedoes, unmanned underwater vehicles (UUVs), and submarines. LIBs are already used in exercise torpedoes and some UUVs, but the technology is still young compared to lead-acid batteries, which were made in the late 19^{th} century [96, 97].

However, LIBs are more effective and reliable than their lead-acid equivalents because of their small size. All-electric and hybrid ships could save a lot of money on fuel, maintenance, and pollution if they stored energy in huge Li-ion batteries. They would also be more responsive, reliable, and safe. The battery is a crucial component of the power system on all hybrid ships. Still, it will typically be a secondary source for the main engines [96].

2.3.4 Battery selection

As mentioned, lithium-ion batteries are the most common for electric vehicles.

These batteries with high energy density and long cycle lives are the primary choice for use in electric vehicles such as the boat of this project. Battery capacity has been calculated by the following Equation (Eq.4) [98]:

$$Ah = \frac{(P)\times(No\ charging\ days)\times(hours)}{(DoD\ [\%])\times(Voltage\ [V])} \qquad \textit{(Eq. 4)}$$

Where,

- P: Required power in W.
- Ah: Battery capacity.
- DoD: Depth of Discharge (%).
- V: Battery voltage in V.

$$Ah = \frac{(17300)\times(1)}{(1)\times(44.4)} = 389.6 \qquad \textit{(Eq. 5)}$$

Power (W) in total for 7-8 hours of running is 17.3 kW. The above Equation is for the case where we have the total power value separately and multiply it by the hours of activity. As the total power consumed during all activity hours is determined, there is no need to put power and hours separately in the formula, and we directly enter the total energy consumed daily. We consider the days when the battery is not charged as one day because we can charge the battery at the dock at the end of the day.

We consider the battery voltage to be 44.4 V and suppose the weather is cloudy during the voyage, making it impossible to use the solar panel. We also consider the capacity in the case when the battery is completely discharged (DoD = 100%). The total capacity of the required batteries (as a pack) for these conditions will be 389.6 Ah. As mentioned in the motor description section, the most suitable battery for the throttle controller and motor set is the Power 48-5000 battery from Torqeedo. The power of one of these batteries is 5000 Wh, and its rated voltage is 44.4 V. As a result, the capacity of a battery in Ah is equal to 112.6 Ah. If four of these batteries are connected in parallel, the total capacity will be slightly more than 450 Ah.

Thus, this battery's four-number parallel pack seems to meet the project boat's requirements. The battery catalogue states that these batteries should never be connected in series. Figure 27 and Table 12 present the Torqeedo Power 48-5000 battery and a summary of its specifications.

Figure 27. Torqeedo Power 48-5000 Battery [99].

Table 12. Specifications of the selected battery [100].

Property	**Value**
Rated voltage	44.4 V
Final charging voltage	50 V
Final discharging voltage	36 V
Maximum voltage at the terminals	50 V
Maximum discharge current	200 A
Ambient temperature, storage	-25 °C to +60 °C
Nominal energy	5275 Wh
Usable energy	5000 Wh

2.4 SOLAR PANEL

2.4.1 Types of solar panels

A solar panel produces energy by allowing photons, or light particles, to knock electrons away from atoms. Solar panels comprise multiple smaller components called photovoltaic cells, which convert sunlight into electrical energy. A solar panel is made of numerous interconnected cells, each representing a sandwich made of two semiconducting material slices [101]. Silicon, the same material used in microelectronics, is commonly used to manufacture solar cells. With this energy and using the existing electric field, this electron moves in a specific direction and with more freedom than before, creating an electric current. Figure 28 indicates the function of the solar cell [102].

It is commonly believed that solar energy is limited to sunny locations. Contrary to what most people think, solar cells can harvest energy even when the sky is overcast, but they do not absorb as much energy. Currently, a lot of research has been conducted on solar energy, leading to the discovery of many new technologies. In recent years, new flexible and lightweight solar panels have been developed that will significantly facilitate the construction of a solar-powered boat [19]. Nowadays, three kinds of photovoltaic cell technologies are leading globally, whose types in constructing electric boats are evaluated in the following [103].

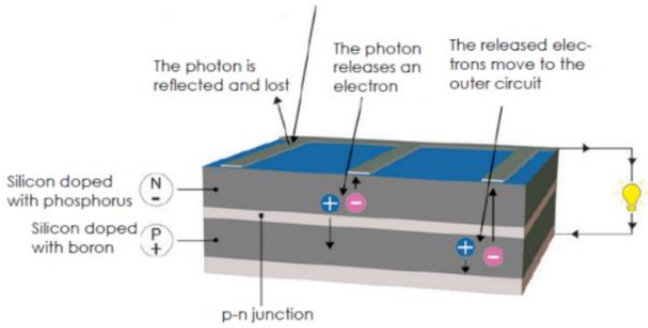

Figure 28. Solar cell functioning [104].

2.4.1.1 Monocrystalline silicon cell

The monocrystalline silicon cell is constructed of pure monocrystalline silicon, which forms a single uniform crystal structure [105]. These cells were also the world's first commercially launched solar cells. This form of the cell is beneficial, but the manufacturing process is slow. It is more expensive than polycrystalline silicon and thin-film cells. Monocrystalline solar panels are among the most widely used types with the highest efficiency, averaging 24%, and a longer average lifespan than other solar panels, ranging from 25 to 40 years [106, 107]. Figure 29 reveals the monocrystalline silicon cell.

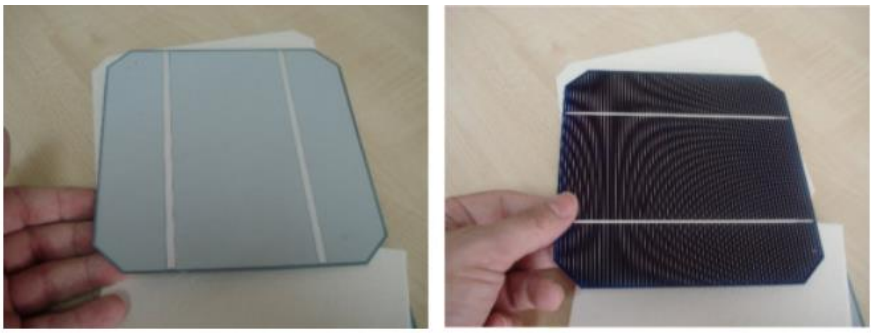

Figure 29. Monocrystalline silicon Cell [108].

2.4.1.2 Polycrystalline silicon cell

Polycrystalline solar panels are made from multiple silicon crystals instead of one. The silicon fragments are melted and poured into a mold, leading to little waste in producing polycrystalline solar cells. Even though polycrystalline silicon PV cells are less efficient but cheaper, they make up about 70% of global PV production and helped lead the world PV cell market in 2015 [109]. The polycrystalline structure consists of several tiny crystal particles, as shown in Figure 30.

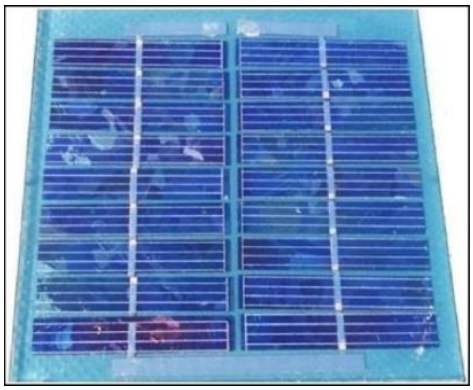

Figure 30. Polycrystalline silicon solar cell [110].

2.4.1.3 Thin-film panels

Thin-film panels are a newer type of solar panel, less commonly used than monocrystalline and polycrystalline. Thin-film PV cells are made from copper indium gallium diselenide (CIGS) and cadmium telluride (CdTe), which improve efficiency more than a-Si [111]. The photovoltaic cells made from a thin film, such as amorphous silicon (a-Si), are incredibly flexible and viable but have a higher manufacturing cost, with an average efficiency of 19% and a lifespan of 10 to 20 years [112]. Figure 31 shows a thin-film panel.

Figure 31. Thin-Film Panel [113].

2.4.2 Selection of solar panels

Solar panels serve as a backup source of power for the boat, ensuring that the batteries' voltage does not drop and the system's working voltage is kept steady. According to battery choice, the battery bank will supply all motor power.

The selected battery can also provide power to other equipment, but if we can get part of this power from solar panels, we can ensure safety to a large extent.

According to Table 8, this boat's equipment will use approximately 2 kWh over an 8 hours operation, regardless of motor consumption. As a result, we have to choose the panels to provide this energy for 8 hours. The SunPower SPR-E-Flex-110 solar panel is a good choice for this purpose and is often found on boats. Each panel has 36 cells in 9 rows of four, as shown in Figure 32.

Figure 32. SunPower SPR-E-Flex-110 [114].

These panels are light and suitable for a boat because they are flexible. The maximum power that a panel produces in 7 hours is equal to 770 W with a maximum voltage of 18.8 V. If solar panels are connected in parallel, the current and the amount of power produced will increase, while if they are connected in series, the voltage and output power will increase.

2.4.2.1 Weight and dimensions

Table 13 provides a brief specification of the PV panel, indicating that the dimensions of each panel are 1165×556×20 mm, and the weight of each solar panel is 2 kg. Each panel can deliver a maximum of 110 W. These 9 panels will occupy an area of approximately 350.0

x 167.0 cm. Since the dimensions of the boat are 23 by 8 feet (701.04 by 243.8 cm), there will be no problem placing these panels on the boat.

Table 13. Specifications of the selected solar panel [114].

Typical Data	
Model	**SPR-E-Flex-110**
Nominal Power (Pnom)	110 W
Rated Voltage (Vmpp)	18.8 V
Rated Current (Impp)	5.9 V
Open-circuit voltage (Voc)	22.8 V
Short-curcuit current (Isc)	6.3 V
Max. System Voltage	45 V
Series Fuse Rating	15 A
Solar Cell	Prime monocrystalline
	25 % and 23 % efficiency SunPower IBS cell
Cables	4 mm^2, 12 AWG
Weight	2 kg
Panel Dimensions mm with Jbox,	1165× 556×20
	2 mm w/o Jbox

2.4.2.2 Solar panel connection type

Output voltage and current are the main differences between series and parallel solar panel wiring. The panels in a series connection add the output voltage and maintain the current, while the parallel connection of the solar panels adds the output current but maintains the voltage, making parallel solar arrays ideal for low-voltage systems [115]. Since wiring several solar panels in parallel does not change the total output voltage, the solar panels are not dependent on each other, which means if one of the panels is shaded or breaks, the rest of the panels will still work as expected [116]. On the other hand, the total voltage output of an array wired in parallel is lower than in series, making the reduction of solar array voltage to battery charge voltage more efficient and resulting in more power storage in the battery.

Thus, if nine parallel panels are placed, 6930 Wh of energy will be produced in 7-8 hours (at rated power). In the autonomous speed calculation section, 80% of the panels' power

was used to calculate this speed because it was practically impossible to produce their rated power. As a result, if we assume an efficiency of about 80%, the panels will produce nearly 5500 Wh of energy. Figure 33 illustrates various connections between the solar panels.

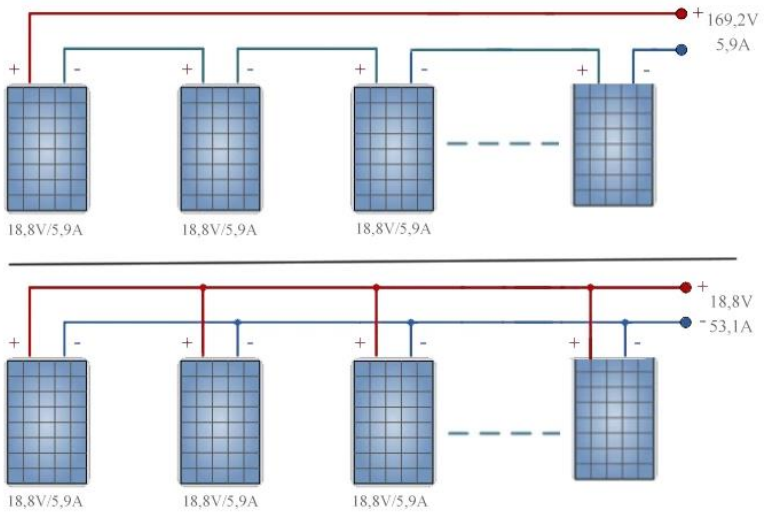

Figure 33. Schematic of series and parallel connected PV modules.

2.5 WEIGHT COMPARISON BETWEEN FUEL AND ELECTRIC PROPULSION SYSTEM

This section compares the weight of the proposed electric propulsion system with the weight of the fuel propulsion components.

2.5.1 Main fuel propulsion components' weight

Fuel outboard**:** A 2- or 4-stroke diesel engine from Mercury or Yamaha with 75 to 90 hp of power can compete with the speed and range of the suggested electric engine. On average, fuel outboards that may provide comparable advantages and are permitted for these boats weigh between 1569.69 and 1667.7 N (160 and 170 kg). As can be seen in Figure 34, a 15–18 gal (56–68 litre) tank capacity is typically used in these cases. Thus, the weight of 56–68 litres of gasoline is 372.5–452.2 N (37.98–46.1 kg), which is added to the nearly 196.2 N weight of the boat's tank (20 kg). Consequently, the total weight of the fuel propulsion components is approximately 2315.16 N (236 kg) [117, 118].

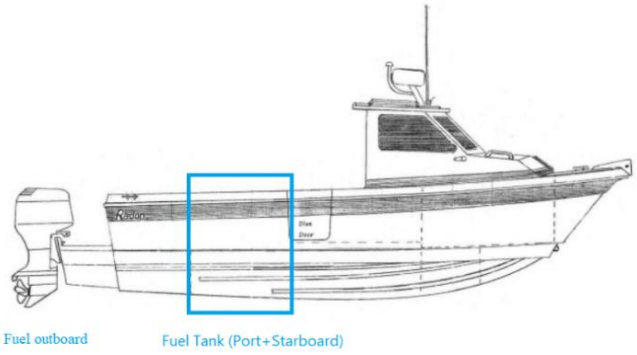

Figure 34. Schematic of fuel propulsion components.

2.5.2 Main electric propulsion components' weight

Electric outboard**:** According to Section 2.2.1.1, the suggested electric motor weighs 613.1 N (62.5 kg).

The suggested batteries weigh 1432.26 N, as mentioned in Section 2.3.4 (146 kg). Each solar panel weighs 19.62 N (2 kg), and the nine solar panels that are part of the propulsion system weigh a total of 176.58 N (18 kg). As a consequence, the overall weight of the electric propulsion system is 404.7 N (228.5 kg). The weight of the electrical system compared to the fuel engine is less, and the system will not have any problems in this regard.

2.6 APPROXIMATED AUTONOMY OF THE ELECTRIC PROPULSION SYSTEM

After selecting the necessary components, an approximation of the boat's autonomy has been determined. In this section, the battery capacity (20 kWh) and the electric motor's power consumption (Equation 1 and Figure 24) are connected. Figure 35 displays the autonomy in hours by the instantaneous speed, calculated using these data. Since solar energy might fluctuate or be unavailable (at night, for instance), the electricity generated by solar panels is excluded from this estimate of autonomy.

Figure 35 shows that the power used at low speeds is very low. Thus, the autonomy is relatively high at low speeds (more than 12 hours at speeds lower than 7 kn). At a speed of

23 kn, the boat's autonomy is reduced to 20 min. Table 14 displays the number of hours of autonomy for various speeds and powers.

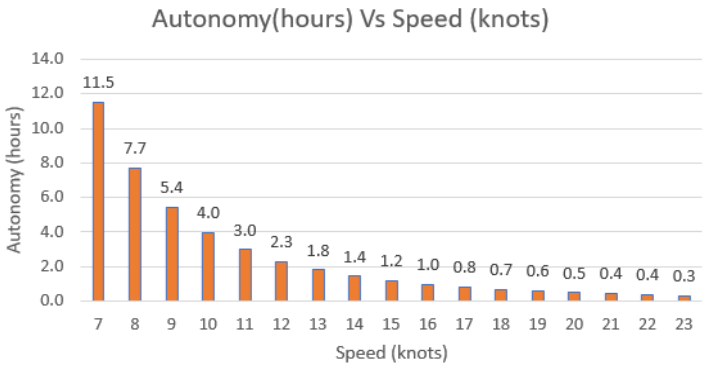

Figure 35. Autonomy vs. speed.

Table 14. Autonomy of the electric propulsion system.

Speed (kn)	Power (kw)	Autonomy (hour)
7	1.736	11.5
8	2.588	7.7
9	3.68	5.4
10	5.024	4.0
11	6.714	3.0
12	8.712	2.3
13	11.078	1.8
14	13.820	1.4
15	16.992	1.2
16	20.614	1.0
17	24.718	0.8
18	29.338	0.7
19	34.4888	0.6
20	40.216	0.5
21	46.5444	0.4
22	53.504	0.4
23	61.1248	0.3

2.7 THE ELECTRICAL SCHEMATIC AND COMPONENT CONNECTION

2.7.1 DC-DC converter

The DC-DC converter changes the voltage level of DC sources from one level to another. In other words, a DC-DC converter takes one DC input voltage and outputs another DC voltage. The output DC voltage can be higher or lower than the input DC voltage. Figure 36 shows a DC-DC converter that works only with DC source.

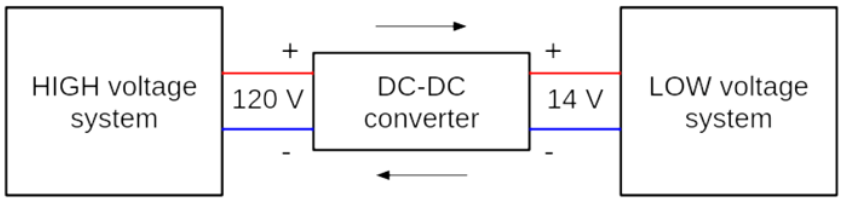

Figure 36. An example of a 120V to 14V converter [119].

A DC-DC converter is additionally known as a DC-DC power converter or transformer. DC/DC converters are usually used in electric vehicles (EVs). The most commonly used DC/DC converters in EVs are the unidirectional and bidirectional converters [120]. The former typically caters to various onboard loads such as sensors, controls, and safety and navigation equipment. These are designed to move power in one direction, from dedicated input to output, while the latter can move power in either direction [121, 122].

There are many types of DC-DC converters in the electrical industry. The most common classification is according to the input and output voltage ratio: boost DC-DC converters and buck DC-DC converters. As seen in Figure 37, in a boost DC–DC converter, the output voltage is higher than the input voltage. However, the output current is lower than the input current due to energy conservation (if we ignore the losses). Based on Figure 38, the output voltage is lower than the input voltage in a buck DC–DC converter. On the other hand, the output current is higher than the input current [122, 123].

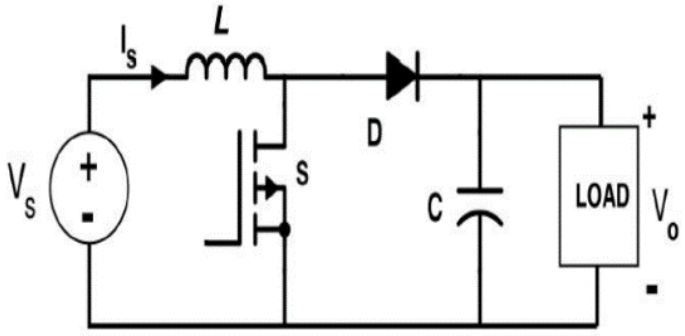

Figure 37. Circuit diagram of the boost converter.

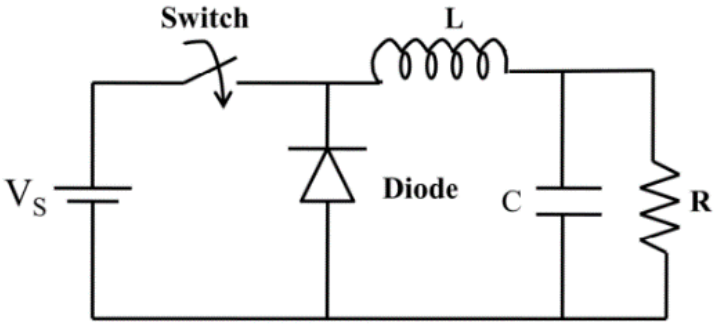

Figure 38. Circuit diagram of the buck converter.

In this thesis, a boost converter made up of an L-C circuit and an IGBT switching device was selected to connect the solar panels, batteries, and motor. The duty cycle (D), which ranges from 0 to 1, controls the switching. The duty cycle is made by the MPPT controller, which then turns it into a pulse signal that goes to the IGBT of the boost converter and hits the gate signal (g). The negative and positive ends of PV are connected to the emitter (E) and collector (C), respectively. Figure 39 shows the boost converter circuit diagram.

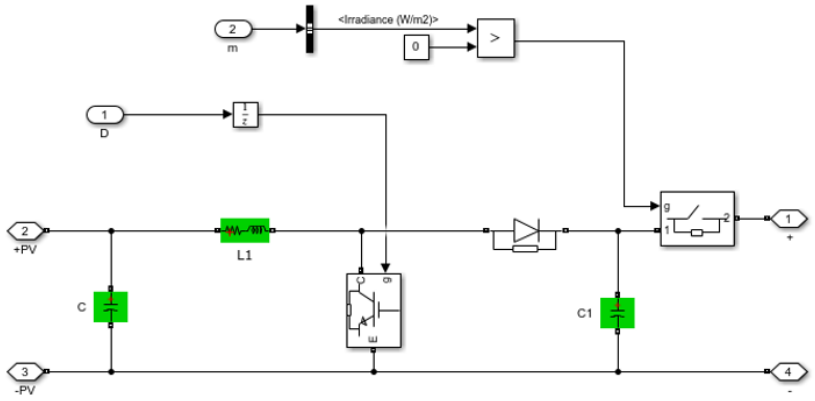

Figure 39. Boost converter in the Simulink model.

2.7.2 AC/DC rectifier function

AC shore power is often available everywhere, while DC power is not. In such a situation, we must be able to convert AC electricity to DC, which is performed by rectifiers. AC switches back and forth between different currents at regular intervals, while DC flows in one direction [124].

We use a transformer, a diode, and a large capacitor to turn an AC signal into a DC signal [125]. The connections are shown in Figure 40. A transformer is used to change the AC voltage level. In this circuit, an AC voltage with a range of 120 V is assumed to be available, but we need 8 to 9 VDC at the output. Thus, we change the transformer coil turn ratio to lower the AC voltage in the secondary coil. A diode will rectify the secondary winding current to generate only positive output voltages. Lastly, a capacitor filters the rectified signal to boost its average.

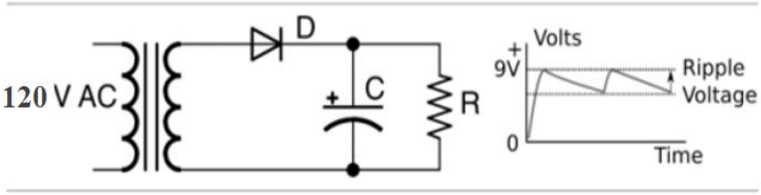

Figure 40. Circuit diagram of rectifier [126].

2.7.2.1 Shore power battery charger

Several choices were evaluated to find the right charger. Finally, a 2900 W charger that can charge batteries quickly in ports was selected. The parameters of the selected charger are compatible with this project's batteries. These 2900 W fast chargers can fully charge a Power 48-5000 battery from 0% to 100% in less than two hours. The selected fast charger is shown in Figure 41.

Figure 41. Fast charger 2900 W Power 48-5000 [127].

The manufacturer suggests using a separate charger for each battery, which means requiring four chargers for this project. Table 15 lists the complete parameters for this chargers.

Table 15. Electrical data for the charger [127].

Charger 2900 W 2212-00	
Property	**Value**
Input voltage	100-240 VAC
Frequency	50-60 Hz
Max. current consumption	16 A
Max. output power (At 100 V input voltage)	2900 W from 185 VAC upwards (1400 W)
Battery type	Power 48-5000 lithium ion
Charging start voltage	36 V
Efficiency	90%

2.7.3 Maximum Power Point Tracking (MPPT)

Maximum power point Tracking (MPPT) is a technology included in charge controllers that regulates voltage and current to extract the maximum possible power from the PV module under specified circumstances. Maximum power is affected by solar radiation, ambient temperature, and the temperature of the solar cell.

Variations in solar irradiance, temperature, and sun direction affect the electrical output of solar photovoltaic (PV) modules. PV modules have unique PV features related to a specific power point for a particular working situation. The PV module should function near this point to have an output close to the maximum power point (MPPT). In this scenario, PV module operation is known as the maximum power point tracking (MPPT), and boosting PV cell application is determined by the maximum PV power harvest [128].

2.7.3.1 The perturbation and observation (P & O) method :

Perturbation and observation (P&O) and incremental conductance (IncCond) have become the most common techniques for Maximum Power point Tracking (MPPT) strategies of PV and wind generation systems [129].

The main reason for selecting the perturbation and observation (P & O) method to execute in the proposed system is to offer superior efficiency against atmospheric circumstances. Oscillation and power loss are the main disadvantages of the P & O method, which arise near the maximum point due to constant perturbation [130]. Figure 42 illustrates the perturbation and observation (P & O) algorithm. Also, Figure 43 reveals the constraint for the perturbation and observation (P & O) method [131].

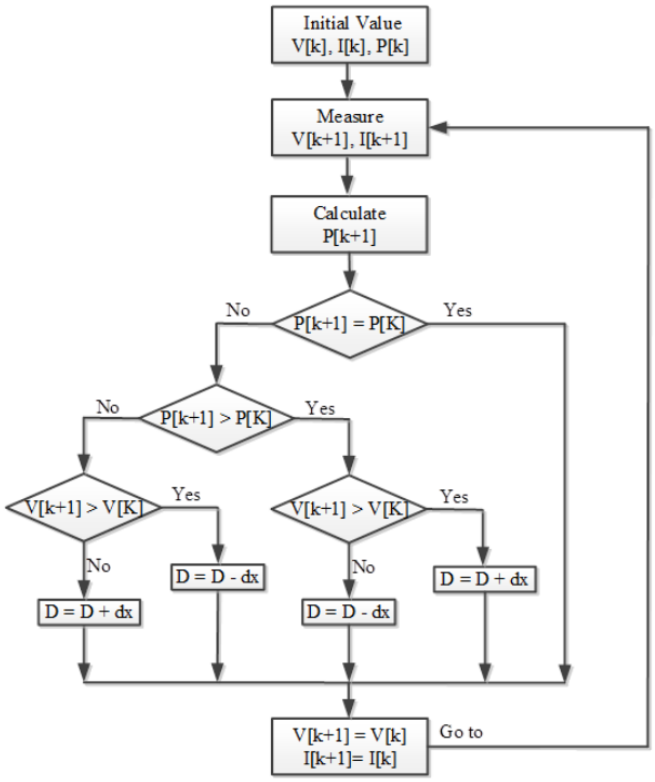

Figure 42. Flowchart of Perturbation and Observation (P & O) method [131].

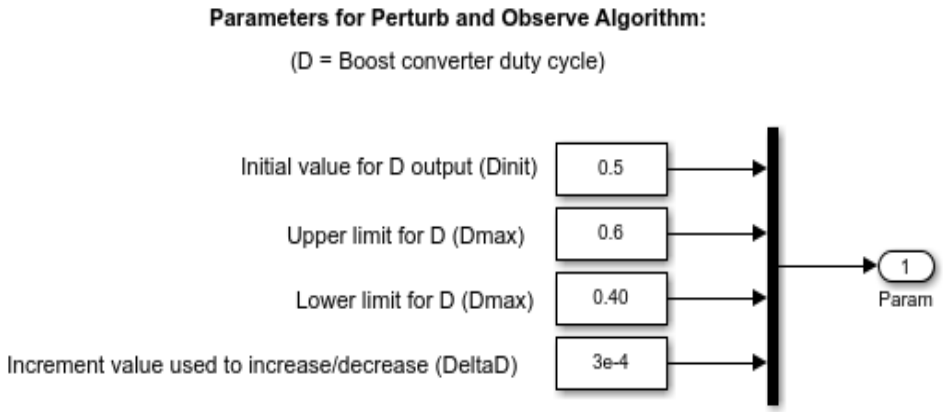

Figure 43. Constraints for Perturbation and Observation (P & O) Method [132].

2.7.3.2 Selection of solar/MPPT charger

The selected solar charge controller, called the Blue Solar MPPT 150/45, is shown in Figure 44. According to Table 16, this device is compatible with a 48 V battery and covers a solar panel with a maximum power of 2600 W and a maximum input voltage of 150 V, which is compatible with this project's elements (each PV array with a maximum power of 990 W and a nominal voltage of 18.8 V). The maximum current allowed for the device is also 50 A, based on the project specifications (about 50 A in the rated power mode). On the other hand, the output or charging voltage of this device can be set to one of the following values: 14.4 V, 28.8 V, 43.2 V, and 43.2 V.

Figure 44. MPPT 150/45 Bluesolar [133].

Table 16. MPPT 150/45 Bluesolar specifications [134].

BlueSolar Charge controller	**MPPT 150/35**	**MPPT 150/45**
Battery voltage	12/24/48V Auto Select (Software tool needed to select 36V)	
Rated charge current	35A	45A
Nominal PV power 1a, b)	35A 12V:500W/24V:1000W/36V:1500W/48V:2000W 45A 12V:650W/24V:1300W/36V:1950W/48V:2600W	
Max. PV short circuit current 2)	40A	50A
Maximum PV open circuit voltage	150V absolute maximum coldest conditions 145V start-up and operating maximum	
Maximum efficiency	98%	
Self-consumption	12V:20 mA 24V: 15 mA 48V: 10mA	
Charge voltage 'absorption'	Default setting: 14.4/28.8/43.2/57.6V (adjustable)	
Charge voltage 'float'	Default setting: 13.8/27.6/41.4/55.2V (adjustable)	
Charge algorithm	Multi-stage adaptive (eight pre-programmed algorithms)	
Temperature compensation	-16mV/-32mV/-64mV/^{o}C	
Protection	PV reverse polarity/output short circuit/ over-temperature	
Operating temperature	-30 to +60 ^{o}C (full rated output up to 40 ^{o}C)	
Humidity	95% non-condensing	

2.8 THE ELECTRICAL CONNECTION FOR THE MAIN COMPONENTS

This system's components operate at a variety of voltages. Therefore, first, we must determine the central voltage. Thus, we review the specifications of the engine, battery, and panels in Table 17 once again. According to this table, we can select 48 V as the main voltage, which is equal to the motor voltage and very close to the battery voltage.

Table 17. Parameters for the motor, battery, and solar panel.

Motor	
Input power	12 kW
Nominal voltage	48 V
Battery	
Capacity	5 kWh
Nominal voltage	44.4 V
Solar panels (one)	
Maximum power	110 W
Maximum voltage	18.8 V
Maximum amperage	5.9 A

The final connections are shown in Figure 45. The orange lines show the central voltage, which is 48 V. The panels are connected to the MPPT and the central network with a DC/DC converter. The battery is also connected to this network with a bi-directional DC/DC converter. This two-way converter provides the possibility of charging and discharging the battery. The battery is charged at the shore with a charger, which typically has an alternating voltage of 120 V and is connected to the central network through an AC/DC rectifier. Since the motor is of the DC type and the voltage of the motor and the central network are the same, no converter is used to connect it to the network. The electric-mechanical loads that feed from the panels are also connected to the central network with converters corresponding to their input voltage.

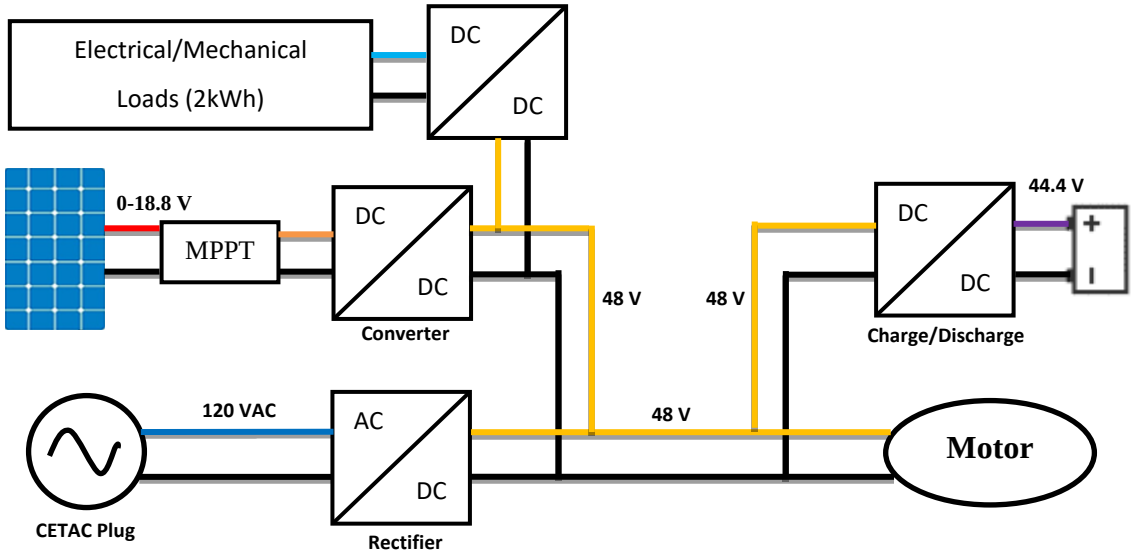

Figure 45. Schematic view of the components connection.

2.8.1 The first working mode: docked at the port

In this case, the boat engine is off, the boat batteries are charged with the help of shore power, and solar panels have output power. Figure 46 shows connections in this mode.

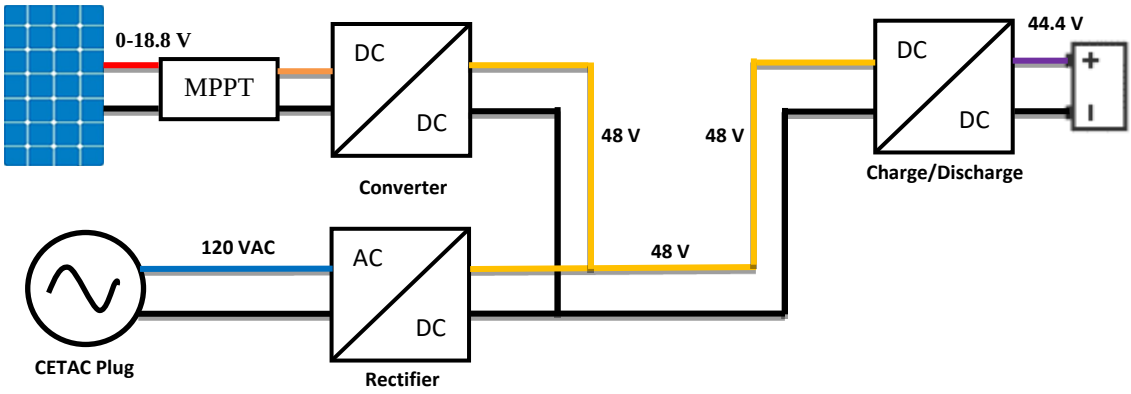

Figure 46. Schematic view of the first scenario.

2.8.2 The second working mode: sailing

The second working mode is sailing from the dock to the fishing location or moving between two rivers. In the second case, the boat sails at maximum speed. In this working mode, there is no shore power connection between the chargers and batteries, and batteries and solar panels power the motor. These connections are shown in Figure 47.

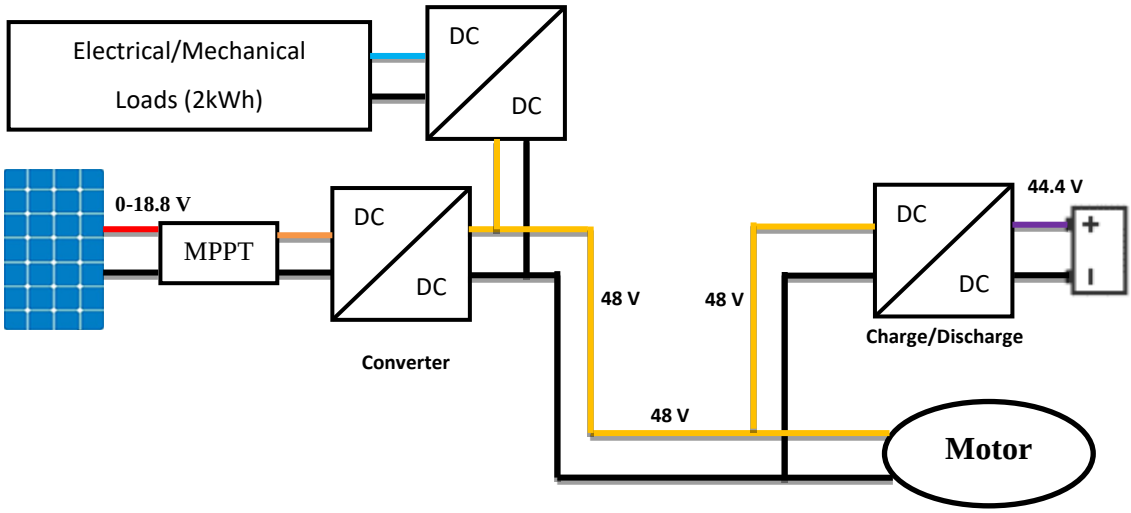

Figure 47. Schematic view of the second scenario.

2.8.3 The third working mode: fishing mode (low speed)

In this case, the motor works with very little power. All the connections are the same as in the second case and, Figure 47 represents it.

2.8.4 The fourth mode: anchored (zero speed)

In this mode, the motor is off and the batteries are unplugged. For example, when the boat is anchored (near the shore), the motor does not consume power, and the power from the solar panels is directly stored in the batteries. These connections are shown in Figure 48.

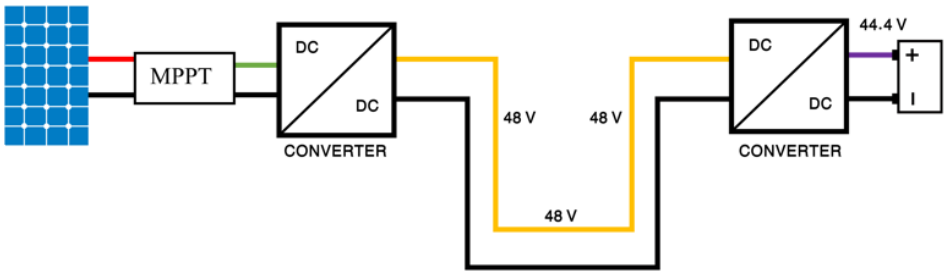

Figure 48. Schematic view of the fourth scenario.

2.9 CONNECTION DIAGRAM OF THE BOAT

Figure 49 is a simplified illustration of a suggested standard wiring diagram that shows how an electrical circuit works and represents the connections for power and signals.

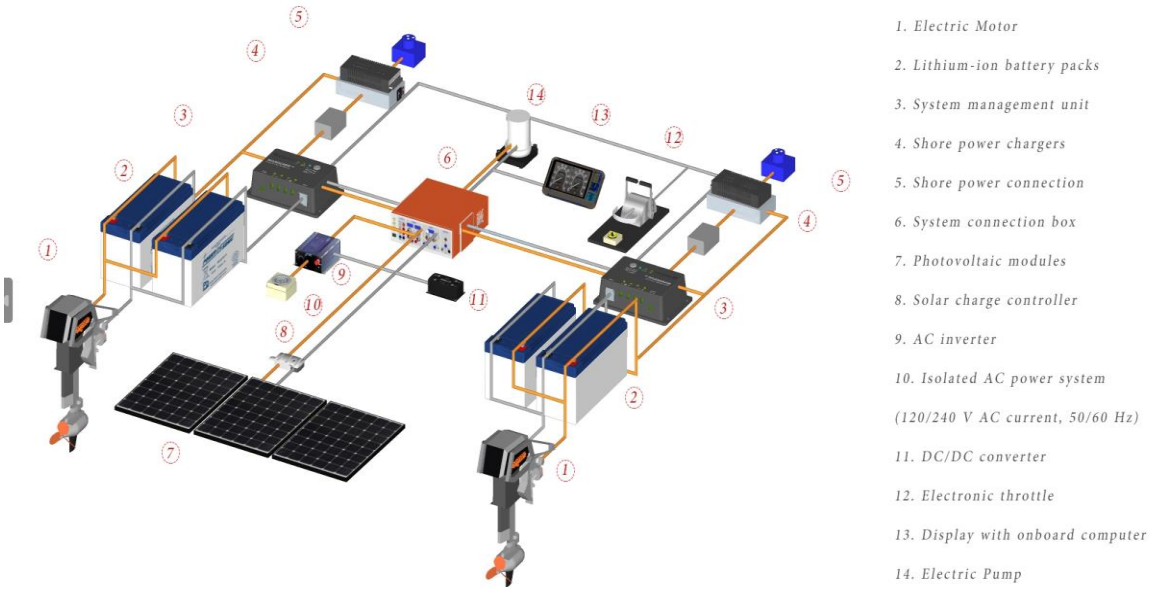

Figure 49. Schematic of the boat's electrical connections.

2.9.1 Selection of the appropriate cable

To make sure a power system works well, it is important to determine the type of cable and cross-section based on the permitted amount of current and voltage drop. After solar panel installation, solar chargers, batteries, and other parts in the right place in a solar system, the parts should be connected using wires and cables with the right insulation.

This section illustrates how the solar boat system is set up and uses math to determine the cable type and size for each part. Solar boat parts include:

1) Solar panels;
2) MPPT controller;
3) Batteries;
4) DC electric motor;
5) Battery charger; and
6) Connecting and disconnecting protective equipment such as CB, connectors, and fuses.

In this system, solar panels use sunlight to make electricity at a specific voltage (18.8 V). The PV array is connected to the charge controller, which changes the input voltage from the panel to the output voltage level (48 V) and tracks the maximum solar power when the temperature and sunlight change. The output of this controller is connected to DC batteries. The batteries and the motor have the same voltage of 48 V. When the boat is in the dock, the batteries and the motor are disconnected by the breaker, and the batteries are connected to the shore's AC power through the battery charger and connector. These chargers are responsible for converting 120 VAC to 48 VDC.

During discharge, the charger is separated from the connector. The batteries are connected directly to the motor. A large cable is needed to connect batteries because they must supply the load's full current and receive the charging current.

In this boat, the system works with DC power, and we can use a two-wire cable (if needed, a three-wire cable with one wire for the neutral) for the equipment cabling. Part of this cabling comes from the panels outside the boat compartment. However, most cabling is done inside the boat. Here, we design the cables for all these parts.

The cable's amperage capacity has been calculated by the below Equation (Eq.6) [135]:

$$I_a = \frac{P}{V} \qquad \textit{(Eq. 6)}$$

Where,

- P: power transmitted through the cable in W.
- V: circuit voltage in V.

The minimum allowable cross section of the cable in mm^2 has been calculated by the following Equation (Eq.7) [136]:

$$a = \frac{200\rho L I_a}{aV} \qquad \textit{(Eq. 7)}$$

Where,

- L: cable length in m.
- a : voltage drop in percent.
- ρ: conductor resistivity (1.724×10^{-8} Ω m (0.0174 μΩ m) for copper).
- I_a: Electric current in A.
- α: Cross-sectional area in m^2.

All cables designed in the following are of the three-wire type with a copper conductor, insulation, and PVC sheath. The percentage of voltage drop for all parts is considered 3%.

First, we consider the cable connecting the panels' output to the controller, with a length of 3 meters. Considering the parallel arrangement of the panels and the panel datasheet, we have an output voltage of about 18.8 V with a current of 53.1 A. Considering that solar panels cannot produce at full capacity in practice, 80% of the panels' rated current is

calculated using the formula. It is noteworthy that the breaker between the panels, the controller, must have a minimum current of 50 A. In this case, the cross-section of the cable from the output of the panels to the breaker is equal to:

$$a_1 = \frac{200 \times 17.2 \times 10^{-9} \times 3 \times 42.1}{3 \times 18.8} = 7.7\ mm^2 \qquad \textit{(Eq. 8)}$$

Now, we consider the cable connected from the MPPT controller to the batteries, with a length of 5 m. The output current of the selected MPPT is equal to:

$$I_0 = 45\ A \qquad \textit{(Eq. 9)}$$

Thus, we consider the permissible current equal to 45 A, assuming that all DC loads are in the circuit. As a result, the cross-section of the desired cable is equal to the following:

$$a_2 = \frac{200 \times 17.2 \times 10^{-9} \times 5 \times 45}{3.0 \times 48} = 5.3\ mm^2 \qquad \textit{(Eq. 10)}$$

We consider this part the cable connecting the battery to the electric motor, with a length of 5.5 m. We assume the batteries are fully charged and the motor works at the maximum speed of the boat. The battery's output voltage to the motor's input power supply is 48 V. The desired motor has an input power of 12 kW, leading to the following input current to the motor:

$$I_t = \frac{P_{in}}{V_a} = \frac{12000}{48} = 250\ A \qquad \textit{(Eq. 11)}$$

$$a_3 = \frac{200 \times 17.2 \times 10^{-9} \times 5.5 \times 250}{3.0 \times 48} = 32.8\ mm^2 \qquad \textit{(Eq. 12)}$$

Now, we calculate the cable size from the battery to the charger. The length of this cable is 7.0 m. In this case, the breaker disconnects the batteries from the motor, and the connector connects the charger to shore power. This 2900 W charger can pass a current of up to 50 A, according to the datasheet [127]. Considering the permissible current, the cross-section of the cable in this part is equal to:

$$a_4 = \frac{200 \times 17.2 \times 10^{-9} \times 50 \times 7}{3.0 \times 48} = 8.3\ mm^2 \qquad \textit{(Eq. 13)}$$

We know that a lot of power from low-voltage systems is wasted along cables because the intensity of the current in the circuit is very high, which causes a lot of power loss [5]. On the other hand, as the current gets stronger, the resistance of the cable or wire also gets stronger, necessitating the application of thicker cables to get around this resistance. If the cable chosen is too weak, there will be a big drop in voltage, which could cause problems with the system's function. To calculate current values, we assume a voltage loss of 3% and a current proportional to the cable's size that is 20% greater than the actual amount. Table 18 lists the sizes of cables needed for the boat according to the AWG standard.

A 15-A fuse is required for each panel in the case of panels connected in parallel. A combiner box is also used to hold the fuse or breaker for each panel, along with one or more combined fuses leading to a charge controller. To select this "combined" fuse or breaker, we must determine the worst-case current flowing through our panels .Fuse 50 A seems to be a good choice for this line.

To turn the solar system on and off, a switch can be placed in the positive wire between the solar array and the MPPT controller. Solar controllers regulate the amount of power going to the battery bank; thus, the positive cable leading to the battery bank should be fused at roughly 10 A above the maximum solar controller output. A 55-A fuse or breaker, which aligns with the maximum capacity of the charge controller selected, should be used in this case to protect this cable set.

The cabling and fuses between a battery and an AC/DC inverter are very important, since this is where most of the current will flow. In the same way, as with the charge controller case, the inverter manual should have the recommended cable and fuse. The recommended inverter charger has a charging current of 50 A, but we use 60 A for safety. The selected motor is 12 kW, which works with a maximum current of 250 A in a 48 VDC system. A 300 A overcurrent protection device is suitable for motor protection.

Table 18. AWG-standard cable selection with 3% voltage drop for 48V DC systems.

Cable	AWG	Cable length (ft)	Wire cross-sectional area mm^2	Protective devices (A)
solar panels connection	16.0	4.0	1.3	Fuse 9 × 15A
Pv array to MPPT	8.0	10.0	8.37	Fuse 1 × 50A and on/off switch
MPPT to battery bank	8.0	16.5	8.37	Fuse /Breaker 1 × 55A
Batteries to shore power (via charger)	6.0	23.0	13.3	Fuse 4 × 60A
Motor to batteries	1/0	18.0	53.5	Main battery switch 300A
Batteries connection	2.0	3.0	33.6	_

CHAPTER 3
BOAT DESIGN

3.1 HULL DESIGN

One of the main designs of the project is the 3D design of the boat and its hard top. The hull design has three main elements: the materials used during construction and the shape and size of the hull. The materials used in hull boats include steel, aluminum, fiber-reinforced plastic (FRP), and polyethylene. Aluminum is widely used now due to its lightweight, which allows for greater boat speed without sacrificing hull integrity or strength [137]. In this project, we designed a catamaran with twin aluminum hulls connected by a deck that measures 23 feet by 8 feet. This design gives the deck a rectangular shape, resulting in more usable deck space than a monohull boat. Figure 50 illustrates a 3D view of our catamaran boat design.

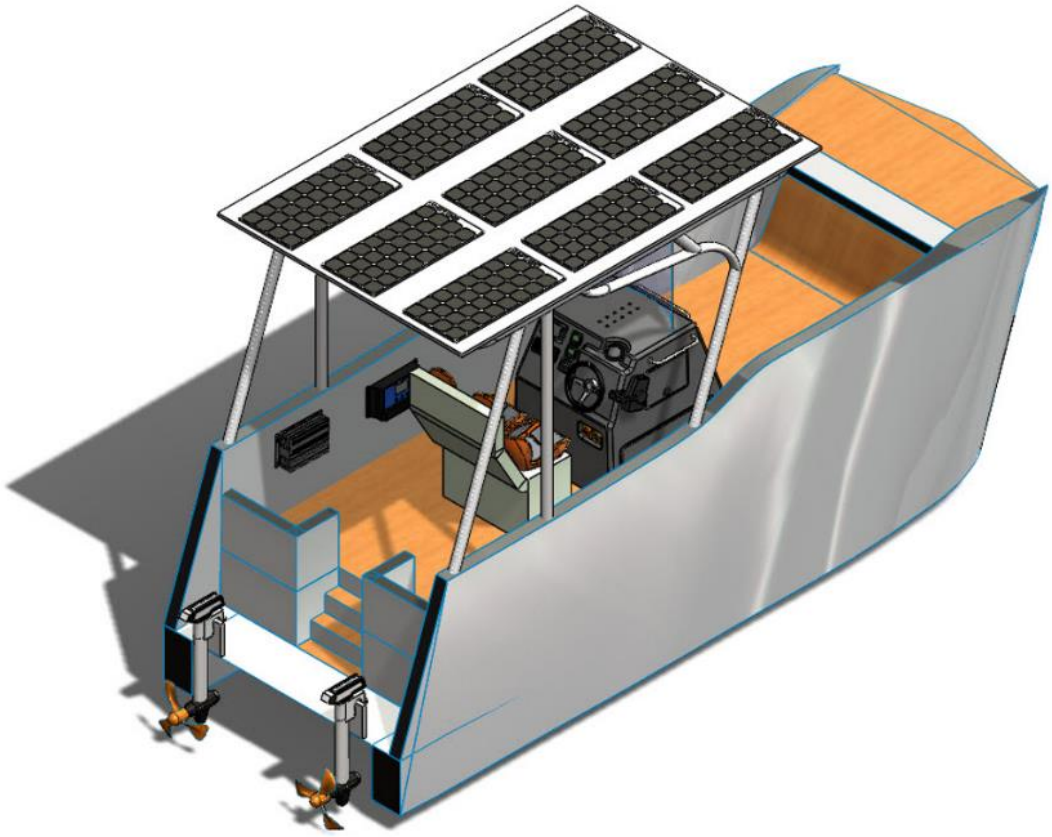

Figure 50. 3D perspective of the designed catamaran boat.

We used SolidWorks, a CAD program, to design this boat. Also, we placed the boat's console in the center and selected an outboard motor to install at the end with a suitable tilt. We determined the appropriate placement of the boat's heavy equipment, which can be seen in Section 3.4, based on the boat's dimensions. In addition, we placed the batteries at the bottom to maintain the boat's stability. The hard top is designed so that it provides shade for the fishermen. The GMDSS equipment is installed on the console of the boat for easy access by the fishermen. Additionally, we considered a water pump and a portable refrigerator for the boat. Figure 51 shows the proposed connection schematic of the designed boat.

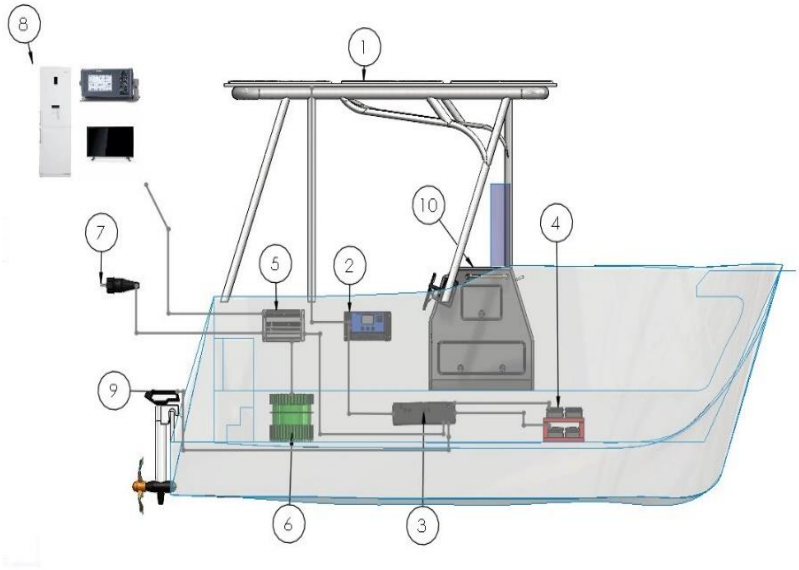

ITEM NO.	Item name
1	Solar roof
2	Solar charge controller
3	Converter
4	Battery bank
5	Inverter/Changer
6	Pump
7	Shore power
8	Appliance
9	Electric motor
10	Console

Figure 51. The schematic of the different parts of the developed catamaran fishing boat.

3.2 HARDTOP DESIGN AND MATERIAL PROPERTIES

The hardtop is one of the designed parts of this project. In our system, the hardtop increases the area available for solar panels. Finding a shadow in the middle of the sea is necessary when the sun is intense. Therefore, hardtops are usually used to cast shadows on boats. Most fishing versions of these boats have complements or additional parts, such as rod supports, in the hardtop structure. Aluminum, stainless steel, and fiberglass are the most common materials used in light boat hardtops. Therefore, to determine which of these three materials is best for making a hardtop, we need to look at them from different perspectives. Table 17 compares aluminum, steel, and fiberglass-based on their physical properties.

Table 19. Physical properties of aluminium, steel, and fiberglass [138, 139].

	Density(kg/m^3)	**Young Modulus (GPa)**	**Poisson's Ratio**	**Yield Strength (Mpa)**
Stainless steel	8030	210	0.3	776
Aluminium	2700	70	0.35	276
Fiberglass	2000	72	0.21	206

The first important point in choosing the material for the hardtop is its weight. According to the densities of the three materials introduced, the weight of aluminum and fiberglass is almost one-third that of stainless steel. Therefore, using stainless steel to make the hardtop causes the weight of the boat to increase unnecessarily. Among the two materials, aluminum and fiberglass, fiberglass can be a better choice due to its lower density. Still, weight is not the only factor in choosing a hardtop material. The next thing to do when choosing a hardtop is to check the selected material's stiffness. Young's modulus is used to measure the resistance of solid materials against elastic deformation, or their stiffness. This quantity relates stress (force applied per unit area) to strain (relative deformation) along a line or axis.

So, to change the shape of a piece of structural steel, we need to apply a very high force and stress. According to Young's modulus of the three selected materials, it is clear that stainless steel has a higher Young's modulus than the other two materials. That is, steel shows a higher resistance against the incoming force. When considering materials, it is essential to consider their durability and longevity against sunlight. Since metals are more durable than fiberglass against sunlight, choosing aluminum or stainless steel can be a better choice than fiberglass. Among the characteristics mentioned above, the most critical factor is the durability and long life of the hardtop, which is preferable to aluminum or stainless steel over fiberglass. In this study, aluminum material is chosen for the hardtop.

The boat's dimensions are 701.04 cm by 243.84 cm. The hull of the boat is made of aluminium and the dimensions of the boat and the solar panels determine the design of the hardtop. Solar panels are installed on the hardtop surface. Figure 52 and 53 show the dimensions and three-dimensional schematic of the designed hardtop. We placed nine panels in three rows three, each measuring 116.5 cm by 55.6 cm. For the design of the solar panel frame, a minimum distance between panels is considered for maintenance and repair.

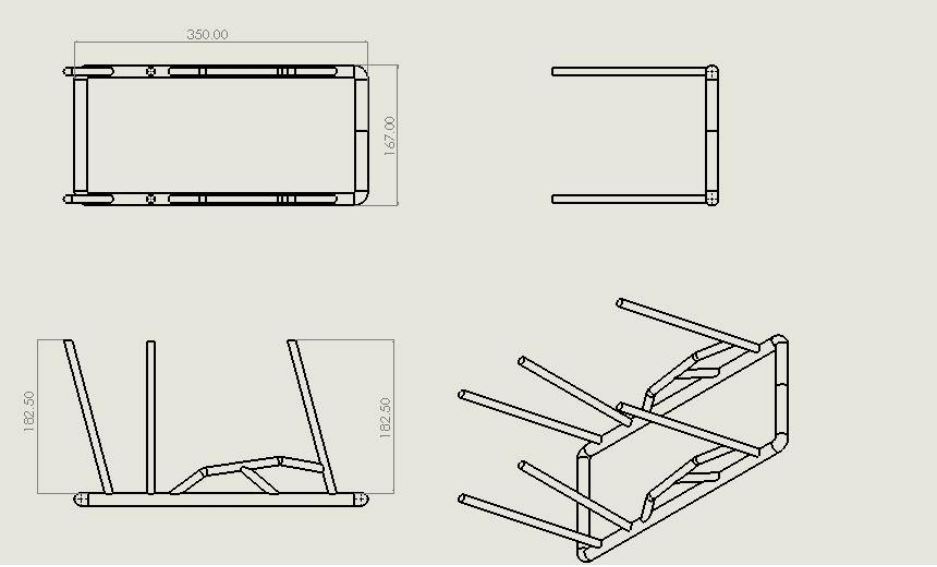

Figure 52. Dimensions of the hardtop.

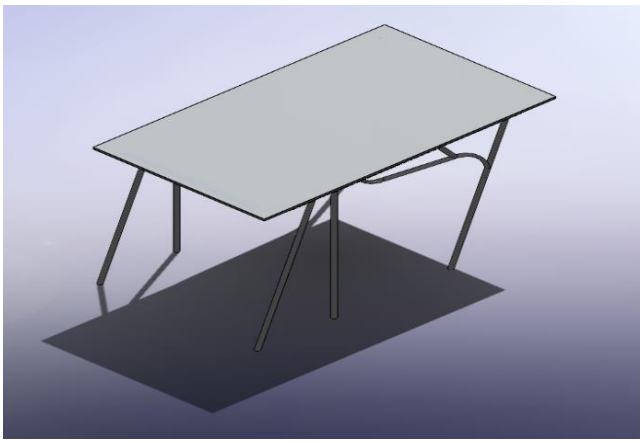

Figure 53. 3D model of the designed hardtop.

3.2.1 Fixing the hard top on the boat

A piece of metal is designed to fix the hardtop structure on the boat body. This piece is shown from different angles in Figure 54.

Figure 54. Hardtop fixation piece.

The designed metal piece can be made of aluminum or galvanized steel (due to the hardness of steel). This pipe can be made and installed in different required angles depending on the hardtop structure's angle with the boat body. To install this part, a screw is used to connect the designed part to the hull, and two smaller screws are used to connect the hardtop structure to the part, which allows the hardtop to be easily separated. Figure 55 shows the designed pieces fixed to the hard top.

To connect the designed piece to the boat body from the bottom, a nut can be welded on the boat body, or if it has a thick body, it can be nailed. With the suggested connection, the hardtop is fixed well on the body.

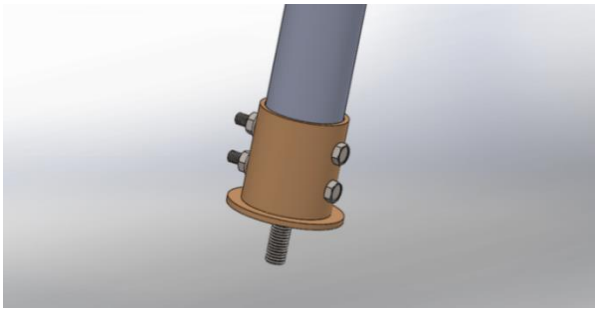

Figure 55. Closed screw schematic.

3.2.2 Solar panels fixation

The solar panel is made of monocrystal, and each panel weighs 2 kg, which is 18 kg for 9 panels. Its framework is made of aluminum. Figure 56 shows the size of the solar panel frame in centimeters. A small space between the panels makes maintenance and cleaning easier.

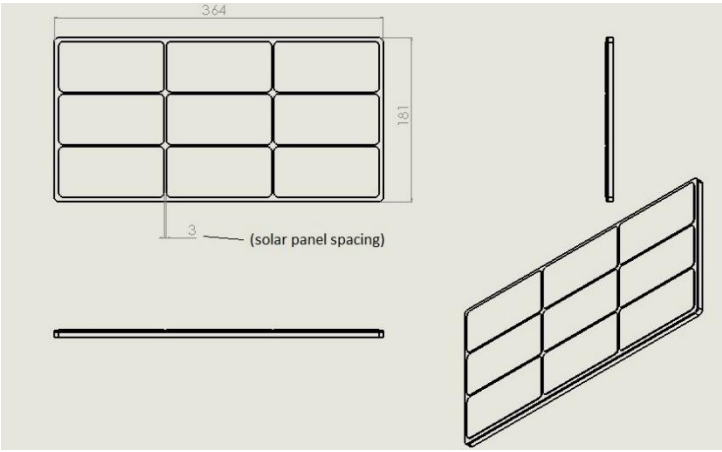

Figure 56. Dimensions of the solar panel frame.

There are different methods to fix the solar panels on the hardtop surface that can be used to connect the panels, depending on the user's interest. This can be done by welding the panels to the plate or by screwing them to the plate. Each method can be chosen based on the boat's use and speed and factors such as ease of opening and closing during replacement or sensitivity.

In this project, the corners of the panels were tightened using four screws because of the low speed of the boat and the possibility of easy replacement. An illustration of how to mount solar panels on the plate surface can be found in Figure 57.

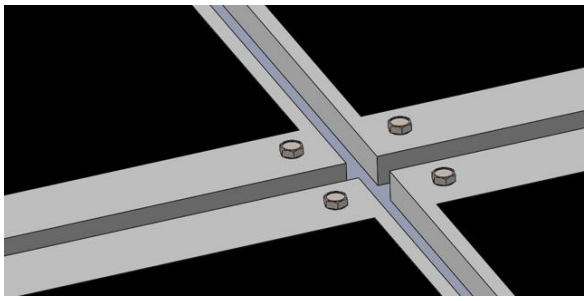

Figure 57. Fixing solar panels on plate.

3.2.3 Solar panel orientation and positioning

3.2.3.1 Electrical parts of the orientation system

The electrical part consists of three main parts: an inclinometer, GPS, and microcontroller. GPS gives the location permanently to the microcontroller. All the information related to the inclinometer and the GPS is sent to a microcontroller. The microcontroller sends the necessary command to the motors in the mechanical part of the system. The microcontroller calculates the optimal angle of the panels by considering three parameters: the latitude (position of the boat), the month of the year, and the boat's direction. Two methods are used to calculate the optimal tilt of solar panels. Table 20 shows different methods for calculating the optimal tilt by season.

Table 20. Calculation for the optimum angle of solar panels [140].

SEASON	TILT ANGLE (METHOD 1)	TILT ANGLE (METHOD 2)
Spring/fall	=latitude	=latitude
Summer	=latitude-15º	=latitude×0.9-23.5º
Winter	=latitude+15º	=latitude×0.9+29º

3.2.3.2 Mechanical parts of the orientation system

For the mechanical part of the solar panel orientation system, four movable arms are used. Each of these arms is made of components that allow frontal inclination rotation and lateral inclination rotation for the panels. These parts consist of a linear motor, a motorized guide, and an electronically controlled brake. A solar panel orientation system is shown in Figure 58.

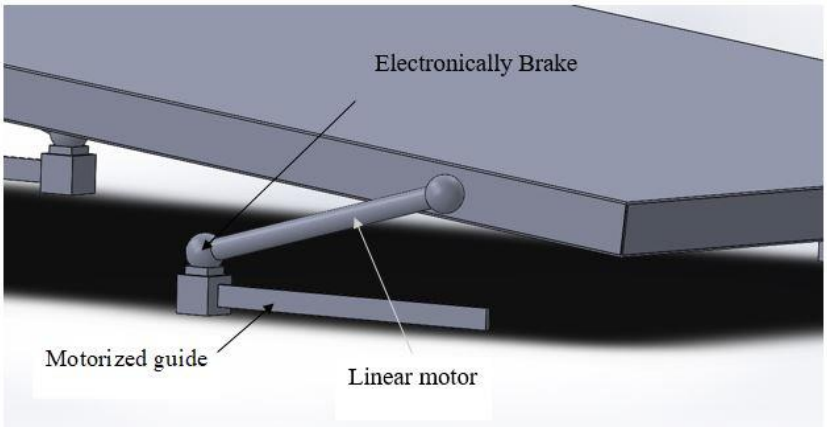

Figure 58. Components of the orientation system.

Due to their lightweight, these panels do not put a lot of pressure on different parts of the arm. These systems are designed to coordinate movement. To raise one side of the solar panels, the brakes, motorized guide, and linear motor block the other side. A motorized guide moves from the minimum to the maximum or desired position to form the optimal angle. When the motorized guide is in the full-length position, the linear motor is in the minimum-length position. If the system wants to give more tilt to the solar modules, the linear motor gives an extra tilt and extends its length to the required amount. In Figure 59 and 60, different inclinations of the solar panel orientation are shown.

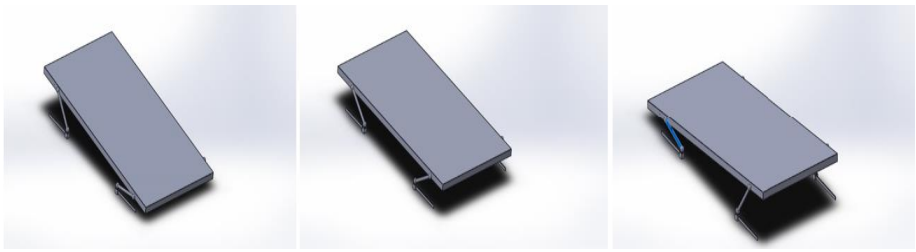

Figure 59. The frontal inclination of the orientation system.

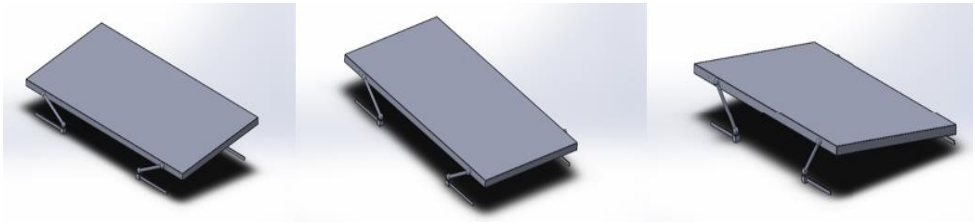

Figure 60. The lateral inclination of the orientation system.

3.3 HARDTOP FEM SIMULATIONS

The hardtop and the whole propulsion system are exposed to weather and gravity conditions during their useful lifetime. These conditions could damage the components of the system. Therefore, it is important to analyze the effects of these conditions, especially on the hardtop. We can confirm the hardtop's mechanical properties by simulating and analyzing its structure. Using ANSYS Workbench, this simulation is conducted. ANSYS is software for finite elements.

This hardtop is fixed to the boat with six fixation points. To translate boundary conditions into our Ansys model, it is imperative to analyze how supports work. The hardtop, which is subject to wind and gravity, holds and places the solar panels. These conditions cause some reactions in the hardtop structure.

The conditions studied are:

- Solar panel's weight
- Wind conditions

3.3.1 Hardtop CAD importing, meshing, material properties, and boundary conditions

Ansys Workbench is used to compute stress and deformations. First, a CAD model of the hardtop has been designed on SolidWorks and imported into the FEM program (using the Ansys extension Design Modeller) in preparation for meshing and solving. The first step in importing CAD is to define the material properties. Based on the information provided in the previous sections, aluminium has been chosen as the material for the hard top.

Throughout these simulations, the weight of the mechanical part of the orientation system has been neglected. Compared to the other boundary conditions applied to the model, the forces caused by this weight are very small. The boundary conditions have been applied to the meshing model. Among all the analyses realized in this chapter, the X-axis direction coincides with the boat direction, the Y-axis is perpendicular to the boat floor, and the Z-axis is the cross product between the X and Y. On the top structure of the solar panels, four forces can be identified based on the conceptual design of the orientation system and the reactions between the junctions and the hardtop.

Six points secure the hardtop. Due to the symmetry of the structure, only anchors 1, 2, and 3 will be studied. In the two figures below, the mesh of the solar panel (nodes=11991) and hardtop (nodes=7986) are placed.

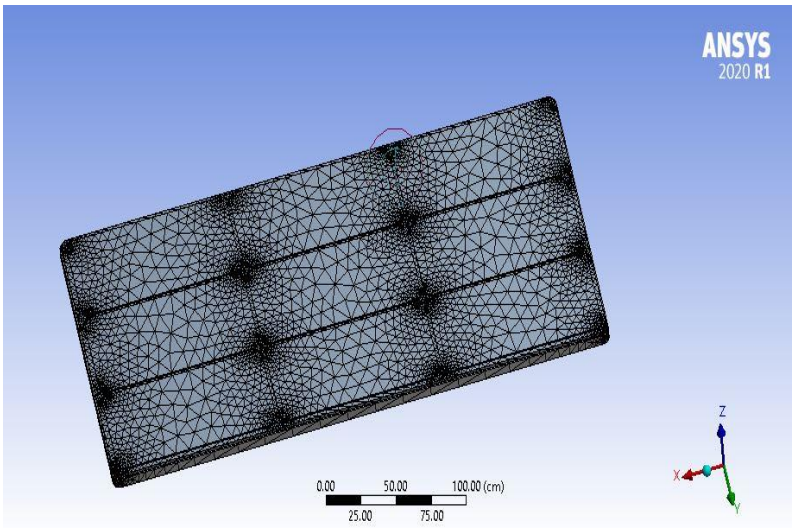

Figure 61. Meshing the solar panel.

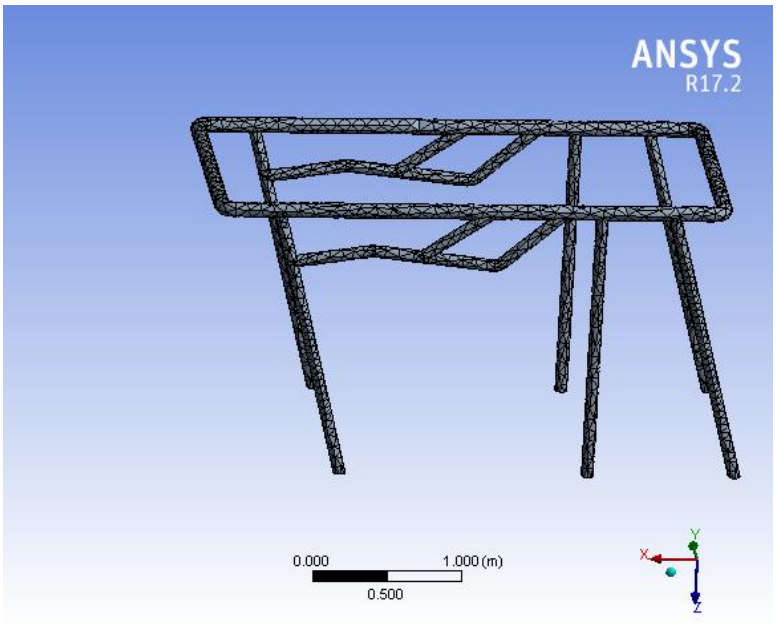

Figure 62. Meshing the hardtop.

3.3.2 Solar panel weight

As explained before, the solar panel system consists of nine panels. Every panel weighs 19.62 N, so the total system weights are 176.58 N. According to the previous explanation, the system's total force acting on the hardtop structure is 176.58 N, distributed among four forces. From the following Equation [141], we have :

$$F_{Total} = m \times g \qquad \textit{(Eq. 14)}$$

Where:

- F: The force pulling objects toward the Earth in N.
- G: The acceleration due to gravity in m/s^2.
- M: Mass of the body in kg.

$$F_{Total} = m \times g = 9.0 \times 2.0 \times 9.81 = 176.58\ N \qquad \textit{(Eq. 15)}$$

- Results analysis:

Here are the results of the analysis of the solar panel's total displacement and von Mises stress. Figure 63 and 64 illustrate displacement plots and boundary conditions due to the weight of solar panels.

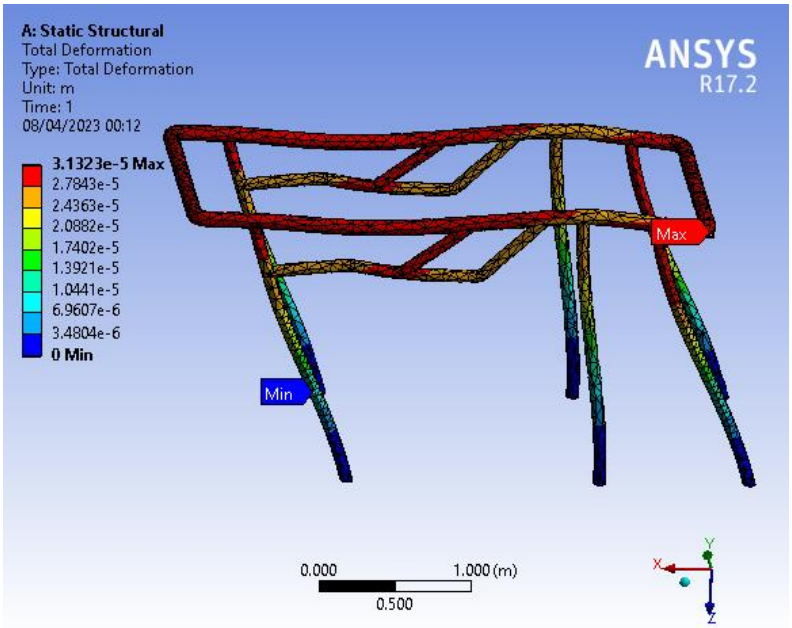

Figure 63. Total deformation (solar panel weight).

During the testing of the hardtop, the minimum displacement was about 0.003 mm, and the maximum displacement was about 0.03 mm , which is a very low displacement.

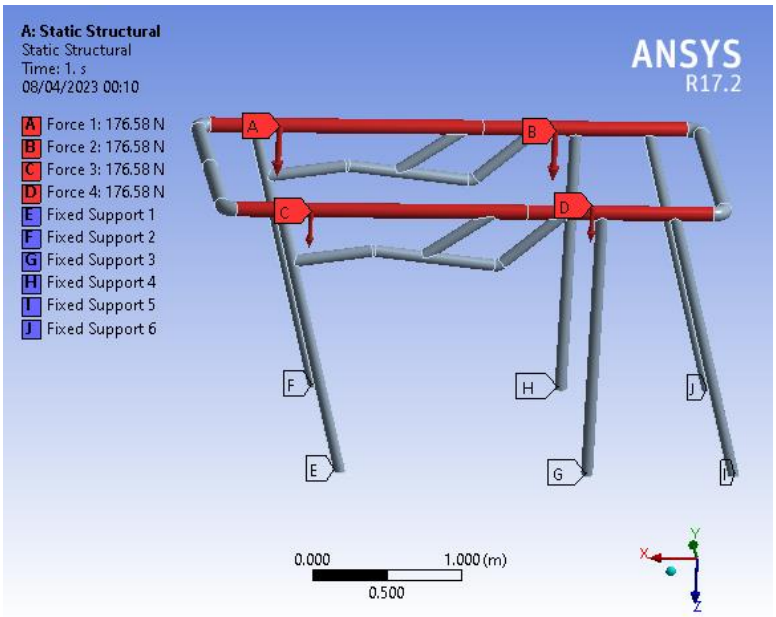

Figure 64. Boundary conditions of the hardtop fixations (solar panel weight).

At the rear and top of the hardtop, the highest and lowest values for this stress are calculated. In this case study, none of the stresses or deformations are very high because the applied loads are very low. However, the safety factor for these loads is extremely high, so it has not been calculated. In Figure 65, we can see the stress distribution due to the weight of the solar panels on the hardtop structure. During the testing of the hardtop, the minimum stress distribution of the hardtop structure was about 0.35×10^{-4} MPa and the maximum stress distribution was about 0.23 MPa.

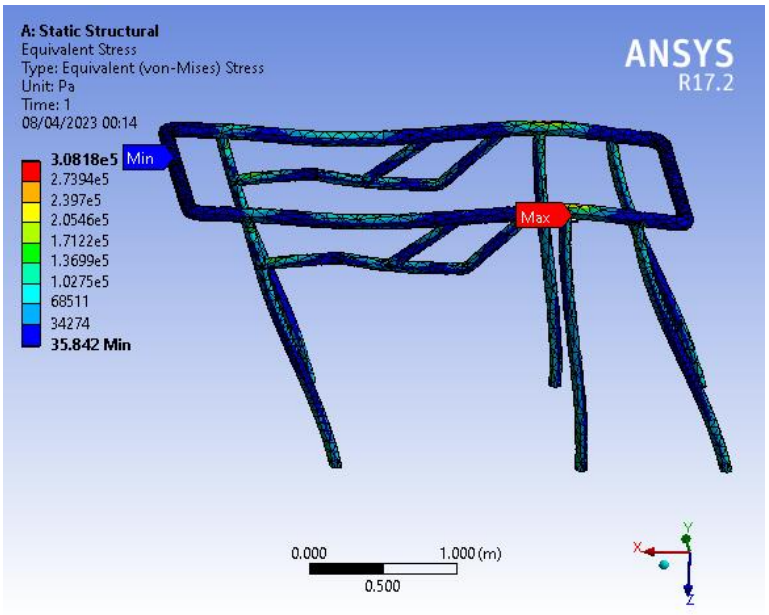

Figure 65. Stress distribution of the hardtop structure (solar panels weight).

3.3.3 Wind conditions

This part discusses the effects of the wind. It is first necessary to simulate the effects and forces caused by wind on solar panels. After finding the wind forces, we can apply them to the mesh model to simulate them. Some factors, such as the panel's orientation, wind direction, wind speed, and boat speed, were considered when studying the wind effects. These factors have been applied in the most harmful way in the wind simulations shown below to present the most extreme cases.

3.3.3.1 First case: boat maximum speed and forward inclined (no wind assumed)

The wind is not assumed in this first case. When the boat is sailing at its maximum motor speed, approximately 25 kn (45 km/h), the hardtop tilts at its maximum angle (30 degrees) against the wind. The airflow simulation is 45 km/h.

This simulation is designed to calculate the forces caused by the wind when the boat is sailing at its maximum speed. The simulation of fluent airflow for the first case is shown in Figure 66. The wind forces (assuming the Y axis is up and the Z axis is parallel to the boat's direction) are:

$$\begin{bmatrix} F_x = 8560 & N \\ F_y = 9320 & N \\ F_z = 0 & N \end{bmatrix}$$

$$F_{R1} = \sqrt{F_x^2 + F_y^2} = \sqrt{(8560^2) + (9320^2)} = 12650\ N \qquad \textit{(Eq. 16)}$$

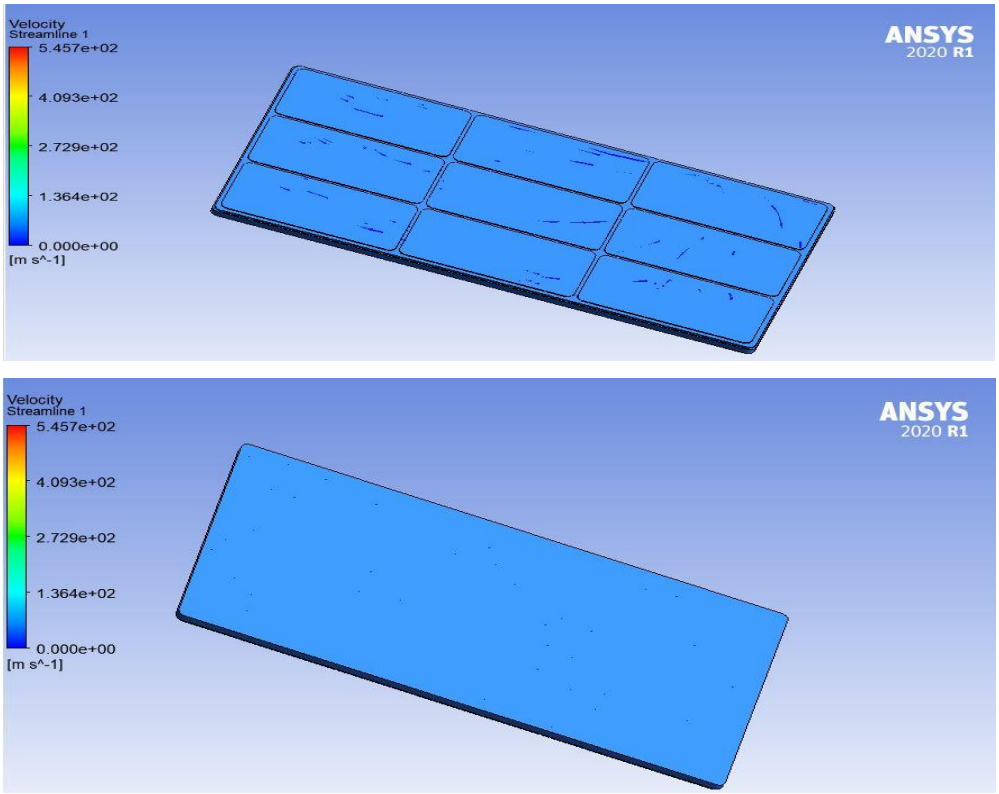

Figure 66. Fluent air flow simulation (case 1).

- Results analysis

The speed distribution of the airflow passing through the surface panel is very low, and its maximum speed is 13.6 m/s. The peak pressure in the airflow passing through the panel is 1.132×10^{-4} Pa.

After that, boundary conditions (forces) were applied using fluent results and the model was solved using the finite element method. Then, the displacement plot and the Von-Misses stress plot were calculated. Boundary conditions and displacement plots for the first case can be seen in Figure 67 and 68. In Figure 69, we can see the stress distribution on the hardtop structure.

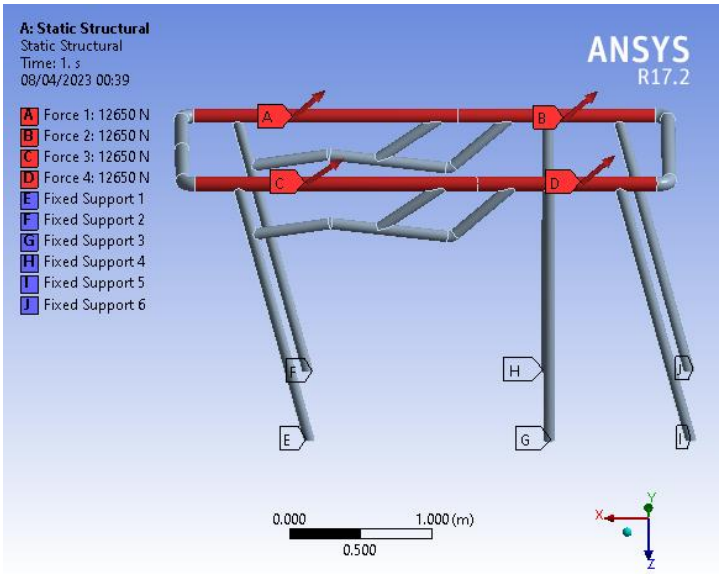

Figure 67. Boundary conditions of the motors' reaction forces (case 1).

According to the Deformation results plot, the maximum deformation occurs at the top of the hardtop. An absolute value of 14 mm gives this maximum deformation. Additionally, a singular point can be detected when analyzing Von-Misses stress results. This structure has a maximum tension of 76 MPa under these boundary conditions.

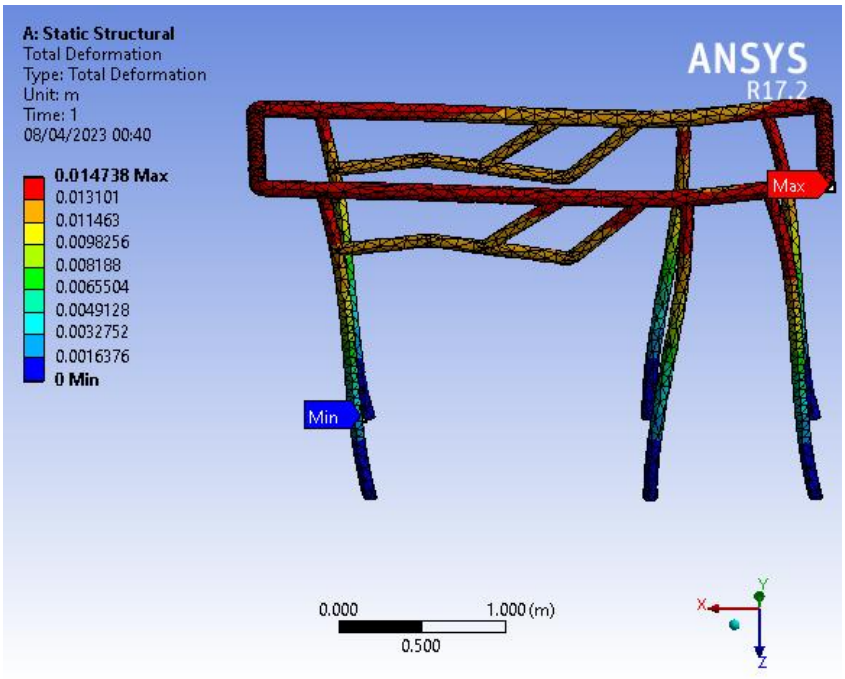

Figure 68. Displacement plot of the hardtop structure (case 1).

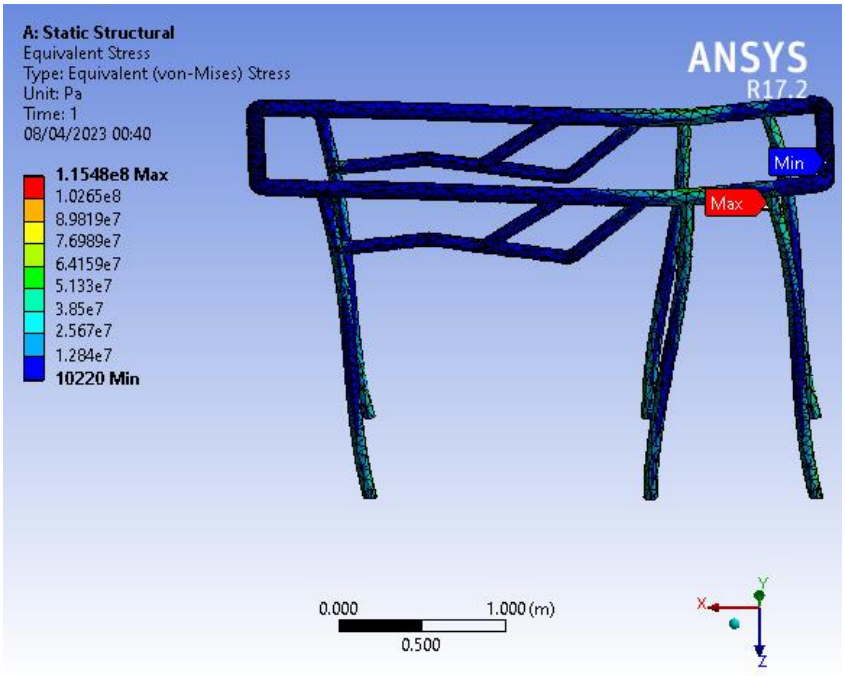

Figure 69. Stress distribution of the hardtop structure (case 1).

The safety factor can be calculated using the following Equation [142]:

$$\gamma = \frac{\sigma_y}{\sigma_{Max}} = \frac{276\ MPa}{76\ MPa} = 3.6 \qquad \textit{(Eq. 17)}$$

Where,

- σ_y: Yield stress of aluminum in Pa.
- σ_{Max}: Maximum stress in Pa.
- γ: Safety factor.

3.3.3.2 Second case: lateral wind gust

In this case study, a lateral wind gust has been applied to the solar panels. The wind speed is 100 km/h, the solar panels' structure has a lateral tilt of 45 degrees (maximum lateral tilt), and the airflow simulation is 100 km/h. To find the forces caused by the wind at a speed of 100 km/h, the affected part (in this case, the solar panel's structure) is simulated. The simulation of fluent airflow for the second case is shown in Figure 70. The wind forces are:

$$\begin{bmatrix} F_x \approx 0 & N \\ F_y = 11500 & N \\ F_z = 9320 & N \end{bmatrix}$$

$$F_{R2} = \sqrt{(11500^2) + (9320^2)} = 14800\ N \qquad \textit{(Eq. 18)}$$

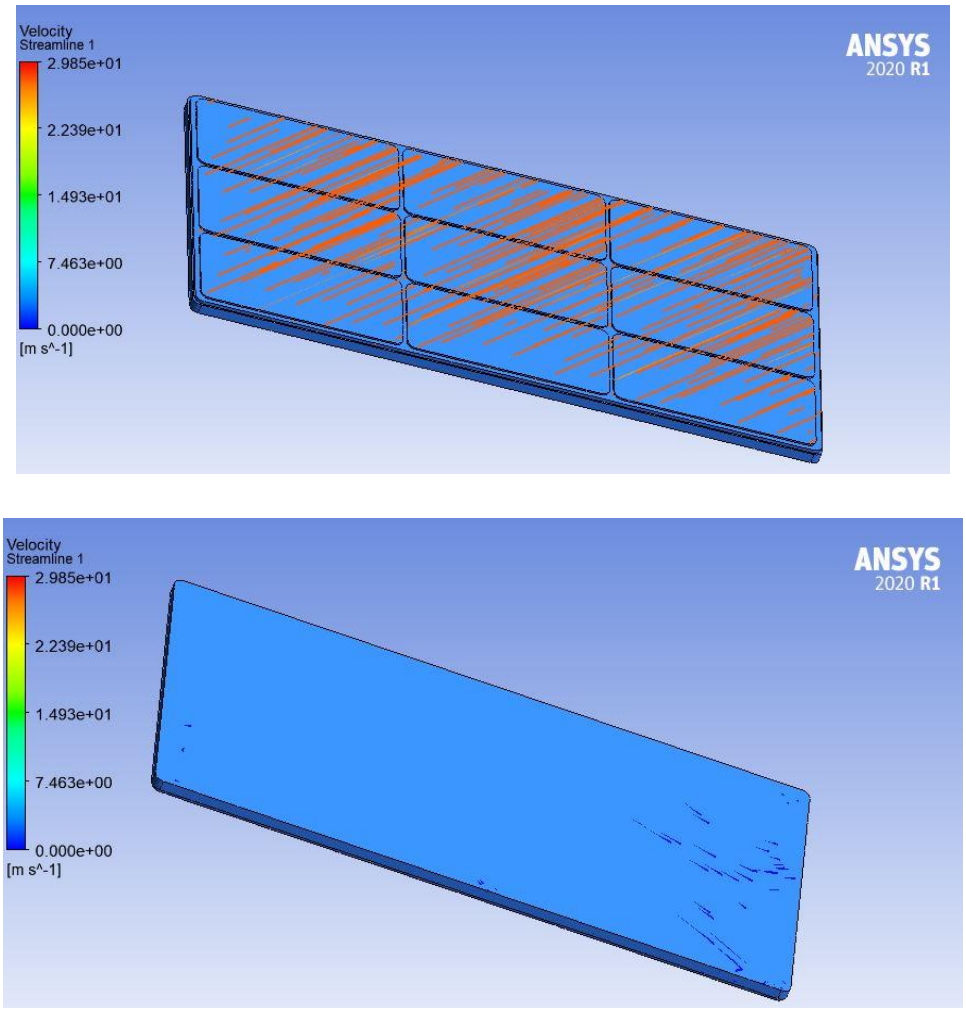

Figure 70. Fluent airflow simulation (case2).

- Results analysis:

The air passes through the panel surface at a higher speed; its maximum speed is 29.8 m/s while the maximum speed of airflow passing under the panel is 5.4 m/s.

As in the first case, the boundary conditions (forces) have to be updated using the Fluent results, and the model has to be solved, and the model has to be solved (Figure 71).

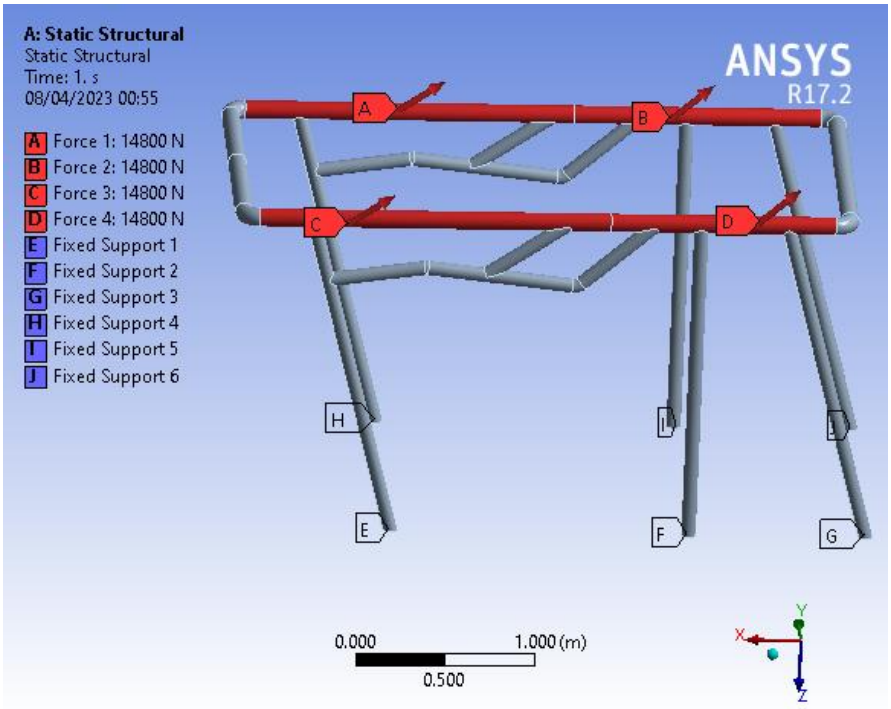

Figure 71. Boundary conditions of the motors' reaction forces (case 2 study).

After solving the system, the deformation plot and the stress plot were obtained. According to the deformation plot, the maximum displacement occurred in the hardtop's top, left, and frontal parts. It has a value of 17 mm and the minimum displacement occurred in the hardtop's bottom. When we approach the maximum stress zone, we see a singular point. If we ignore these affected nodes, the maximum stress value would be 75 MPa. Displacement plots and stress distributions for the hardtop are shown in Figure 72 and 73.

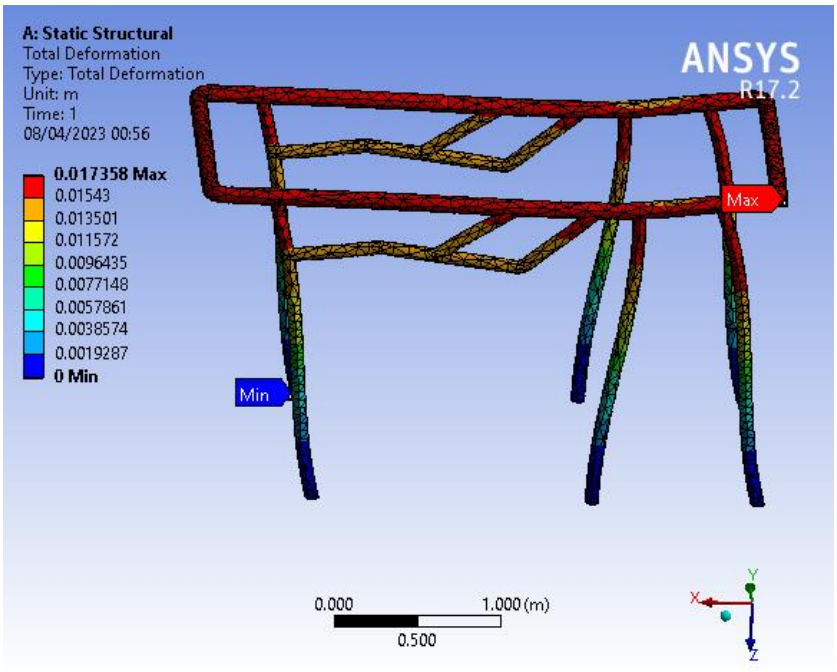

Figure 72. Displacement plot of the hardtop structure (case 2).

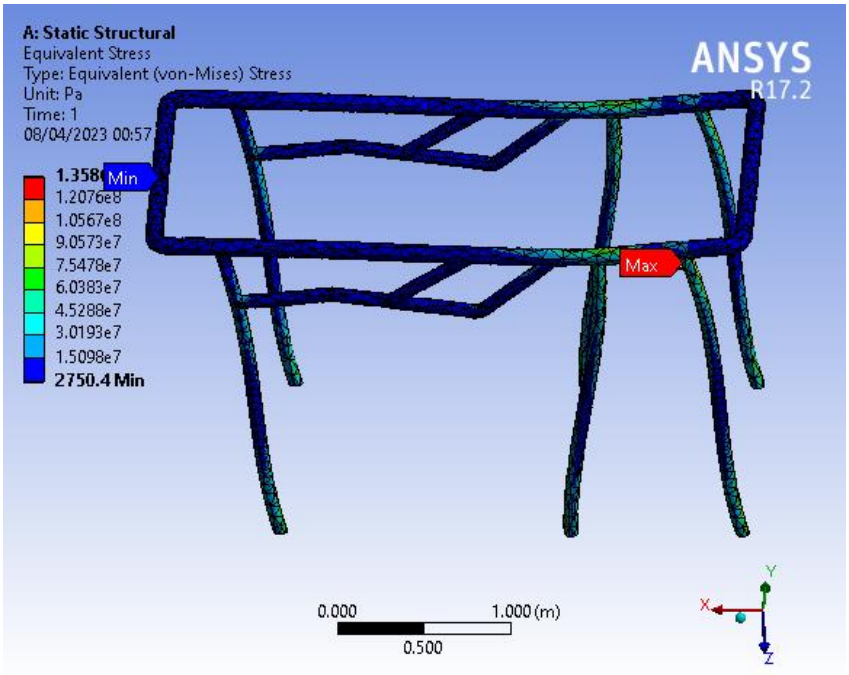

Figure 73. Stress distribution of the hardtop structure (case 2).

The safety factor has a value:

$$\lambda = \frac{\sigma_y}{\sigma_{Max}} = \frac{276\ MPa}{75\ MPa} = 3.7 \qquad \textit{(Eq. 19)}$$

3.3.3.3 Third case: rear wind gust

In this case study, we simulate the effects of a rear gust of wind (100 km/h) on the structure of solar panels. The solar panels' structure is tilted (rear part up) at the maximum angle (35 degrees). The simulation of the flowing air flow for the third case is shown in Figure 74. The wind forces are:

$$\begin{bmatrix} F_x \approx 0 & N \\ F_y = 4800 & N \\ F_z = 6225 & N \end{bmatrix}$$

$$F_{R3} = \sqrt{(4800^2) + (6225^2)} = 7861\ N \qquad \textit{(Eq. 20)}$$

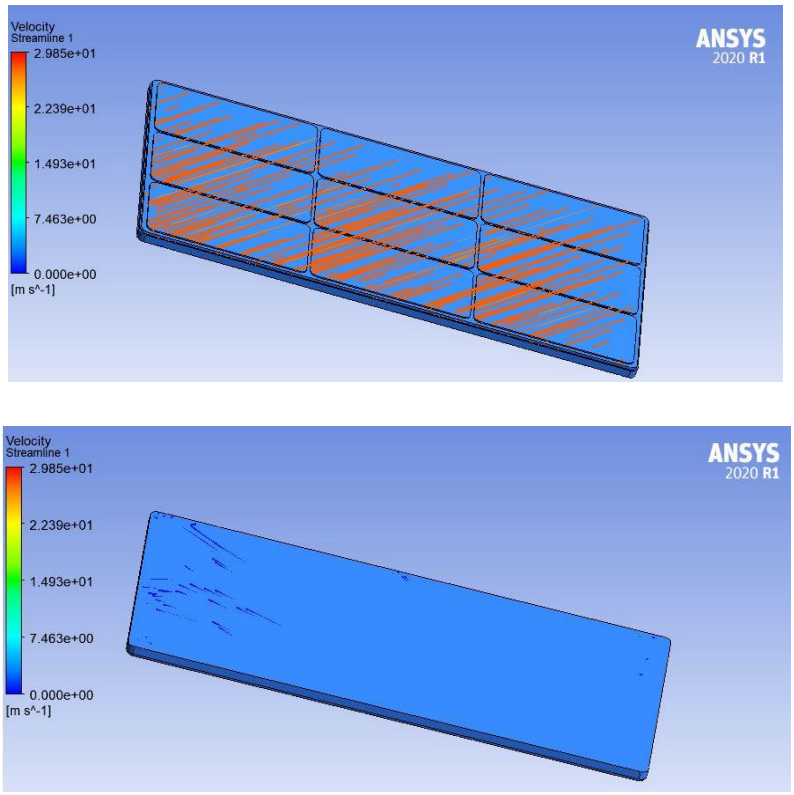

Figure 74. Fluent airflow simulation (case3).

- Results analysis:

The maximum speed of the air flow passing through the surface of the panel is 29.8 m/s, while the maximum speed of the air flow passing under the panel is 7.5 m/s. The boundary conditions of the motors' reaction forces for the third case can be seen in Figure 75.

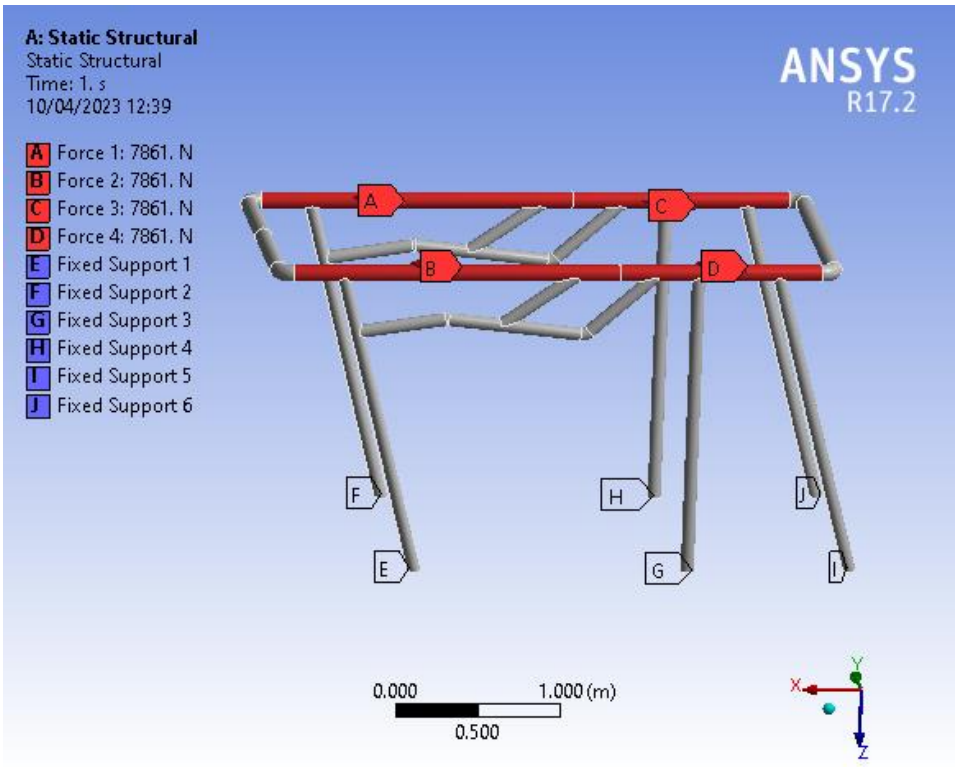

Figure 75. Boundary conditions of the motors' reaction forces (case study 3).

There is a maximum displacement of 10 mm in the top part of the structure due to the airflow passing through the solar panel surface. The airflow passing behind the solar panel is average. There is a singular point in the Von-Misses stress study. In the absence of this singular point, the maximum stress value is 54 MPa. The displacement and stress distribution plot for the third case is shown in Figure 76 and 77.

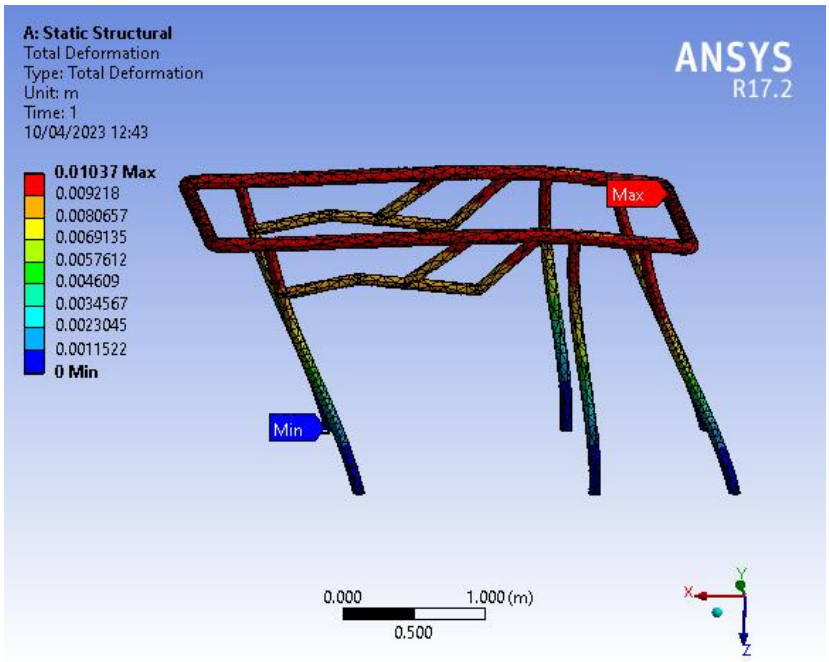

Figure 76. Displacement plot of the hardtop structure (case 3).

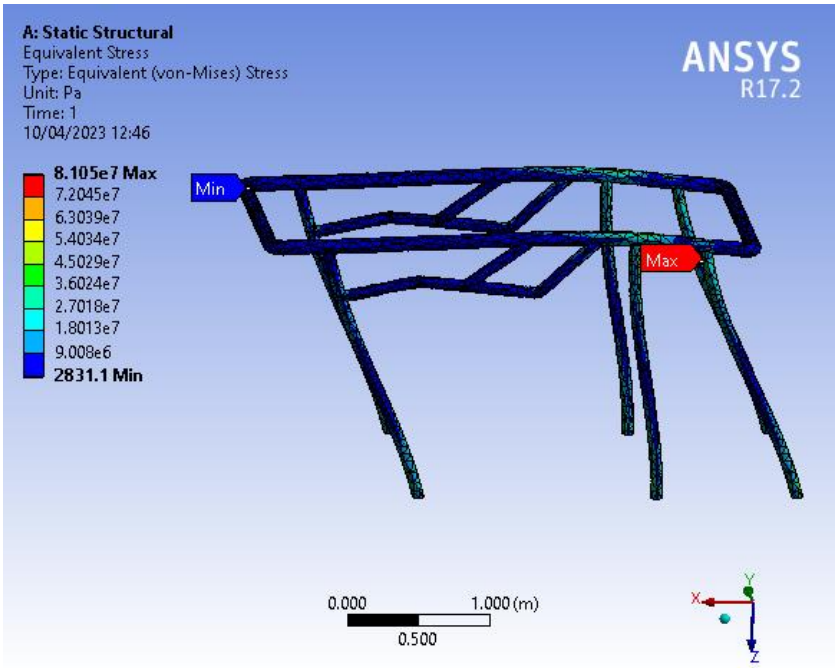

Figure 77. Stress distribution of the hardtop structure (case3).

Thus, the safety factor, in this case, has a value of:

$$\gamma = \frac{\sigma_y}{\sigma_{Max}} = \frac{276\ MPa}{54\ MPa} = 5.1 \qquad \textit{(Eq. 21)}$$

3.3.3.4 Fourth case: frontal wind gust along with maximum boat speed (forward inclined)

In this case, wind effects have been studied when the boat is sailing at maximum speed (as in the first case). We consider a frontal gust of wind (100 km/h) in this case. The airflow simulation is 150 km/h. The simulation of the flowing air flow for the third case is shown in Figure 78. The wind forces are:

$$\begin{bmatrix} F_x = 5050 & N \\ F_y = 4920 & N \\ F_z = 0 & N \end{bmatrix}$$

$$F_{R4} = \sqrt{(5050^2) + (4920^2)} = 7050\ N \qquad \textit{(Eq. 22)}$$

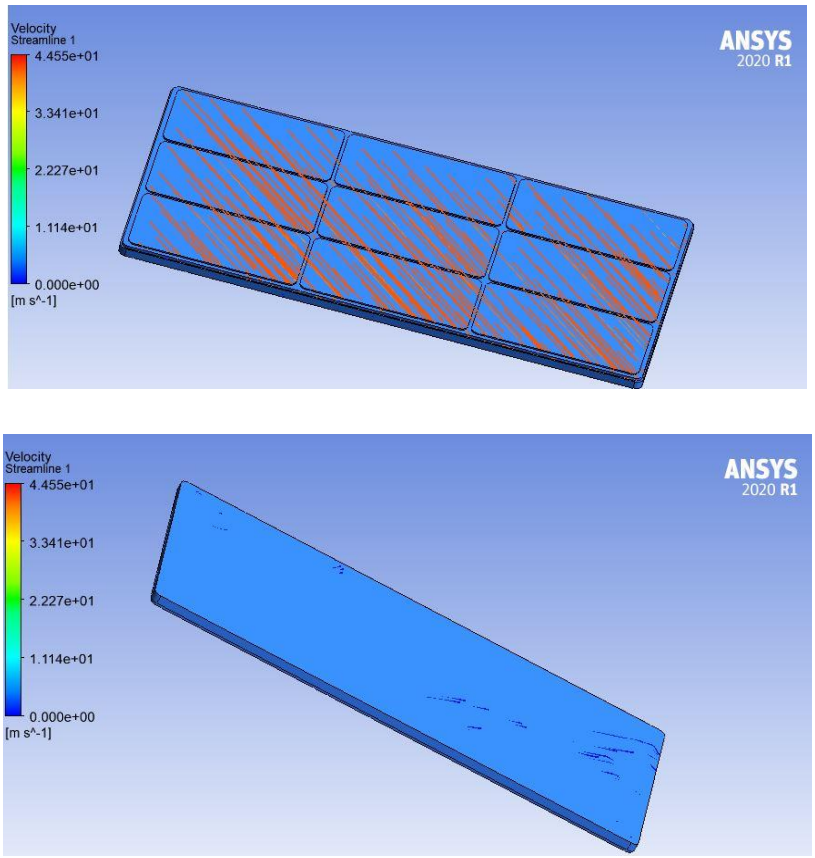

Figure 78. Fluent airflow simulation (case 4).

- Results analysis:

As in the other cases, the boundary conditions (forces) have to be updated using the fluent results, and the model has to be solved using the finite element method. There is a maximum airflow speed passing through the solar panel, and its value is 44.5 m/s. On the panel bottom, the speed of the airflow is 11.1 m/s. The boundary conditions of the reaction forces of the motors for the fourth case can be seen in Figure 79.

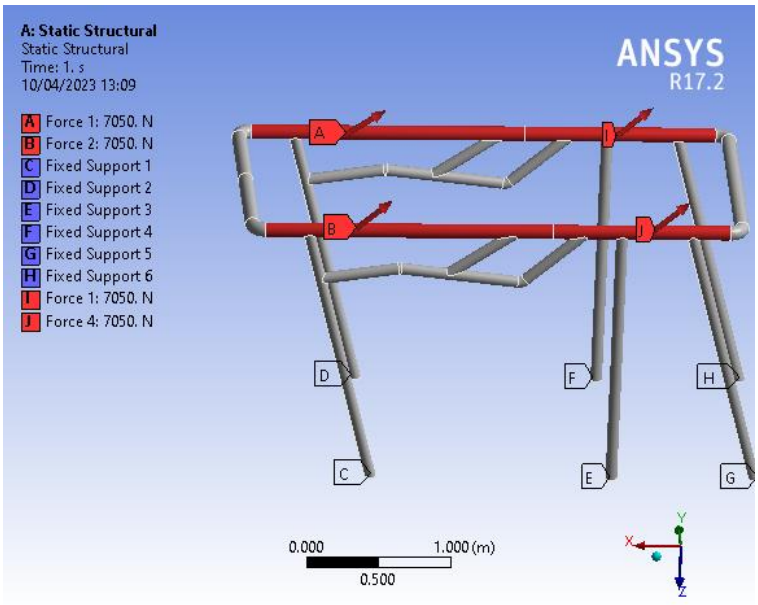

Figure 79. Boundary conditions of the motors' reaction forces (case study 4).

Then, the system has been solved, and the displacement plot and the Von-Misses stress plot were obtained. Displacement plots and stress distributions for the hardtop are shown in Figure 80 and 81. Similarly to the first case, maximum deformation with a 8.1 mm value occurs around the top and upper legs of the hardtop. The highest stress is in the hardtop legs, which have the maximum amount 42 MPa.

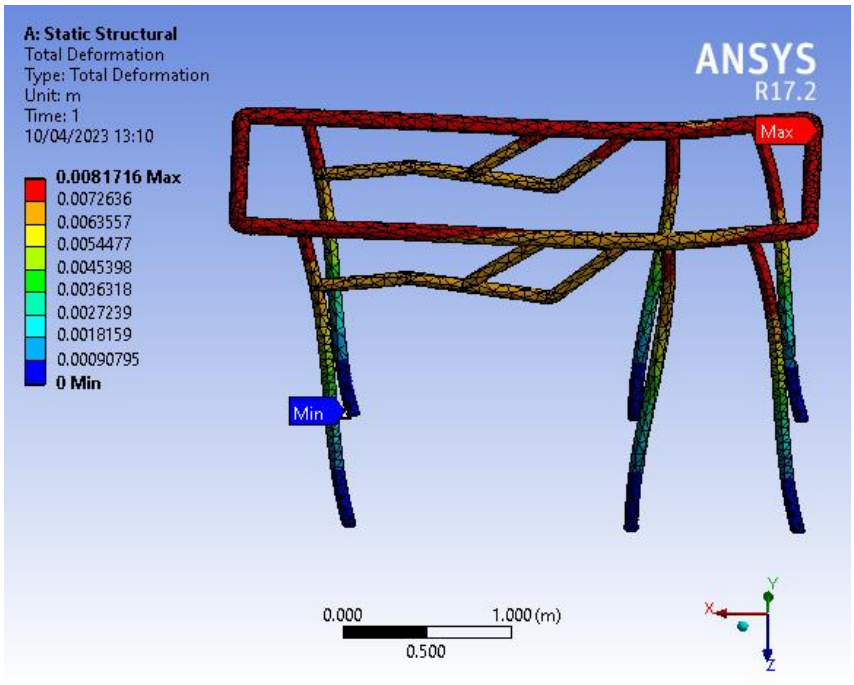

Figure 80. Displacement plot of the hardtop structure (case 4).

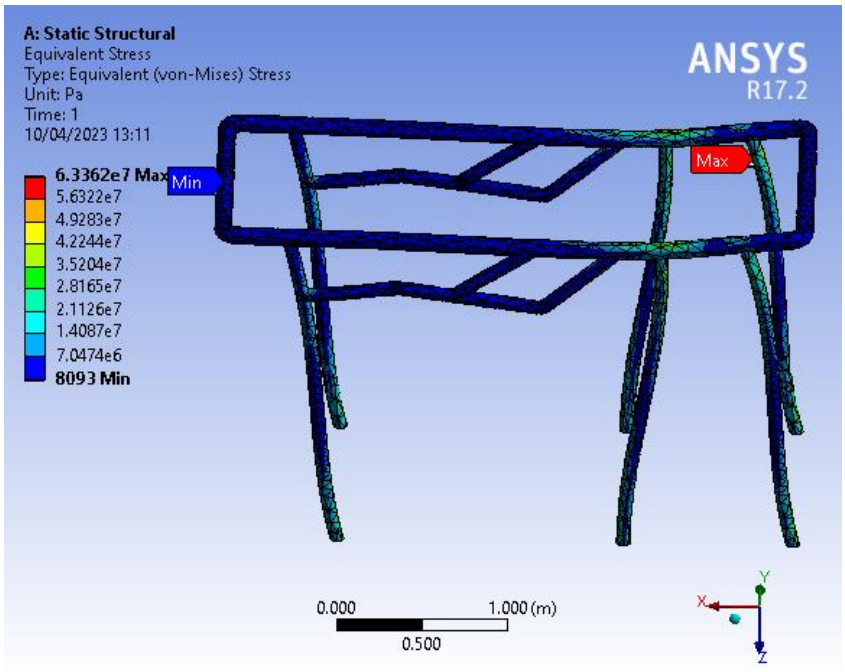

Figure 81. Stress distribution of the hardtop structure (case 4).

Thus, the safety factor is:

$$\lambda = \frac{\sigma_y}{\sigma_{Max}} = \frac{276\ MPa}{42\ MPa} = 6.6 \qquad \textit{(Eq. 23)}$$

3.4 STABILITY AND LOAD DISTRIBUTION

Since the location of the motor, solar panel, and passengers are fixed, calculations related to the loading distribution and stability of a boat must be done to find the right place for the batteries. First, we define the problem's assumptions:

- All masses are assumed to be points.
- The location of the motor, solar panel, and passengers is considered fixed and clear.
- The location of the buoyancy force is determined and considered at point (x_0, y_0)
- The names are considered as follows:

m_1=motor mass, m_2=mass of solar panels, m_3=mass of passengers, m_4=mass of batteries, l_1=Boat width, l_2=Boat length

- The coordinates of the center of mass (gravity) of each mass are considered as follows:

(x_0, y_0) : coordinates of center of buoyancy

(x_1, y_1) : Coordinates of the center of mass of the motor

(x_2, y_2) : Coordinates of the center of mass of the solar panel

(x_3, y_3) : Coordinates of the center of mass of passengers

(x_4, y_4) : Coordinates of the center of mass of batteries

To analyze the stability of boats, it is first necessary to define the terms:

Centre of gravity (G) of a ship: In a boat, the center of gravity is measured from the keel. It is the point where the weight of the boat is applied and has three components: longitudinal, transverse, and vertical [143].

Buoyancy force (B): Buoyancy is the force that supports objects in a liquid or gas. As a ship floats in still water, the pressure of water below the waterline pushes upward, creating buoyancy [144, 145].

Suppose the boat's center of gravity is always lower than the center of buoyancy of the boat. In that case, the created torque arm will create a torque against the deflection of the boat and return it to its original state, so the boat should be designed so that it has a lower center of gravity than it does a buoyancy center. Place all heavyweights (such as motors and batteries) at the bottom of the boat.

This principle is demonstrated using two different model boats. When the boat rolls, the center of buoyancy does not shift because it has a semicircular hull shape (in cross-section). During a roll, the center of gravity shifts very little, so very little torque is needed to right the boat. On the other hand, a rectangular hull can have its center of buoyancy shift considerably, creating a torque couple that tends to right the boat and result in a very stable float. Figure 82 shows how gravity and buoyancy affect the float.

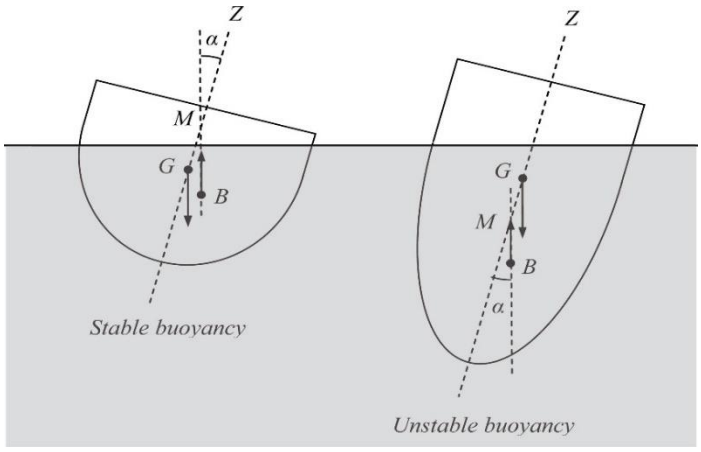

Figure 82. Effects of gravity and buoyancy on float [146].

Determination of the center of gravity of the boat [147]:

$$X_G = \frac{m_1x_1+m_2x_2+\cdots+m_nx_n}{m_1+m_2+m_3+\cdots+m_n} \quad \textit{(Eq. 24)}$$

$$Y_G = \frac{m_1y_1+m_2y_2+\cdots+m_ny_n}{m_1+m_2+m_3+\cdots+m_n} \quad \textit{(Eq. 25)}$$

$$Z_G = \frac{m_1z_1+m_2z_2+\cdots+m_nz_n}{m_1+m_2+m_3+\cdots+m_n} \quad \textit{(Eq. 26)}$$

For the least rolling and deviation and the stability of the boat, the center of buoyancy and the center of gravity of the ship should be located on the same plane in the longitudinal and latitudinal planes. The boat's center of gravity must always be lower than the center of buoyancy for the restoring arm to return the boat to its original state and not overturn it [146].

Figure 83 shows the schematic shape of the boat from its top view, in which gravity accelerates towards the inside of the plane and the approximate locations of the centers of mass are visible. Because the center of gravity on the boat must correlate with the center of buoyancy, the center of mass of the batteries must be determined based on the locations of each of these centers of mass, and then the batteries should be placed there.

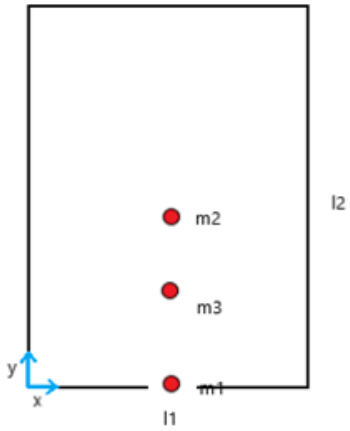

Figure 83. The boat's mass distribution.

The coordinate system is considered as follows, and the following calculations are performed:

$$m_1 + m_2 + m_3 + m_4 = M\ Boat's\ total\ mass \qquad \textit{(Eq. 27)}$$

$$x_0 = \frac{m_1x_1+m_2x_2+m_3x_3+m_4x_4}{M} \qquad \textit{(Eq. 28)}$$

$$y_0 = \frac{m_1y_1+m_2y_2+m_3y_3+m_4y_4}{M} \qquad \textit{(Eq. 29)}$$

$$(x_0, y_0) = \left(\frac{l_1}{2}, \frac{2l_2}{5}\right), (x_1, y_1) = (l_1, 0), (x_2, y_2) = \left(\frac{l_1}{2}, \frac{l_2}{2}\right), (x_3, y_3) = (\frac{l_1}{2}, \frac{l_2}{3})$$

$$l_1 = 8\ ft\ , l_2 = 23\ ft\ , m_1 = 70Kg\ , m_2 = 9 \times 2 = 18\ Kg, m_3 = 4 \times 70 = 280\ kg$$

$$m_4 = 4 \times 36.5 = 146\ Kg$$

$$x_0 = \frac{\frac{m_1l_1}{2}+\frac{m_2l_1}{2}+\frac{m_3l_1}{2}+m_4x_4}{M} \rightarrow Mx_0 = \frac{(m_1+m_2+m_3)l_1}{2} + m_4x_4 \qquad \textit{(Eq. 30)}$$

$$x_4 = \frac{Mx_0}{m_4} - \frac{(m_1+m_2+m_3)l_1}{2} \qquad \textit{(Eq. 31)}$$

$$y_0 = \frac{m_1(0)+\frac{m_2 l_2}{2}+\frac{m_3 l_2}{3}+m_4 y_4}{M} \quad \textit{(Eq. 32)}$$

$$My_0 = \frac{m_2 l_2}{2} + \frac{m_3 l_2}{3} + m_4 y_4 \quad \textit{(Eq. 33)}$$

$$y_4 = \frac{My_0}{m_4} - \frac{m_2 l_2}{2} - \frac{m_3 l_2}{3} \quad \textit{(Eq. 34)}$$

By placing the parameters, we are now able to locate the batteries:

$$x_4 = \frac{514*4}{146} - \left(\frac{70+18+280}{146}\right).(4) \rightarrow x_4 = 4.027\ feet \quad \textit{(Eq. 35)}$$

$$y_4 = \frac{514*8.8}{146} - \frac{18*23}{2*146} - \frac{280*23}{3*146} \rightarrow y_4 = 14.87\ feet \quad \textit{(Eq. 36)}$$

Following the assumptions stated above, the batteries are placed so that the centre of mass coincides with the centre of buoyancy.

Now the masses must be placed so that the center of mass (gravity) is much lower than the center of buoyancy so that the steering arm is large enough.

As such, the boat is stable against larger deflections. So, heavyweights such as the motor and battery must be placed to lower the boat's center of gravity as much as possible.

In Figure 84, the schematic view of the boat from the back can be seen, where the height of each mass is specified. That is, the acceleration of gravity in the figure below is downward. We consider the z coordinate that determines the height of each mass from the lowest point of the boat.

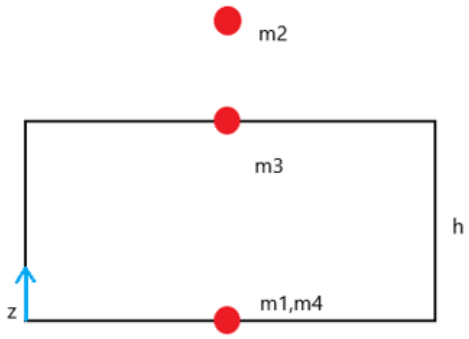

Figure 84. Schematic view of the boat's mass distribution from back.

$$Z_G = \frac{m_1(0)+m_4(0)+m_3(h)+m_2(h_p)}{M} \quad \textit{(Eq. 37)}$$

$$Z_G = \frac{m_3 h+m_2 h_p}{M} \quad \textit{(Eq. 38)}$$

$\mathrm{h} = \text{boat height} = 5 \text{ feet}, \ \mathrm{h_p} = \text{height of solar panel} = 11 \text{ feet}$

As long as this value is lower than the height of the center of buoyancy, the boat will not overturn, and the steering arm will return to its original position. The following parameters are assumed based on the boat's size:

$$Z_G = \frac{m_3 h+m_2 h_p}{m_1+m_2+m_3+m_4} \quad \textit{(Eq. 39)}$$

$$Z_G = \frac{(280*5)+(18*11)}{70+18+146+280} \quad \textit{(Eq. 40)}$$

$$Z_G = 3.1 \ feet \quad \textit{(Eq. 41)}$$

The boat must be designed so that the center of buoyancy is always 3.1 feet above the lowest point of the boat.

.

CHAPTER 4
SIMULATION OF THE PROPOSED SYSTEM IN SIMULINK

4.1 SIMULATION OF THE FIRST SCENARIO

We have modeled this part using three Simulink models. First, there is a Simulink model in which the charger and the solar panels charge the batteries. In the other one, only the charger is working; in the last one, only the panels produce energy. The first model is the most complete, so we explain here its components. Figure 85 shows this model.

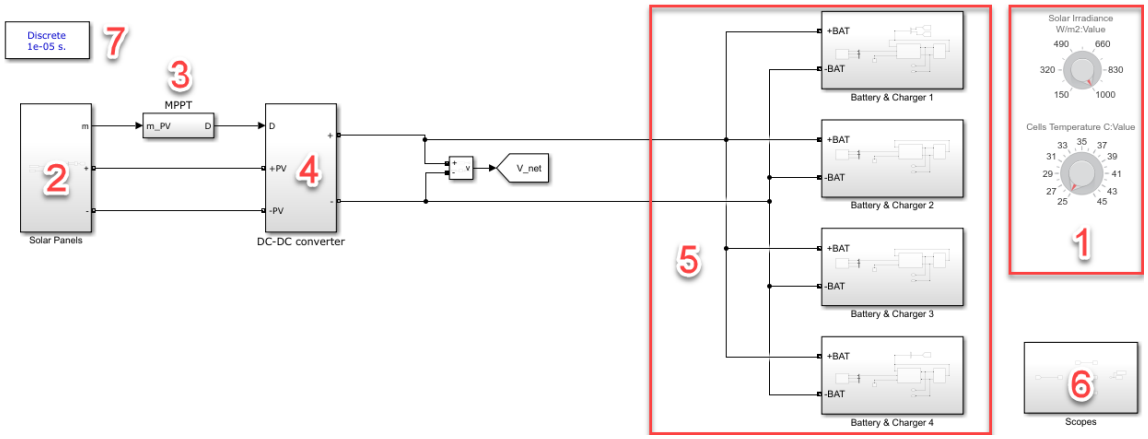

Figure 85. Simulink model of the first scenario.

Block 1: These two tools allow us to adjust the amount of radiation and temperature of the solar cells inside the block.

Block 2: The simulation of solar panels is shown in this part. Figure 86 illustrates the inside of this block. On the left side, there are two rectangular blocks. The two blocks represent the cells' inputs of radiation and temperature. It is also possible to make changes to these entries. Within this block is a solar panel block. This block has been designed to have specifications equivalent to nine parallel panels.

Figure 87 illustrates this specification. We can observe that a panel has a power of 110 W. Moreover, the upper part of the figure shows nine parallel panels arranged in a series.

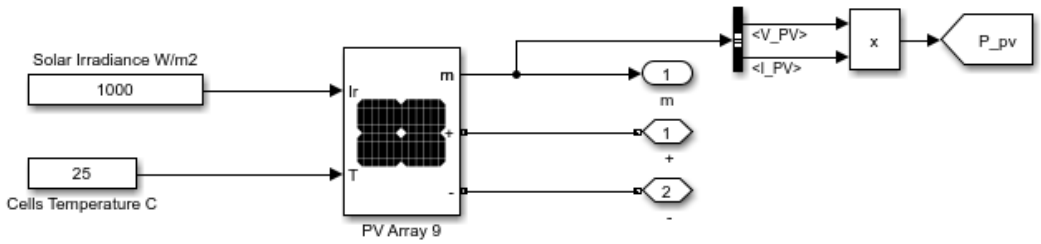

Figure 86. Photovoltaic Simulink block.

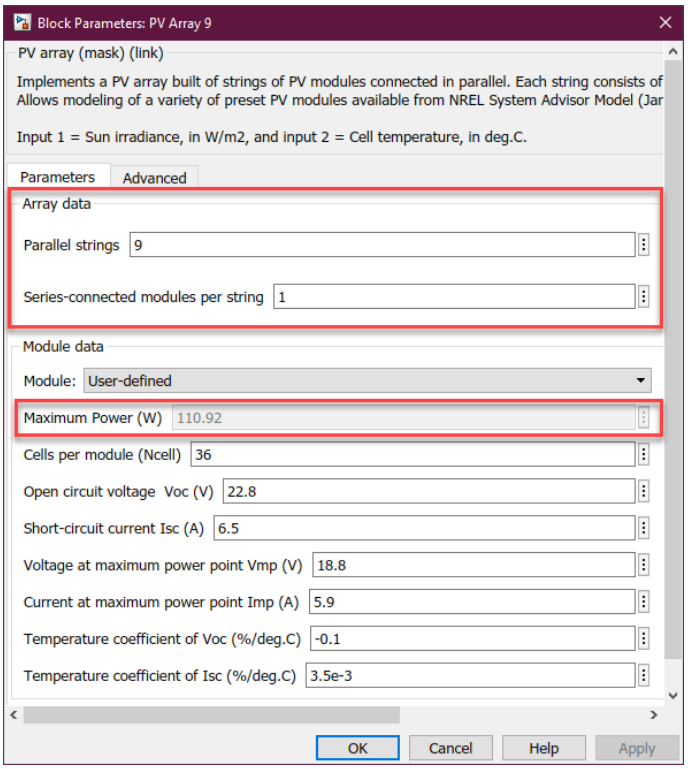

Figure 87. Solar panel's parameters.

Figure 88 shows how the solar panel power and current vary with voltage at a temperature of 25 **°C**.

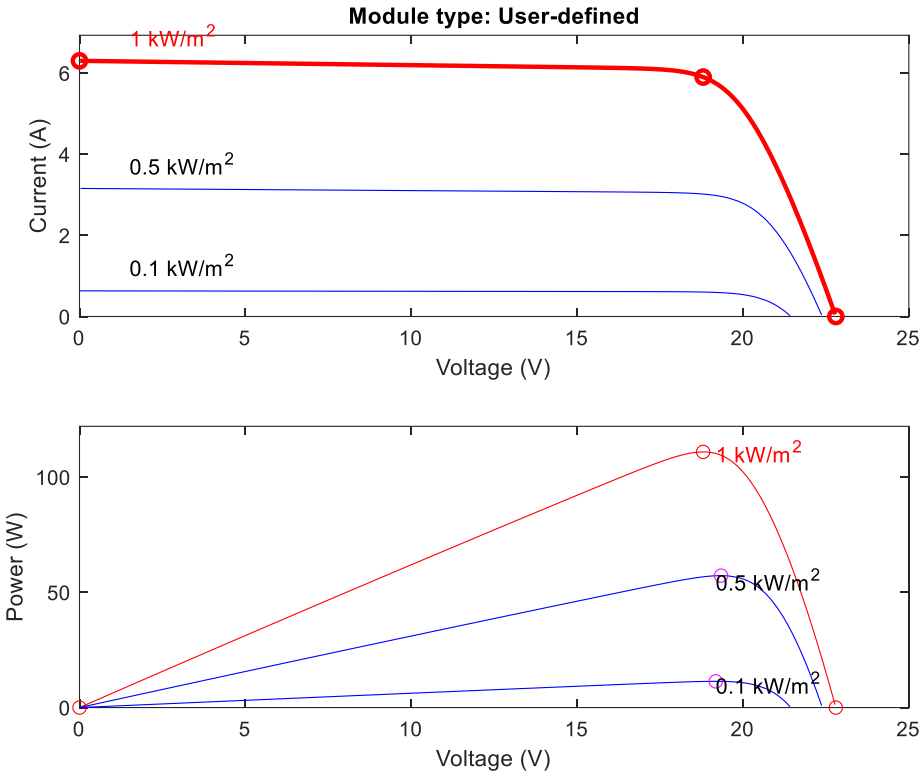

Figure 88. P-V and V-I characteristics of PV arrays for various solar irradiances.

Inside Block 3 is the MPPT controller. Typically, solar panels perform most efficiently when they are connected to an MPPT controller. Figure 89 displays this block's inside.

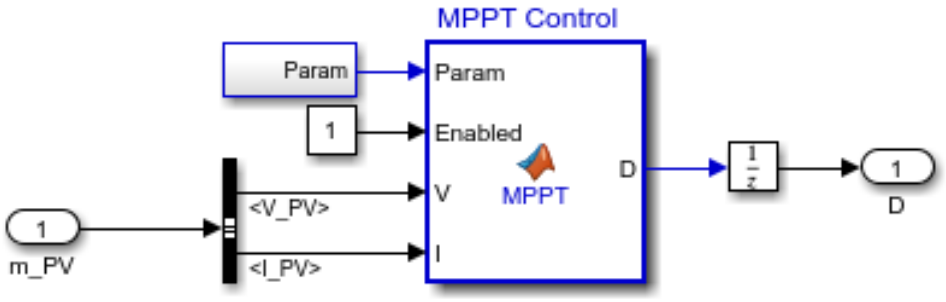

Figure 89. Inside the MPPT block.

In Block 4, a DC/DC converter is simulated to increase the parallel panel voltage. Figure 90 shows the inside of this block. An L-C model and an IGBT switch make up the boost converter. Duty cycle input switch g has only two output values, 0 and 1.

MPPT controllers generate duty cycle values. The collector, or C, is connected to the solar panel's positive terminal, and the emitter, or E, is connected to the negative terminal.

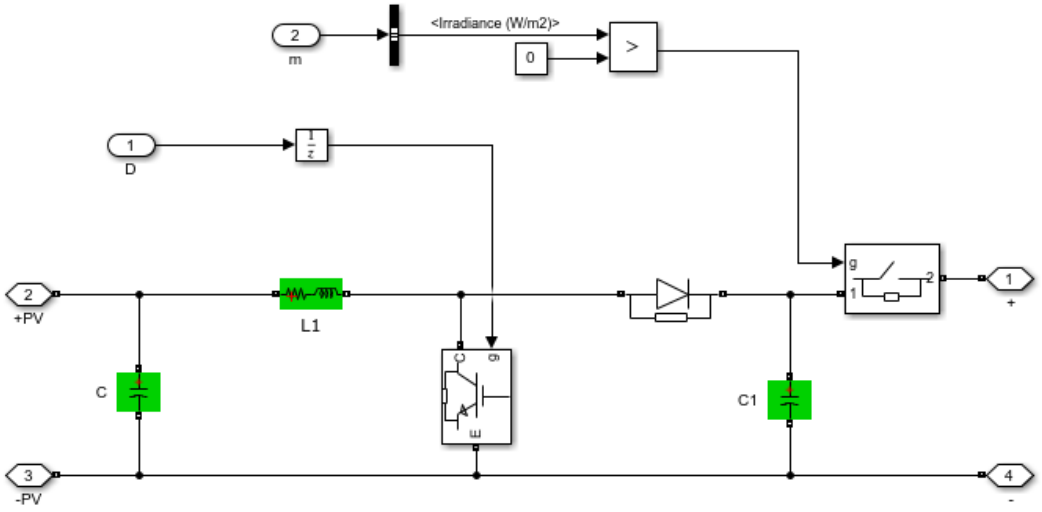

Figure 90. Boost converter in the Simulink model.

Block 5: There are four parallel batteries in each block, along with their chargers. All blocks have the same content. Next, we consider the first block. The inside of this block is shown in Figure 91.

A three-phase AC voltage source is shown on the left side. This block has a peak voltage of 120 V and a phase angle of 60 degrees. One of the phases of the voltage source is utilized to feed the charger. Finally, we find the battery on the right side of Figure 91. This lithium-ion battery has the same specifications as the selected battery (Figure 92). Again, a value of 0% is set as the initial value of the battery capacity.

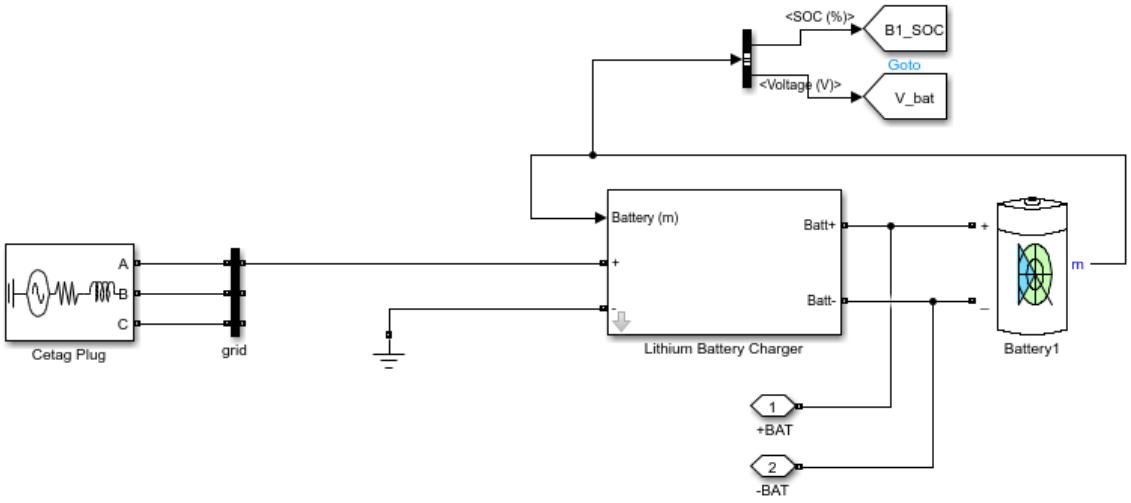

Figure 91. Details of the battery and charger in the Simulink model.

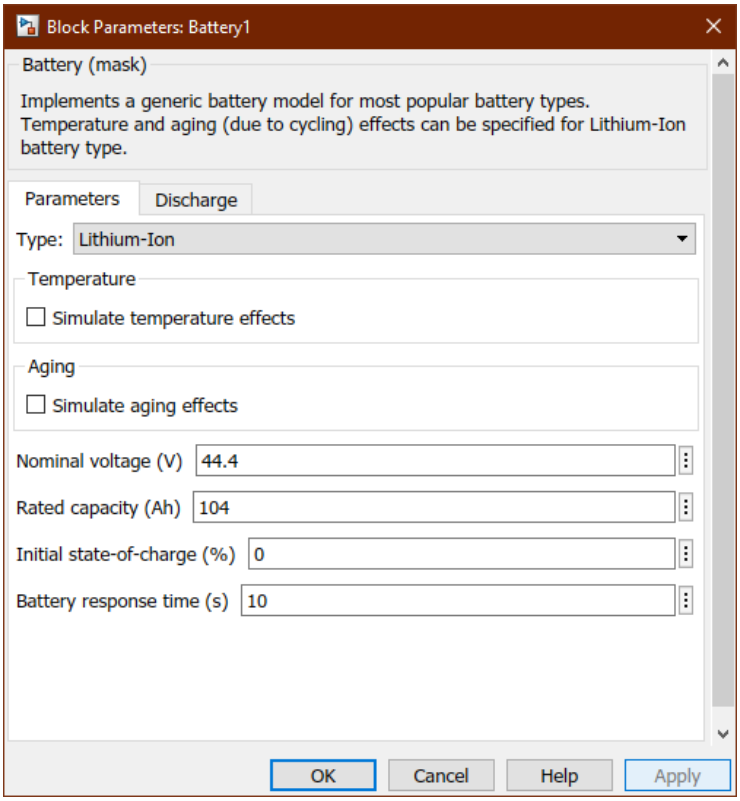

Figure 92. Nominal parameters of the lithium-ion battery in the Simulink block.

Block 6: This block displays the system's output (battery capacity).

Block 7: The simulation time step is equal to 10^{-5}

4.1.1 Panels and chargers work simultaneously

After running this simulation, Figure 93 shows each battery's charging in the presence of chargers and panels simultaneously. In about 8054 sec, the batteries were charged from 0 to 100 %.

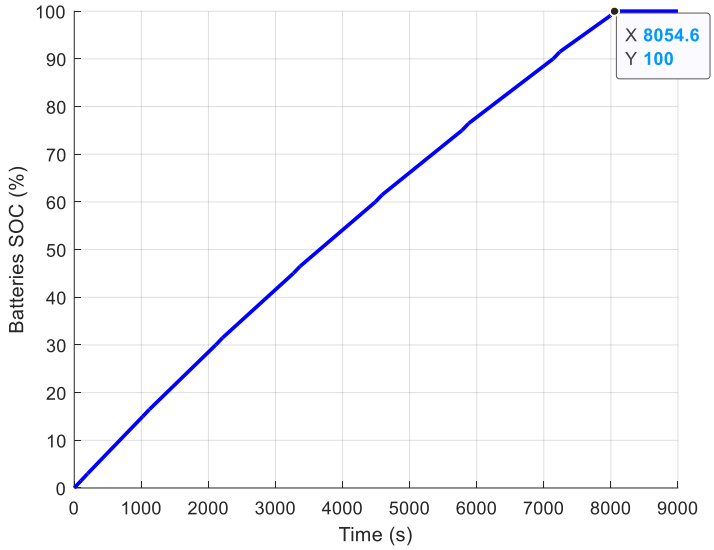

Figure 93. Battery charging process time (charger-solar panel working mode).

In Figure 94, it can be seen that the solar panels' power is around 800 W. The central network voltage is shown in Figure 95, and the battery voltage is shown in Figure 96. Both are very close to 48 V. After the solar panel's current remained constant, its power reached its maximum final value in a short period and remained constant. In Figure 95 and 96, like Figure 94, after a short period, the voltages have reached the desired value (about 48 V). The voltage fluctuations in these two forms are around the desired value.

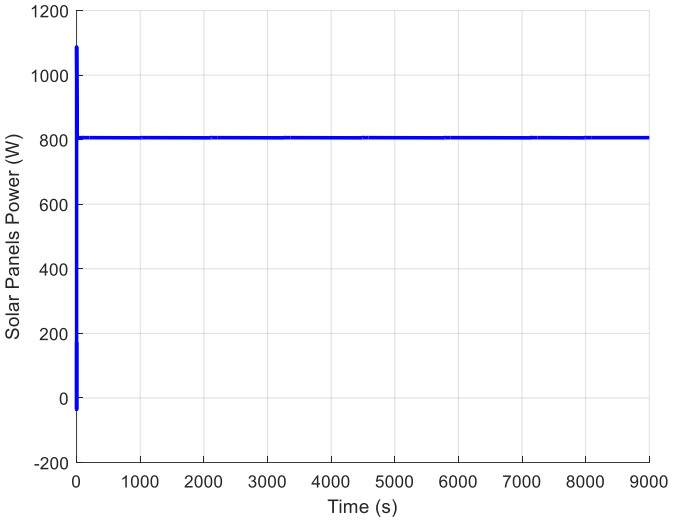

Figure 94. PV power (charger-solar panel working mode).

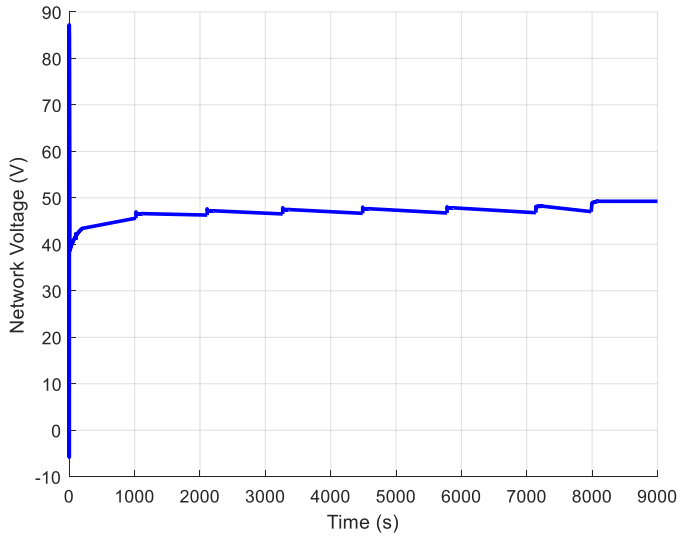

Figure 95. Central network voltage (charger-solar panel working mode).

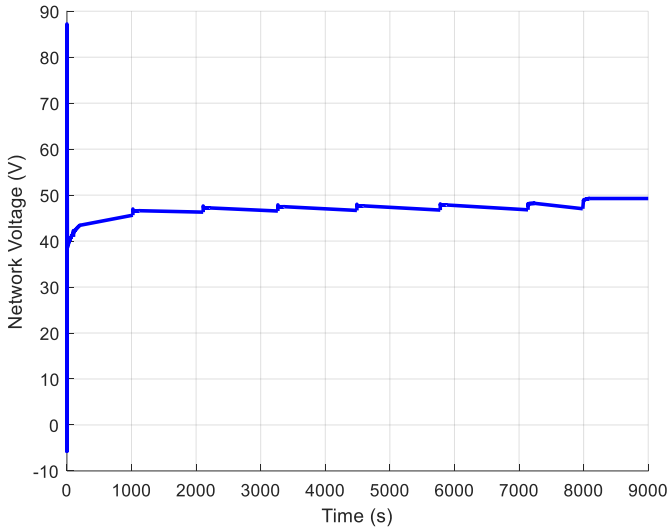

Figure 96. Battery voltage (charger-solar panel working mode).

4.1.2 Charging only via chargers

Two more simulations were done to check charging process where only the charger or solar panels work. Figure 97 shows the battery charging process through a charger.

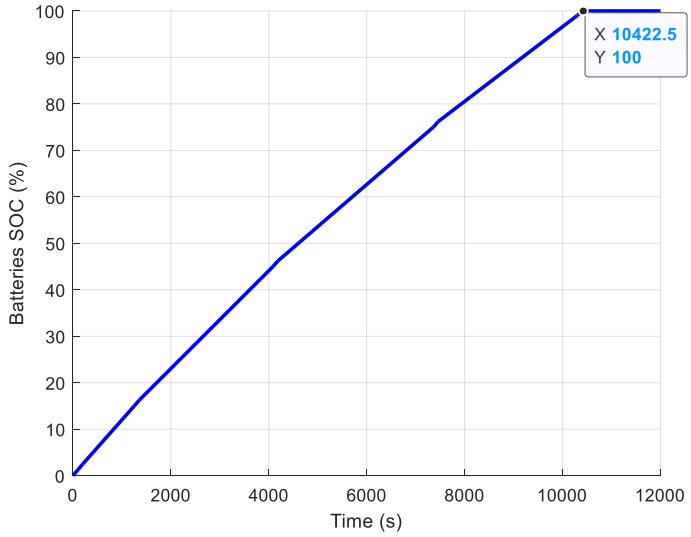

Figure 97. Battery charging (charger working mode).

Because of the absence of solar panels, the battery charging time has increased (by about 10400 sec). The central voltage and battery voltage are also shown in Figure 98 and 99. It can be seen that both voltages are still in the range of 48 V and have only minor changes.

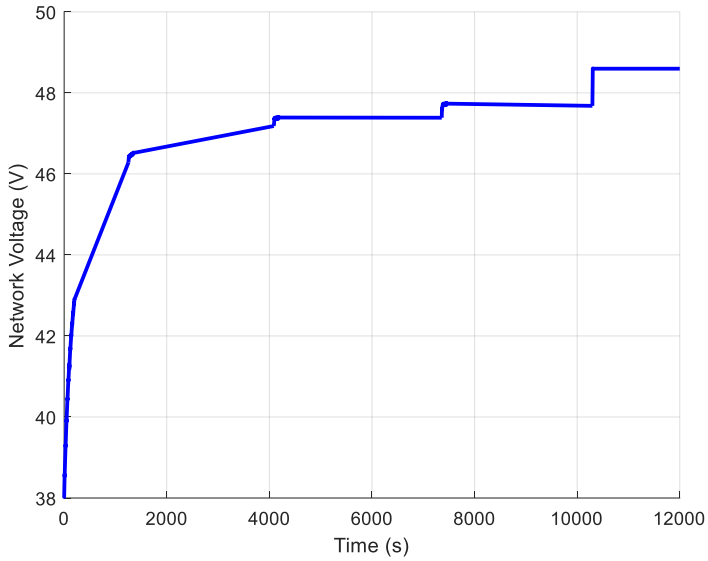

Figure 98. Central network voltage (charger working mode).

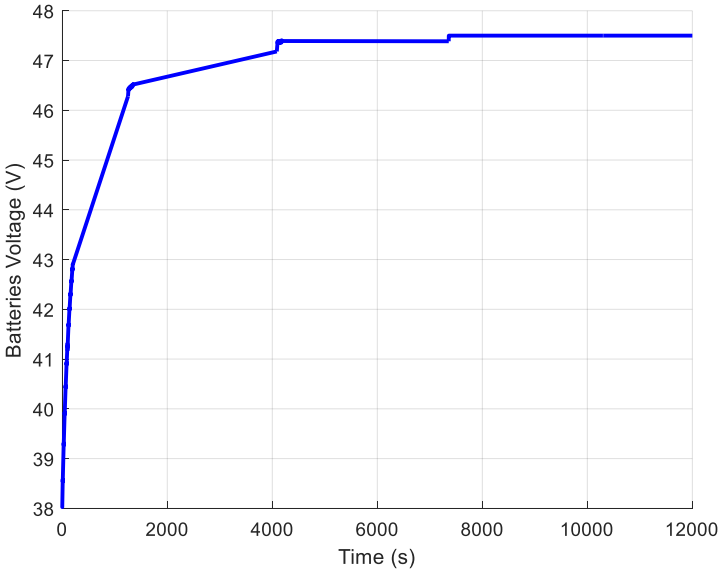

Figure 99. The voltage of battery (charger working mode).

4.1.3 Charging batteries (with solar panels only)

It takes 33480 sec to fully charge the battery (about 9 h and 20 min). Due to the absence of chargers, charging time is much longer than before (because solar panels have less power than chargers). The central voltage and batteries are the same and have reached their peaks after a short time. Figure 100 shows the battery charging time. Figure 101 shows the solar panel power.

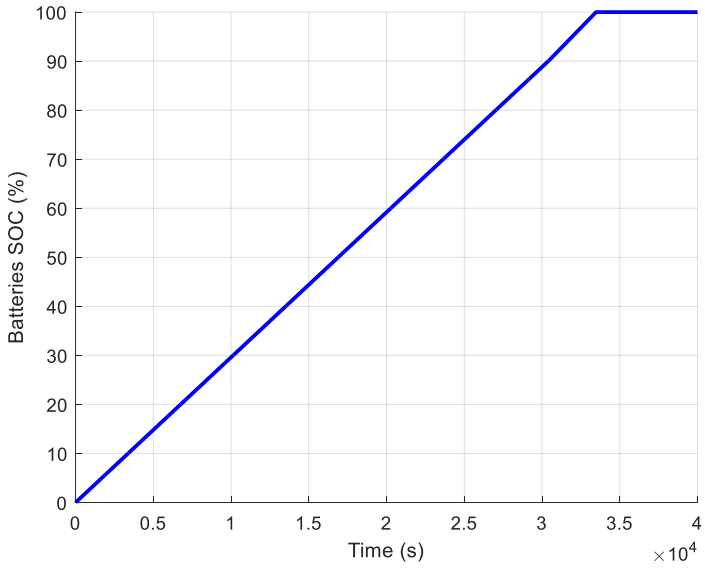

Figure 100. The battery-charging process (solar panels' working mode).

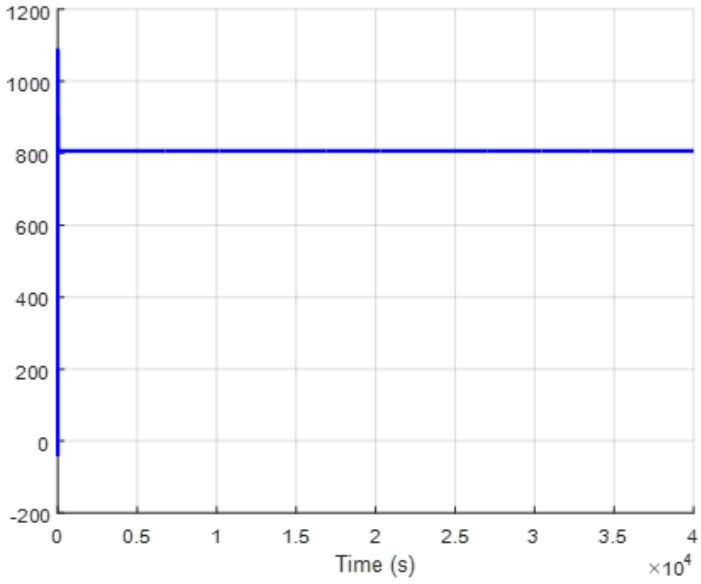

Figure 101. PV output power (solar panels' working mode).

Figure 102 and 103 show the central network voltage and battery voltage, respectively.

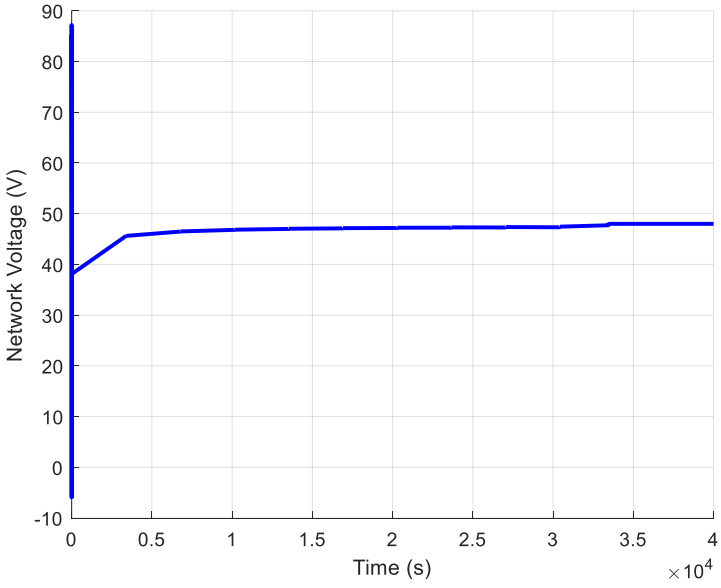

Figure 102. The central network voltage (solar panels' working mode).

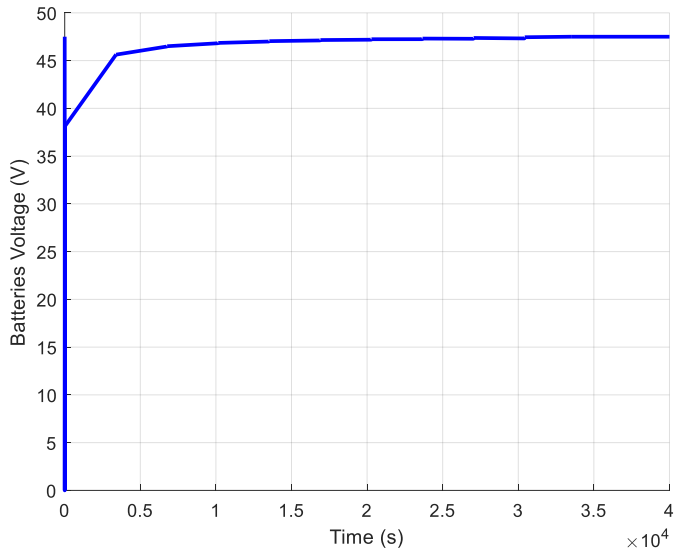

Figure 103. Battery voltage (solar panels' working mode).

4.1.4 Panels performance with solar radiation variations

According to Figure 104, a radiation function lasting 100 sec is designed to determine the effect of changes in solar radiation.

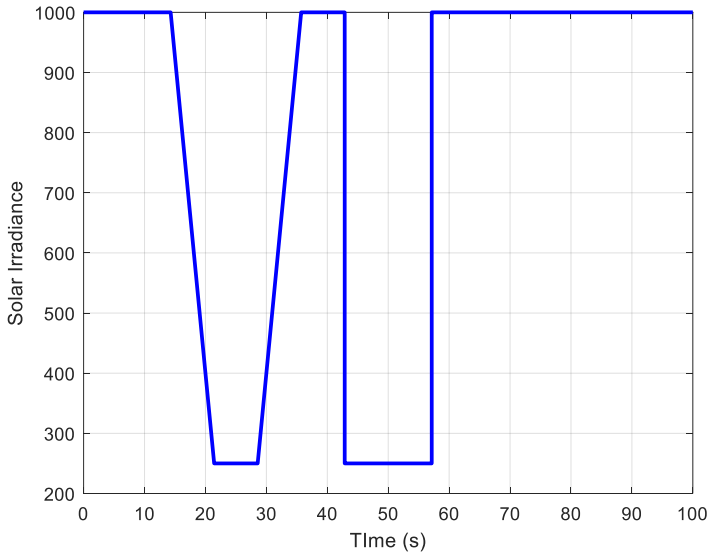

Figure 104. Unpredictable solar irradiance function.

Figure 105 shows the panels' power and battery charging based on the simulation. Again, the power and slope of the charge graph increase with the increase of radiation, while with the decrease of radiation, the opposite results occur.

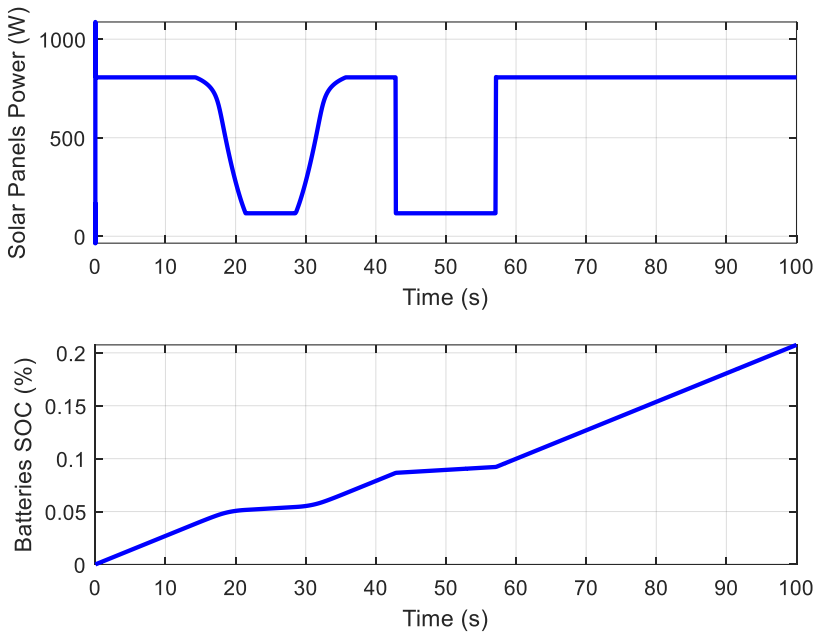

Figure 105. Solar panel power and battery charging for time-varying solar radiation.

4.2 SIMULATION OF THE SECOND AND THIRD SCENARIOS

First, we check the Simulink model related to the motor test before entering the main simulation. As shown in Figure 106, this model simulates a DC motor (No. 2) connected to two batteries (No. 1). In its initial state, the battery has a capacity of 100%. Within the motor block (Figure 107), speed and current controllers are also included (the motor is numbered 1, the speed controller is numbered 2, and the current controller is numbered 3).

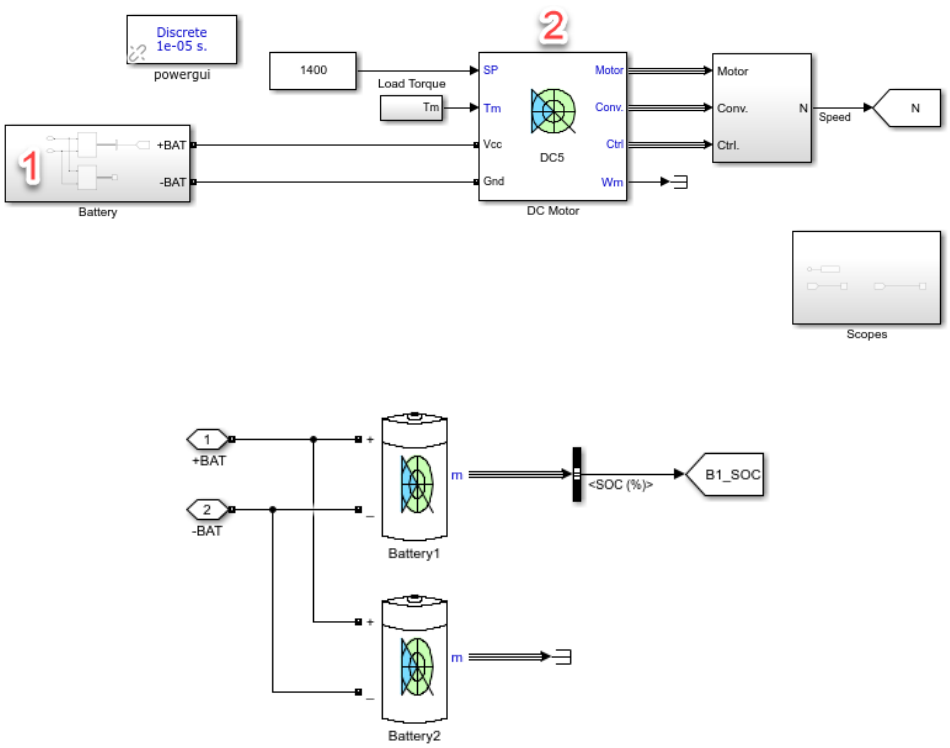

Figure 106. Simulation model for motor testing.

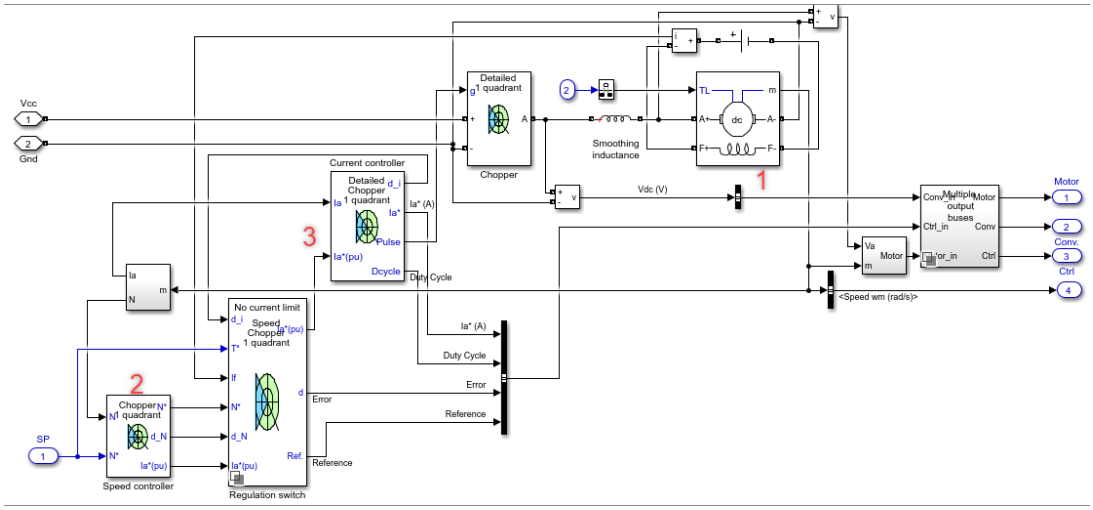

Figure 107. Dc motor model with speed and current controller.

The motor's actual speed and desired speed are shown in Figure 108 and 109. The first value of the actual motor speed is expressed in rad/sec. Figure 109 states that the desired motor speed is 1400 rpm (the highest selected motor speed). This speed is used for all simulations.

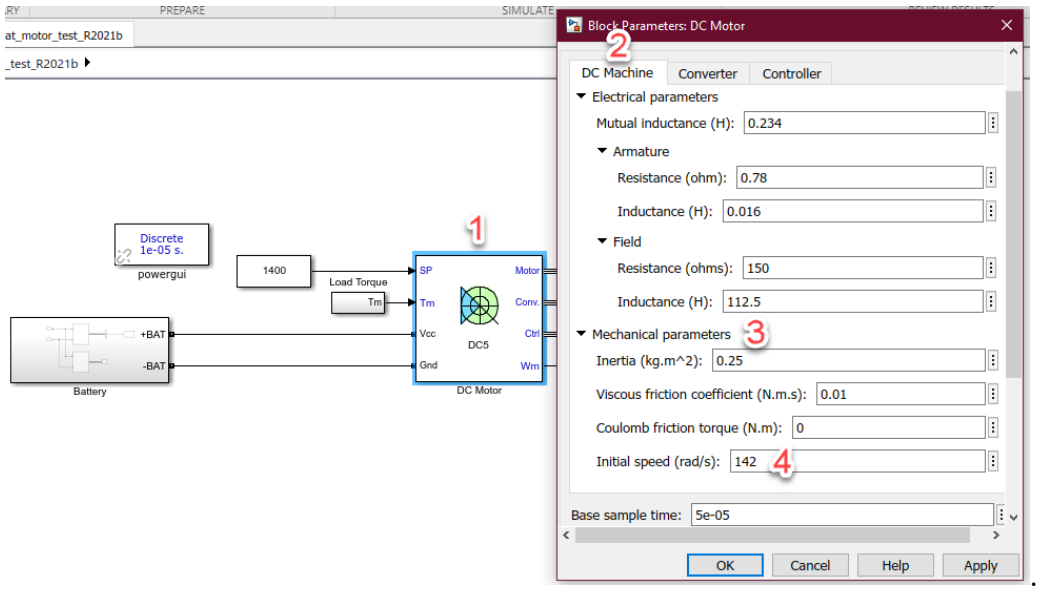

Figure 108. The actual initial speed setting for the motor.

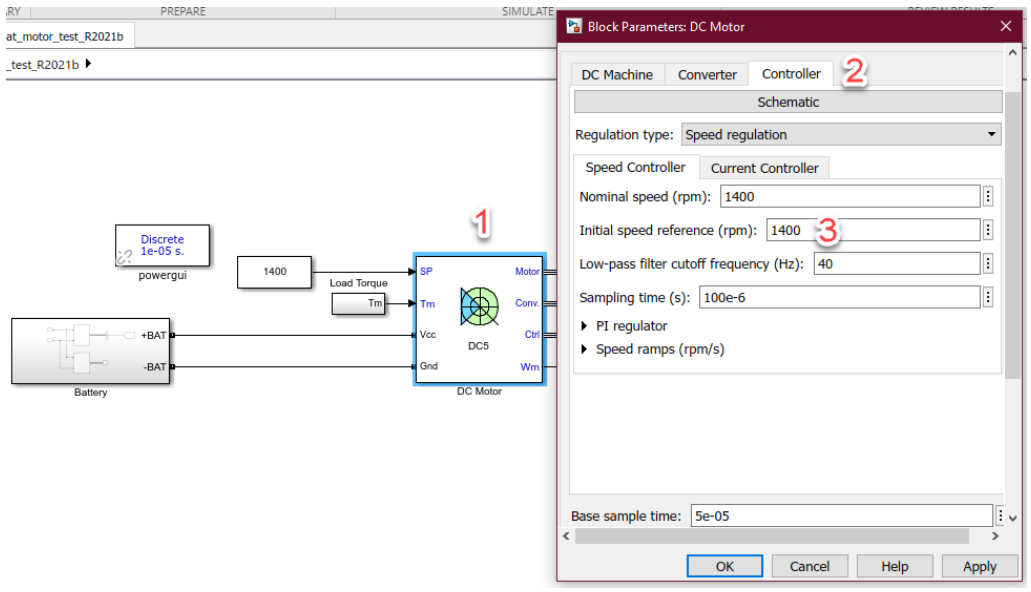

Figure 109. The desired initial speed setting for the motor.

The battery charge percentage is shown in Figure 110. The battery is discharged in about 2988 sec or less than 50 min. The timing is consistent with the information in Table 6.

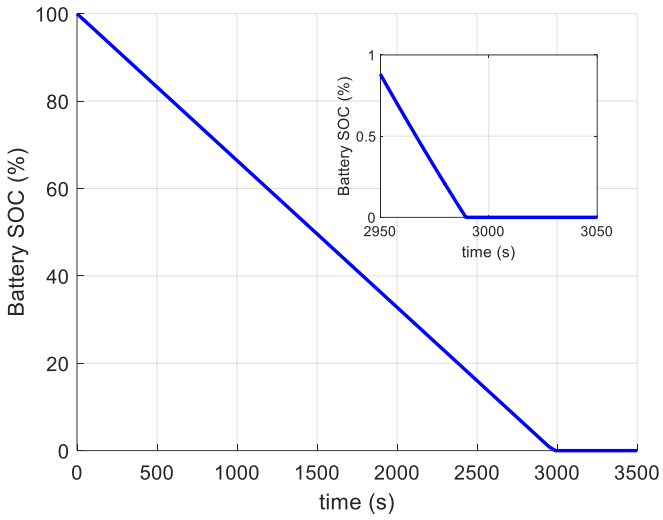

Figure 110. Battery capacity percentage in the motor test.

In Figure 111, the real and desired speed of the motor are also shown. Since the motor speed is constant throughout the simulation, the results of the first 20 sec and the end have been shown. Throughout the entire process, the actual speed tracked the desired speed, and when the battery is empty, the real speed is zero.

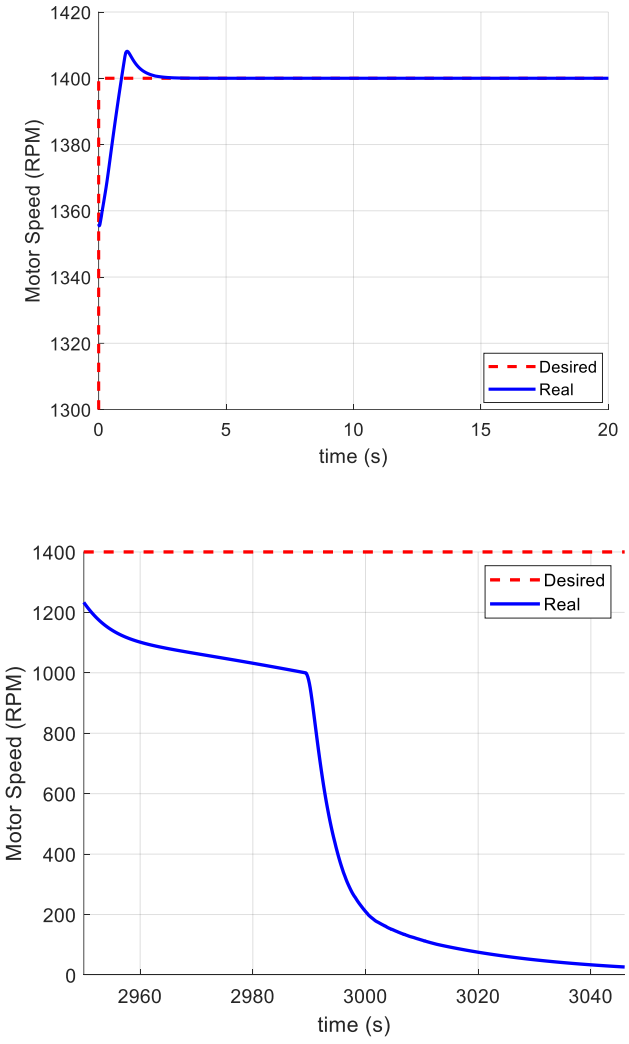

Figure 111. Motor speed change curves for real and desired speeds.

The next step is to simulate scenarios 2 and 3. This model is shown in Figure 112.

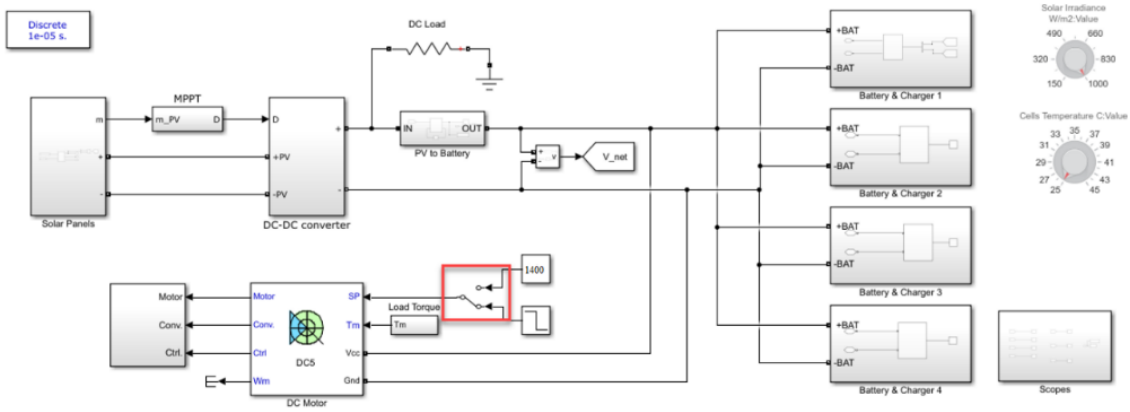

Figure 112. The Simulink model of scenarios 2 and 3.

In Figure 112, we can see that a DC load is connected to the DC-DC converter of the solar panels. Figure 113 illustrates the specifications of this load. It is estimated that this load generally consumes about 2 kW for seven to eight hours. Additionally, the load voltage is determined to be 48 V, equal to the voltage of the central network.

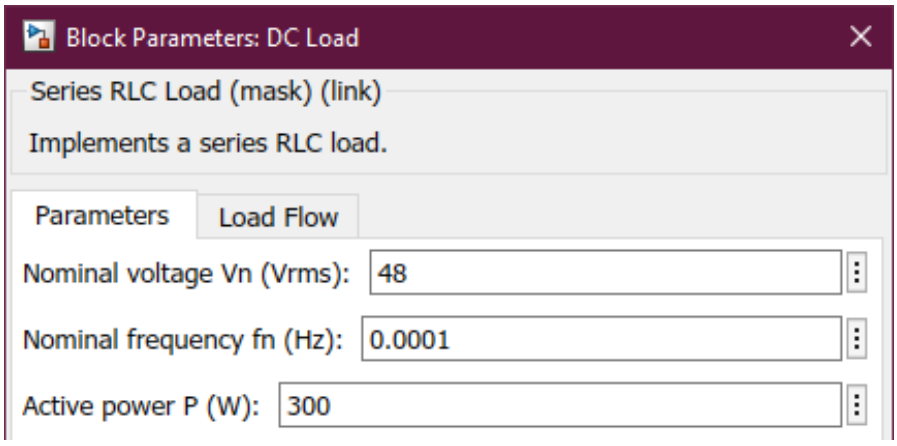

Figure 113. DC load profile.

A block is placed in front of the DC load. Whenever the battery charge percentage reaches less than 55%, the panels are connected to the battery with this block, and the battery is charged as a result. There will be a cut-off to this current when the charging percentage reaches 62%. We see from the results that the battery will be charged at a very low rate. This

is because the charging process is very long with the panels. Therefore, reaching 62% is pretty much impossible. However, it will be evident in the results that the battery will be charged at a very low rate. The red rectangle at the bottom of the Simulink model represents an input switch that receives two desired speed inputs and switches them accordingly as needed. The upper input is set to a constant speed of 1400 rpm, equivalent to the maximum motor speed (equivalent to case 2), and the lower input is set to a step input, equivalent to case 3. We considered the duration of the simulation to be 200 sec because it is not possible to simulate the entire voyage. The initial SOC value is set at 57%. Up to 140 sec, the motor works at its highest speed (1400 rpm), after which the speed decreases to 390 rpm (as shown in Figure 114 by the desired speed diagram in red colour). The Equation (33) can be used to determine the motor's actual speed in scenario 3 because the angular speed of the motor is linearly related to the linear speed [148].

$$\frac{R_3[rpm]}{1400[rpm]} = \frac{4\left[\frac{km}{hr}\right]}{14.5\left[\frac{km}{hr}\right]} \qquad \textit{(Eq. 42)}$$

$$\rightarrow R_3 \approx 390\ [rpm] \qquad \textit{(Eq. 43)}$$

Figure 114 demonstrates that the actual motor speed follows the desired speed closely. When the motor speed lowers, it takes about 30 sec for the actual speed to settle to the desired speed, which is a reasonable time.

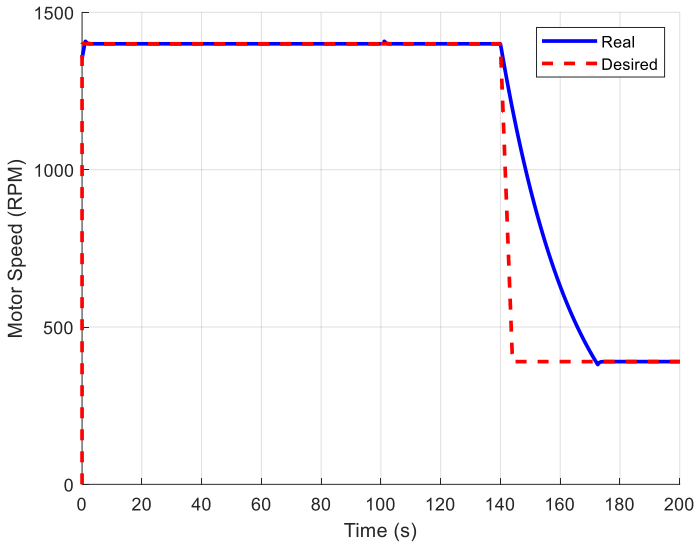

Figure 114. Motor speed changes for scenarios 2 and 3.

Figure 115 shows the motor current. We can see that when the speed is at its highest, the motor current is around 245 A, but when the speed decreases, the current decreases to around 5 A.

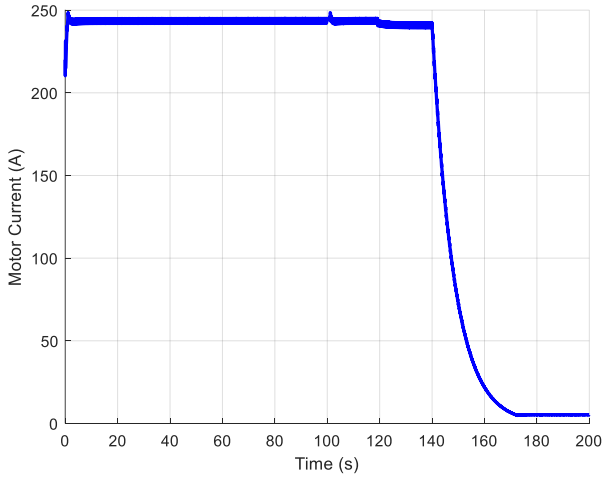

Figure 115. Motor current changes for scenarios 2 and 3.

We can calculate the changes in motor torque using Equation (44) [149]. Figure 116 shows the results of this calculation. When the motor speed is at its highest value, the motor

torque is around 8 N.m. As the motor speed lowers, the torque drops below 1 N.m (around 0.6).

$$T = Power \times 9.549/Speed\ (n) \qquad \textit{(Eq. 44)}$$

Where,

- T: torque (Nm).
- P: power (W).
- n: revolution per minute (rpm).

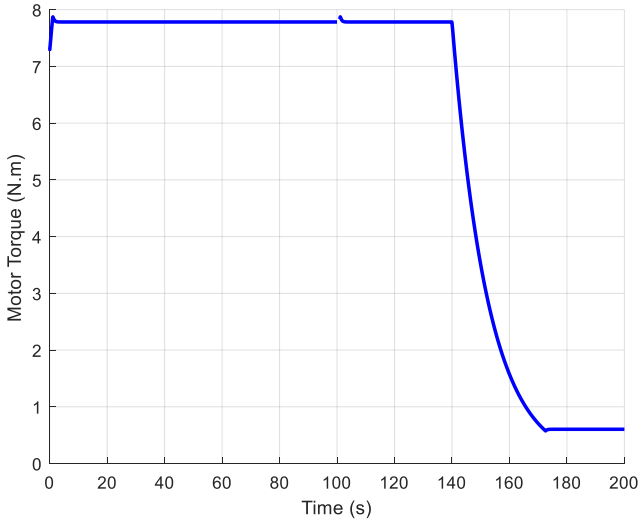

Figure 116. Motor torque changes for scenarios 2 and 3.

Figure 117 illustrates the PV output. We can see that, with the use of MPPT, their power remains constant (about 800 W). Also, convergence at this maximum power occurs in a short time.

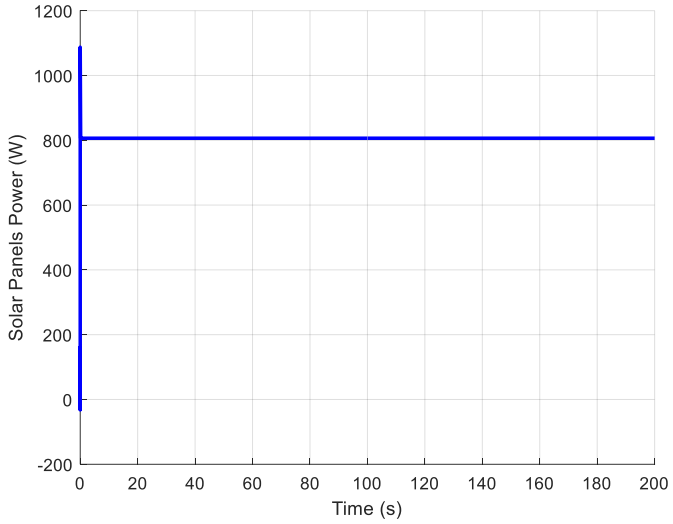

Figure 117. Solar panel output changes for scenarios 2 and 3.

The central and battery bank voltages are shown in Figure 118 and 119. It can be seen that both voltages are very close to 48 V. Also, by changing the speed of the motor, the voltage increases by a very small amount.

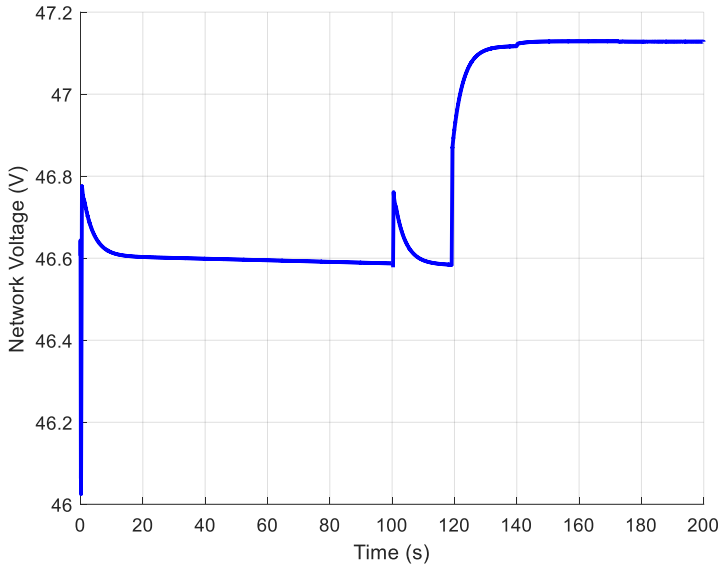

Figure 118. Central voltage changes for scenarios 2 and 3.

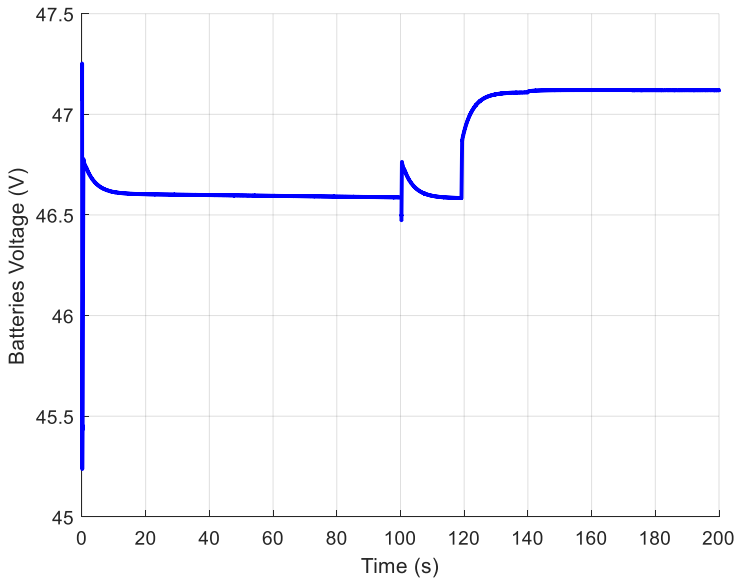

Figure 119. Battery voltage changes for scenarios 2 and 3.

The batteries' SOC is shown in Figure 120. We can see that the battery starts charging as soon as the SOC percentage is reduced to 55%. We can see that the discharge rate of batteries is much higher than their charging rate, and this is due to the solar panel's output.

In addition, as the motor speed decreases, the slope of charging the batteries increases slightly.

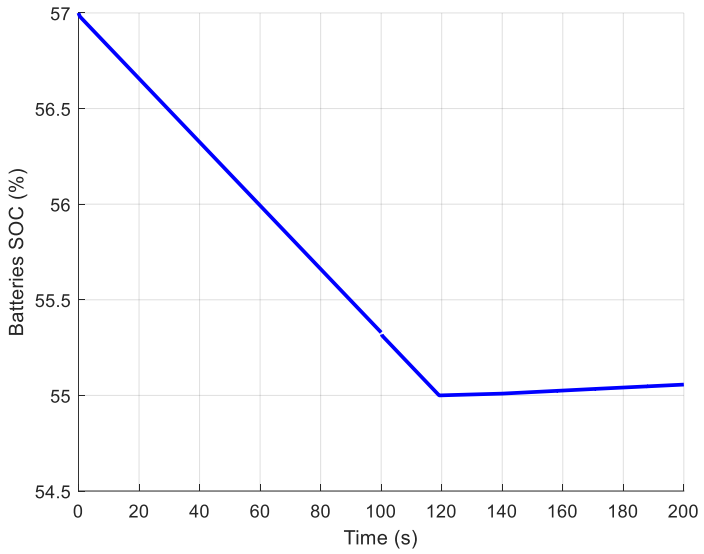

Figure 120. Battery charge percentage changes for scenarios 2 and 3.

CHAPTER 5
CONCLUSION AND FUTURE DEVELOPMENT

5.1 GENERAL CONCLUSION

This study suggests that a diesel engine on a medium-sized catamaran boat could be replaced by electric propulsion using batteries and solar panels. This project's main objective is to establish the continuous operation of the electric boat and a stable speed regardless of the time of day and weather conditions that could affect solar irradiance, which is directly related to the solar panel that charges the batteries. The main parts of the boat's electrical system are the photovoltaic panel, the battery system, and the installation of equipment on board. To achieve the goals of this project, component sizing, electrical design, and implementation of an MPPT charge controller and a DC motor with an IGBT controller are presented. We have also developed a connection proposal. Designing a hardtop is necessary to create a shadow and place solar panels on the boat, so we designed an aluminium roof for the boat. By analyzing similar diesel engines and comparing them with the electric propulsion system, we found a 12 kW electric motor would be suitable for propulsion system development. We calculated the amount of power required on a daily voyage by considering the boat's length and width, its maximum speed (8.0 kn), and electrical equipment consumption. The electrical energy required for each trip is 17.3 kWh. It is understood that there will be excess electrical power to be generated by the two sources (battery and solar panels). We designed the boat in 3D perspective using SolidWorks software. With only a few changes, the proposed hardtop and the designed electric propulsion system can be put on any boat up to 10 tons with the same range and weight.

Ansys Workbench was used to test the designed hardtop's stability during extreme weather and load conditions. The wind flow was applied at different speeds and directions to

measure the hard top's safety, and the solar panels were tilted in various directions (maximum position). Results confirm that the hardtop's safety factor is acceptable. An orientation system is necessary for boats to maximize efficiency and reach the optimal angle of the solar panels. The suggested system has movement restrictions, but the panels' efficiency can be improved to an acceptable level by tilting them. The electrical connection between all the components has also been designed for different scenarios (sailing mode, fishing mode, docked position, and off position).

Matlab Simulink was used to model the dynamic behavior of the designed system, which was made up of PV (990 W), MPPT controller (50 A), a battery bank (44.4 V, 450 Ah), and a DC motor (12 kW, 1400 rpm). Since the system contains several complex blocks and the boat's voyage lasts eight hours, the simulation was only run for 200 seconds because computing the full time would take many days.

During the dynamic simulation, the random function of the sun's irradiance was used to test the charging process and power supply of the boat's equipment. The MPPT was designed using the Perturb & Observe method. The solar panel's output power is stored in the battery bank, so the boat's onboard electronics can use it. We considered a switching circuit for charging batteries with solar panels. Whenever the battery charge percentage reaches 55%, the panels start charging the battery at a low current rate. We designed the battery bank so that the system is entirely independent of weather conditions (solar panel efficiency).

Even though the solar irradiance changes over time, the boat motor's output speed maintains the same thanks to switching circuit blocks and the PV panels' MPPT system.

The proposed design results demonstrated that it maintained stable operation and speed compared with other designs from the previous work that had trouble with power stability and continuity when weather conditions like solar irradiance changed. In all simulations, successful results were reported. The results prove that it is possible to replace the standard fuel engine with an electric one without changing the boat's weight or dimensions.

5.2 FUTURE DEVELOPMENT

- Developing larger hardtops for ocean boats would be an interesting future project.
- Due to the computer's slow processing speed, a Matlab dynamic simulation was run for 200 sec to observe equipment behavior over time. The solution to this problem is to simulate a computer with a faster processing speed or a simple model that can run for eight hours.
- For more complicated designs, a microcontroller is recommended to manage power for the PV array, battery bank, DC motor, and other equipment.
- In the future study, we can consider an orientation mechanism for hardtop solar panels that can rotate in any direction (which was designed conceptually in this project).
- Since the electrical propulsion system parts chosen for this thesis are typical for medium-sized catamaran boats, a detailed economic analysis of the system and hardtop design should be conducted before large-scale manufacture.
- This research covers solar panel size, battery size, MPPT, dynamic modeling, instrumentation design, and battery-powered boat control. A physical system is required to validate the transportation system's feasibility.
- Future research could design and install different kinds of solar PV cells, implement a boat control system, and improve weather forecasts to increase renewable energy efficiency and storage.
- During the rainy and winter seasons, solar power is low. To solve this problem, this study uses a highly advanced battery bank as one of the main power sources. Further research may be done on implementing other renewable energy sources as a backup.

BIBLIOGRAPHIC REFERENCES

[1] Issa, M., et al., *A review and economic analysis of different emission reduction techniques for marine diesel engines.* Open Journal of Marine Science, 2019. 9(03): p. 148.

[2] Issa, M., A. Ilinca, and F. Martini, *Ship Energy Efficiency and Maritime Sector Initiatives to Reduce Carbon Emissions.* Energies, 2022. 15(21): p. 7910.

[3] Lindstad, E. and A. Rialland, *LNG and cruise ships, an easy way to Fulfil regulations—versus the need for reducing GHG emissions.* Sustainability, 2020. 12(5): p. 2080.

[4] Mihanović, L., et al. *Experimental investigation of exhaust emission from marine diesel engines*. in *2020 5th International Conference on Smart and Sustainable Technologies (SpliTech)*. 2020. IEEE.

[5] Fernández, G., et al., *Photovoltaic generation impact analysis in low voltage distribution grids.* Energies, 2020. 13(17): p. 4347.

[6] Breuer, J.L., et al., *How to reduce the greenhouse gas emissions and air pollution caused by light and heavy duty vehicles with battery-electric, fuel cell-electric and catenary trucks.* Environment international, 2021. 152: p. 106474.

[7] Abbas, T., M. Issa, and A. Ilinca, *Biomass cogeneration technologies: A review.* Journal of Sustainable Bioenergy Systems, 2020. 10(1): p. 1-15.

[8] Barbosa, R., et al., *Variable Speed Diesel Electric Generators: Technologies, Benefits, Limitations, Impact on Greenhouse Gases Emissions and Fuel Efficiency.* Journal of Energy and Power Technology, 2022. 4(1): p. 1-21.

[9] Bleviss, D.L., *Transportation is critical to reducing greenhouse gas emissions in the United States.* Wiley Interdisciplinary Reviews: Energy and Environment, 2021. 10(2): p. e390.

[10] Elrawy, W., *Developing a Business Plan for an Innovative Electric Boats Trading Company in UAE.* 2022.

[11] Nguyen, H.P., et al., *The electric propulsion system as a green solution for management strategy of CO2 emission in ocean shipping: A comprehensive review.* International Transactions on electrical energy systems, 2021. 31(11): p. e12580.

[12] Kapuścik, W., et al. *AGH Solar Boat–the analysis of energy and ecological parameters of the solar powered boat*. in *IOP Conference Series: Earth and Environmental Science*. 2019. IOP Publishing.

[13] Haxhiu, A., et al., *Electric power integration schemes of the hybrid fuel cells and batteries-fed marine vessels—An overview.* IEEE Transactions on Transportation Electrification, 2021. 8(2): p. 1885-1905.

[14] Spagnolo, G.S., et al., *Solar-electric boat.* Journal of Transportation Technologies, 2012. 2(2): p. 144-149.

[15] Utama, I., et al. *New concept of solar-powered catamaran fishing vessel*. in *Proceeding of the 7th International Conference on Asian and Pasific Coasts*. 2013.
[16] Shahira, U., et al. *Electrical Design of Solar-powered Recreational Boat in Malaysia*. in *2022 IEEE International Conference on Power and Energy (PECon)*. 2022. IEEE.
[17] research, D.b.m. *Global Electric Boat Market – Industry Trends and Forecast to 2028*. 2023; Available from: https://www.databridgemarketresearch.com/reports/global-electric-boat-market.
[18] research, A.m. *Electric boat market*. 2023; Available from: https://www.alliedmarketresearch.com/electric-boat-market-A08766.
[19] Pan, P., et al., *Research progress on ship power systems integrated with new energy sources: A review*. Renewable and Sustainable Energy Reviews, 2021. 144: p. 111048.
[20] Sharma, K. and P. Syal, *A Review on Solar Powered Boat Design.* International Research Journal on Advanced Science Hub, 2021. 3: p. 1-10.
[21] Sousa, G.C., D.S. Simonetti, and E.E. Norena. *Efficiency optimization of a solar boat induction motor drive*. in *Conference Record of the 2000 IEEE Industry Applications Conference. Thirty-Fifth IAS Annual Meeting and World Conference on Industrial Applications of Electrical Energy (Cat. No. 00CH37129)*. 2000. IEEE.
[22] Postiglione, C.S., et al. *Propulsion system for an all electric passenger boat employing permanent magnet synchronous motors and modern power electronics*. in *2012 Electrical Systems for Aircraft, Railway and Ship Propulsion*. 2012. IEEE.
[23] Mahmud, K., S. Morsalin, and M.I. Khan, *Design and fabrication of an automated solar boat.* International Journal of Advanced Science and Technology, 2014. 64: p. 31-42.
[24] Salleh, N., W. Muda, and S. Abdullah. *Feasibility study of optimization and economic analysis for grid-connected renewable energy electric boat charging station in Kuala Terengganu*. in *2015 IEEE Conference on Energy Conversion (CENCON)*. 2015. IEEE.
[25] Chakraborty, S., S.S. Ullah, and M. Razzak. *Quantifying solar potential on roof surface area of fishing trawlers in Chittagong Region in Bangladesh*. in *2016 IEEE Innovative Smart Grid Technologies-Asia (ISGT-Asia)*. 2016. IEEE.
[26] Kabir, S.L., et al. *Solar powered ferry boat for the rural area of Bangladesh*. in *2016 International Conference on Advances in Electrical, Electronic and Systems Engineering (ICAEES)*. 2016. IEEE.
[27] Leung, C. and K. Cheng. *Zero emission solar-powered boat development*. in *2017 7th International Conference on Power Electronics Systems and Applications-Smart Mobility, Power Transfer & Security (PESA)*. 2017. IEEE.
[28] Obaid, W., A.-K. Hamid, and C. Ghenai. *Hybrid Power System Design for Electric Boat with Solar Irradiance Forcasting*. in *2018 6th International Renewable and Sustainable Energy Conference (IRSEC)*. 2018. IEEE.
[29] Chao, R.-M., H.-K. Lin, and C.-H. Wu. *Solar-powered boat design using standalone distributed PV system*. in *2018 IEEE International Conference on Applied System Invention (ICASI)*. 2018. IEEE.

[30] Ghenai, C., et al. *Design of solar PV/fuel cell/diesel generator energy system for Dubai ferry*. in *2019 Advances in Science and Engineering Technology International Conferences (ASET)*. 2019. IEEE.
[31] Padwad, D. and H.K. Naidu. *A Review of Electrical Boat Vehicle Solar Generation for Energy Sustainability and Development*. in *2022 10th International Conference on Emerging Trends in Engineering and Technology-Signal and Information Processing (ICETET-SIP-22)*. 2022. IEEE.
[32] Maimon, D., *Electric propulsion of ships and its advantages for anchor lifting towing vessels.* Annals of" Dunarea de Jos" University of Galati. Fascicle XI Shipbuilding, 2021. 44: p. 51-58.
[33] technica, C. *Electric boats will be a 16.6 billion market by 2031*. 2023; Available from: https://cleantechnica.com/2022/07/19/electric-boats-will-be-a-16-6-billion-market-by-2031/.
[34] Kedong, Y., et al., *Analysis and forecast of marine economy development in China.* Marine Economics and Management, 2022. 5(1): p. 1-33.
[35] Grand_View_Research_company. *Electric Ship Market Size & Share, Industry Report, 2020-2027*. 2020; Available from: https://www.grandviewresearch.com/industry-analysis/electric-ship-market.
[36] Vance, J.E. *History of ships*. 2022; Available from: https://www.britannica.com/technology/ship/History-of-ships.
[37] Knighton, A. *Galleys: The First Great Warships – They Dominated The Seas For Centuries*. 2017; Available from: https://www.warhistoryonline.com/ancient-history/galleys-first-great-warships-m.html?chrome=1.
[38] CAVENAGH, B. *Square Rigs for Small Boats An update for an ancient rig*. 2015; Available from: https://smallboatsmonthly.com/article/square-rig-for-small-boats/.
[39] Vance, J.E. *The steamboat*. 2018; Available from: https://www.britannica.com/technology/ship/The-steamboat.
[40] Skiff, C. *news events*. 2022; Available from: https://www.carolinaskiff.com/news-events/.
[41] Bernardo. *What is a Deck Boat?* 2021; Available from: https://www.nauticalventures.com/blog/what-is-a-deck-boat.
[42] Callahan, J. *20 Different Types of Fishing Boats (Small, Mid-Sized and Large Options)*. 2022 Available from: https://boatbiscuit.com/20-different-types-of-fishing-boats-small-mid-sized-and-large-options/.
[43] Tarjan, G., *Catamarans: The complete guide for cruising sailors*. 2007: McGraw Hill Professional.
[44] Denison's_team. *top 5 convertible sportfishing boats under 500k*. 2019; Available from: https://www.denisonyachtsales.com/2019/03/top-5-convertible-sportfishing-boats-under-500k/.
[45] Woodford, C. *How outboard motors work.* 2021; Available from: https://www.explainthatstuff.com/outboardmotors.html.
[46] Hendricks, J. *Twin Outboards Versus Single Outboard*. 2017; Available from: https://www.sportfishingmag.com/one-or-two-outboard-motors-for-boat/.

[47] Dale, V. *Outboard Motor Installation Guide*. 2022; Available from: https://www.powerequipmentdirect.com/stories/1693-How-to-Install-an-Outboard-Motor-for-Your-Small-Boat.html.
[48] Yanmar. *Inboard_motor/media*. 2007; Available from: https://en.wikipedia.org/wiki/Inboard_motor#/media/File:Yanmar.jpg.
[49] matsonauto. *whats the difference between inboard outboard and sterndrive*. 2018; Available from: https://matsonauto.com/whats-the-difference-between-inboard-outboard-and-sterndrive/.
[50] Greenboatsolutions. *Electric pod motor for your boat*. 2023; Available from: https://www.greenboatsolutions.com/shop/motor/pod.
[51] Boatsafe. *Inboard vs Outboard Motors: What's the Difference?* 2020; Available from: https://www.boatsafe.com/inboard-vs-outboard/.
[52] Fortey, I. *Understanding Different Kinds of Boat Propulsion*. 2021; Available from: https://www.boatsafe.com/propulsion-requirements/.
[53] Torqeedo. *Inboards - Electric motors from Torqeedo*. 2015; Available from: https://www.torqeedo.com/us/en-us/products/inboards.
[54] Johnson_Outdoors_Inc. *E-drive electric outboard motor product manuals*. 2023; Available from: https://minnkota.johnsonoutdoors.com/us/support/manuals/trolling-motors/e-drive.
[55] Ray_Electric_Outboards. *Ray Electric Outboards* 2018; Available from: https://rayeo.com/.
[56] Marine, A. *28 cabin electric*. 2020; Available from: https://alfastreet-marine.com/electric-range/28-cabin-electric/.
[57] Blazeby, M. *DutchCraft Reveals Fully Electric DutchCraft 25 Tender*. 2019; Available from: https://www.boatinternational.com/yachts/news/dutchcraft-reveals-fully-electric-dutchcraft-25-tender--42131.
[58] silent-yachts. *SILENT 60*. 2023; Available from: https://www.silent-yachts.com/silent60/.
[59] Aquawatt. *aquawatt Green Electric Marine Technologies*. 2022; Available from: https://www.aquawatt.at.
[60] Tvaronavičienė, M., *Effects of climate change on environmental sustainability*. 2021.
[61] Paul, D., *A history of electric ship propulsion systems [history]*. IEEE Industry Applications Magazine, 2020. 26(6): p. 9-19.
[62] Merve, Ş.K., *The Use of Induction Motors in Electric Vehicles*, in *Induction Motors-Recent Advances, New Perspectives and Applications*. 2023, IntechOpen.
[63] Sailor, S. *5 Best Electric Outboard Motors*. 2021; Available from: https://www.solarsailor.com/best-electric-outboard-motor/.
[64] Torqeedo_Company. *about torqeedo company*. 2005; Available from: https://www.torqeedo.com/us/en-us/about-torqeedo/company.html.
[65] Vaez-Zadeh, S., *Control of permanent magnet synchronous motors*. 2018: Oxford University Press.
[66] Turqeedo. *Superior Drive Train Engineering*. 2017; Available from: https://www.torqeedo.com/us/en-us/technology-and-environment/propulsion-technology.html.

[67] Uttern. *Quicksilver Activ Performance Data*. 2014; Available from: https://www.uttern.com/media/220726/activ_performance_data_rev_k.pdf.
[68] Torqeedo-inc. *Cruise Outboards, the ultimate power packs for sailing or motorboats*. 2023; Available from: https://media.torqeedo.com/downloads/flyer/EN/torqeedo-onepager-cruise-rt-en.pdf.
[69] Torqeedo-inc. *Torqeedo cruise 12r manual*. 2023; Available from: https://media.torqeedo.com/downloads/manuals/torqeedo-cruise-12-r-manual-DE-EN.pdf.
[70] Torqeedo-inc. *The ultimate power packs for sailing or motorboats*. 2023; Available from: https://media.torqeedo.com/downloads/flyer/EN/torqeedo-onepager-cruise-rt-en.pdf.
[71] Julie. *Autonomous Boat*. 2017; Available from: https://angusadventures.com/propulsion-system-for-autonomous-boat.
[72] Agarwal, M. *What is The Speed of a Ship at Sea?* 2019; Available from: https://www.marineinsight.com/guidelines/speed-of-a-ship-at-sea/.
[73] Torqeedo-inc. *Cruise 12.0 rs torqlink*. 2023; Available from: https://www.torqeedo.com/us/en-us/products/outboards/cruise/cruise-12.0-r-torqlink/M-1280-00.html.
[74] Torqeedo_inc. *TorqLink throttle with colour display*. 2023; Available from: https://www.torqeedo.com/en/products/accessories/cables-and-steering/torqlink-throttle-with-colour-display/1976-00.html.
[75] Revankar, S.T., *Chemical energy storage*, in *Storage and Hybridization of Nuclear Energy*. 2019, Elsevier. p. 177-227.
[76] Washington-edu. *Batteries*. 2023; Available from: https://depts.washington.edu/matseed/batteries/MSE/battery.html.
[77] Lipschultz, A., *Batteries in a portable world.* Biomedical Instrumentation & Technology, 2015. 49(2): p. 134-134.
[78] Rajanna, B. and K.K. Malligunta, *Comparison study of lead-acid and lithium-ıon batteries for solar photovoltaic applications.* International Journal of Power Electronics and Drive Systems, 2021. 12(2): p. 1069.
[79] Zhou, L., et al., *Recent developments on and prospects for electrode materials with hierarchical structures for lithium-ion batteries.* Advanced Energy Materials, 2018. 8(6): p. 1701415.
[80] Yin, J., et al., *Lead-carbon batteries toward future energy storage: from mechanism and materials to applications.* Electrochemical Energy Reviews, 2022. 5(3): p. 2.
[81] Jafari, H. and M.R. Rahimpour, *Pb acid batteries.* Rechargeable Batteries: History, Progress, and Applications, 2020: p. 17-39.
[82] Lopes, P.P. and V.R. Stamenkovic, *Past, present, and future of lead–acid batteries.* Science, 2020. 369(6506): p. 923-924.
[83] Boddula, R., R. Pothu, and A.M. Asiri, *Rechargeable Batteries: History, Progress, and Applications*. 2020: John Wiley & Sons.

[84] Chumchal, C. and D. Kurzweil, *Lead–acid battery operation in micro-hybrid and electrified vehicles*, in *Lead-Acid Batteries for Future Automobiles*. 2017, Elsevier. p. 395-414.
[85] KITARONKA, S., *Lead-Acid Battery*. 2022, Figshare.
[86] Spiers, D.J., *Battery issues*, in *Photovoltaics in Cold Climates*. 2019, Routledge. p. 46-58.
[87] Williams, J. and J. Williams, *Portable Power: Batteries.* The Electric Century: How the Taming of Lightning Shaped the Modern World, 2018: p. 84-92.
[88] Zelinsky, M., et al., *Storage-integrated PV systems using advanced NiMH battery technology.* 2010.
[89] Petrovic, S. and S. Petrovic, *Nickel–cadmium batteries.* Battery Technology Crash Course: A Concise Introduction, 2021: p. 73-88.
[90] Yang, Y., et al., *On the sustainability of lithium ion battery industry–A review and perspective.* Energy Storage Materials, 2021. 36: p. 186-212.
[91] Ren, W.-F., et al., *Si anode for next-generation lithium-ion battery.* Current Opinion in Electrochemistry, 2019. 18: p. 46-54.
[92] Spitthoff, L., P.R. Shearing, and O.S. Burheim, *Temperature, ageing and thermal management of lithium-ion batteries.* Energies, 2021. 14(5): p. 1248.
[93] Zhou, Z., et al., *A review of energy storage technologies for marine current energy systems.* Renewable and Sustainable Energy Reviews, 2013. 18: p. 390-400.
[94] Fichtner, M., et al., *Rechargeable batteries of the future—the state of the art from a BATTERY 2030+ perspective.* Advanced Energy Materials, 2022. 12(17): p. 2102904.
[95] Verma, J. and D. Kumar, *Recent developments in energy storage systems for marine environment.* Materials Advances, 2021. 2(21): p. 6800-6815.
[96] Wang, Z., et al., *A review of marine renewable energy storage.* International Journal of Energy Research, 2019. 43(12): p. 6108-6150.
[97] Hannan, M., et al., *Review of energy storage systems for electric vehicle applications: Issues and challenges.* Renewable and Sustainable Energy Reviews, 2017. 69: p. 771-789.
[98] Alexander, C. and M. Sadiku, *Part1: DC circuits fundamentals of electric circuits*. 2017, New York: McGraw-Hill Education.
[99] Torqeedo_inc. *Power 48-5000*. 2023; Available from: https://www.torqeedo.com/en/products/batteries/power-48-5000/2104-00.html.
[100] Torqeedo-inc. *Power 48-5000 and chargers,Translation of the original operating instructions*. 2023; Available from: https://media.torqeedo.com/downloads/manuals/torqeedo-power-48-5000-manual-DE-EN.pdf.
[101] Khan, K. and M.A. Salek, *Solar photovoltaic (SPV) conversion: a brief study.* IJARIIE, 2019. 5(5): p. 187-204.
[102] Jmdonev. *Types of photovoltaic cells*. 2018 [cited 2022; Available from: https://energyeducation.ca/wiki/index.php?title=Types_of_photovoltaic_cells&oldid=7275.

[103] Bagher, A.M., M.M.A. Vahid, and M. Mohsen, *Types of solar cells and application.* American Journal of optics and Photonics, 2015. 3(5): p. 94-113.
[104] Planete-energies. *How Does a Photovoltaic Cell Work?* 2019; Available from: https://www.planete-energies.com/en/media/article/how-does-photovoltaic-cell-work.
[105] Prajapati, T. and A. Priyam, *A Review on Photovoltaic Cells.* Smart Energy and Advancement in Power Technologies, 2023: p. 497-512.
[106] Pujahari, R., *Solar cell technology*, in *Energy Materials*. 2021, Elsevier. p. 27-60.
[107] Goodrich, A., et al., *A wafer-based monocrystalline silicon photovoltaics road map: Utilizing known technology improvement opportunities for further reductions in manufacturing costs.* Solar Energy Materials and Solar Cells, 2013. 114: p. 110-135.
[108] Bayod-Rújula, A.A., *Solar photovoltaics (PV)*, in *Solar Hydrogen Production*. 2019, Elsevier. p. 237-295.
[109] Ahmad, L., et al., *Recent advances and applications of solar photovoltaics and thermal technologies.* Energy, 2020. 207: p. 118254.
[110] Cano, J., *Photovoltaic modules: Effect of tilt angle on soiling*. 2011: Arizona State University.
[111] Lutz, A. *TYPES OF SOLAR PANELS FOR HOMES (2022 GUIDE)*. 2022; Available from: https://www.architecturaldigest.com/reviews/home-improvement/types-of-solar-panels.
[112] Dharmadasa, I., *Advances in Thin-Film Solar Cells, Second Edi*. 2018, Jenny Stanford Publishing, Boulevard.
[113] SUSTAINIA. *Efficient Flexible Thin-Film Solar Cells*. 2018; Available from: https://goexplorer.org/efficient-flexible-thin-film-solar-cells/.
[114] SunPower. *Flexible Solar Panels | SPR-E-Flex-110*. 2023; Available from: https://us.sunpower.com/sites/default/files/110w-flexible-panel-spec-sheet.pdf
[115] Shaikh, M.R.S., *A review paper on electricity generation from solar energy.* 2017.
[116] Kazem, H.A., et al. *Effect of Shadows on the Performance of Solar Photovoltaic*. in *Mediterranean Green Buildings & Renewable Energy*. 2017. Cham: Springer International Publishing.
[117] Plueddeman, C. *Mercury Debuts All-New 75 HP, 90 HP, and 115 HP FourStroke Outboards*. 2014; Available from: https://www.boats.com/reviews/mercury-debuts-new-75-hp-90-hp-115-hp-fourstroke-outboards/.
[118] Yamaha_Motor_Canada_Ltd. *Yamaha Motor* 2023; Available from: https://www.yamaha-motor.ca/en/water/outboard-motor?gclid=Cj0KCQjwnP-ZBhDiARIsAH3FSRdeo-KVXa6wNxm6FLG2N9qbqleRUxl46WOOTkG3PPD-wiNcauDVxTQaArP6EALw_wcB.
[119] x-engineer. *What is a DC-DC converter*. 2022; Available from: https://x-engineer.org/dc-dc-converter/.
[120] Khan, M.A., et al., *Performance analysis of bidirectional DC–DC converters for electric vehicles.* IEEE transactions on industry applications, 2015. 51(4): p. 3442-3452.
[121] Emadi, A., *Advanced electric drive vehicles*. 2014: CRC Press.

[122] Kumar, S., R. Kumar, and N. Singh. *Performance of closed loop SEPIC converter with DC-DC converter for solar energy system*. in *2017 4th International Conference on Power, Control & Embedded Systems (ICPCES)*. 2017. IEEE.
[123] Babes, B., et al. *Design of a robust voltage controller for a DC-DC buck converter using fractional-order terminal sliding mode control strategy*. in *2019 International Conference on Advanced Electrical Engineering (ICAEE)*. 2019. IEEE.
[124] Chai, M., et al., *Alternating current and direct current-based electrical systems for marine vessels with electric propulsion drives.* Applied Energy, 2018. 231: p. 747-756.
[125] Leaf-Group-Ltd., *How Does a Rectifier Work?* 2023.
[126] Arora, K., S. Katiyar, and R. Patel. *Design and analysis of AC to DC converters for input Power Factor Correction*. in *2016 2nd International Conference on Applied and Theoretical Computing and Communication Technology (iCATccT)*. 2016. IEEE.
[127] Torqeedo-inc. *fast charger 2900 w power 48.5000*. 2023; Available from: https://www.torqeedo.com/us/en-us/products/accessories/charging-equipment/fast-charger-2900-w-power-48-5000/2212-10.html.
[128] Gupta, R., et al. *Modeling and design of MPPT controller for a PV module using PSCAD/EMTDC*. in *2010 IEEE PES Innovative Smart Grid Technologies Conference Europe (ISGT Europe)*. 2010. IEEE.
[129] Ram, J.P., N. Rajasekar, and M. Miyatake, *Design and overview of maximum power point tracking techniques in wind and solar photovoltaic systems: A review.* Renewable and Sustainable Energy Reviews, 2017. 73: p. 1138-1159.
[130] Reisi, A.R., M.H. Moradi, and S. Jamasb, *Classification and comparison of maximum power point tracking techniques for photovoltaic system: A review.* Renewable and sustainable energy reviews, 2013. 19: p. 433-443.
[131] Fahim, K.E., et al. *Overview of maximum power point tracking techniques for PV system*. in *E3S Web of Conferences*. 2021. EDP Sciences.
[132] Aurairat, A. and B. Plangklang, *An Alternative Perturbation and Observation Modifier Maximum Power Point Tracking of PV Systems.* Symmetry, 2021. 14(1): p. 44.
[133] Victronenergy. *BlueSolar Charge Controller MPPT 150/35 & 150/45*. 2023; Available from: https://www.victronenergy.com/upload/documents/Datasheet-BlueSolar-charge-controller-MPPT-150-35-&-150-45-EN-.pdf.
[134] VictronEnergy. *BlueSolar Charge Controllers with screw- or MC4 PV connection*. 2023; Available from: https://www.victronenergy.com/upload/documents/Datasheet-BlueSolar-charge-controller-MPPT-150-45-up-to-150-70-EN.pdf.
[135] Kirtley, J.L., *Electric power principles: sources, conversion, distribution and use*. 2020: John Wiley & Sons.
[136] J Chapman, S., *Electric machinery fundamentals*. 2004: McGraw-hill.
[137] Palomba, G., et al., *Aluminium honeycomb sandwich as a design alternative for lightweight marine structures.* Ships and Offshore Structures, 2022. 17(10): p. 2355-2366.

[138] MatWeb. *MatWeb, Your Source for Materials Information*. 2022; Available from: https://www.matweb.com/.
[139] Kováčik, J., L. Marsavina, and E. Linul, *Poisson's ratio of closed-cell aluminium foams.* Materials, 2018. 11(10): p. 1904.
[140] SolarSena. *How to Calculate Solar Panel Tilt Angle?* 2022; Available from: https://solarsena.com/how-calculate-solar-panel-tilt-angle/.
[141] Tupper, E.C., *Introduction to naval architecture*. 2013: Butterworth-Heinemann.
[142] Callister Jr, W.D., *Fundamentals of materials science and engineering: an integrated approach*. 3 ed. 2008: John Wiley & Sons.
[143] Bagué, A., et al., *Dynamic stability analysis of a hydrofoiling sailing boat using CFD.* Journal of Sailing Technology, 2021. 6(01): p. 58-72.
[144] Barrass, C.B. and D.R. Derrett, *Ship Stability for Masters and Mates*. 2012: Elsevier Ltd.
[145] Santander, J., *A problem regarding buoyancy of simple figures suitable for Problem-Based Learning.* Revista Brasileira de Ensino de Física, 2017. 39.
[146] Bar-Meir and 2021Genick, *Stability of Ship and Other Bodies*.
[147] Ginsberg, J., *Advanced engineering dynamics*. 1998: Cambridge University Press.
[148] Barraza, J.F. and N.M. Grzywacz, *Measurement of angular velocity in the perception of rotation.* Vision research, 2002. 42(21): p. 2457-2462.
[149] Engineering_ToolBox. *Electric Motors - Torque vs. Power and Speed*. 2009; Available from: https://www.engineeringtoolbox.com/electrical-motors-hp-torque-rpm-d_1503.html.